Development of Flotation Enhanced Stirred Tank (FEST) Process for Petroleum Hydrocarbons Removal from Drill Cuttings
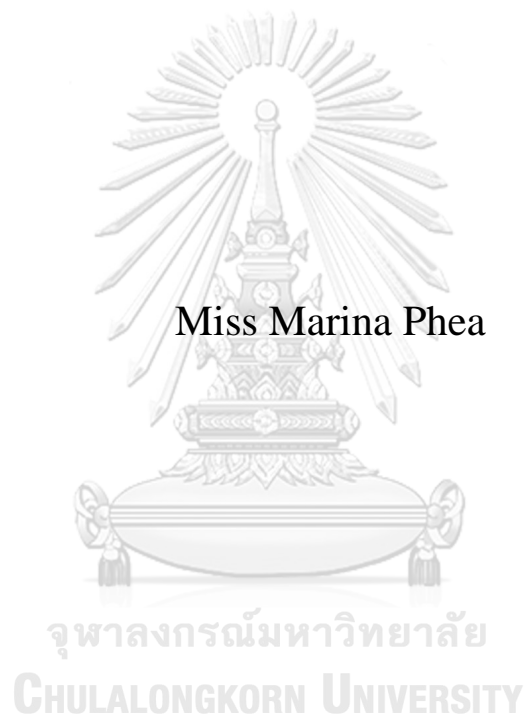
Miss Marina Phea

การพัฒนาระบบบำบัดดินปนเปื้อนจากอุตสาหกรรมปิโตรเลียมโดยใช้ถังปฏิกรณ์แบบกวนร่วมกับกระบวนการทำให้ลอย

น.ส.มารีนา เพีย

Thesis Title   Development of Flotation Enhanced Stirred Tank
                      (FEST) Process for Petroleum Hydrocarbons Removal
                      from Drill Cuttings
By   Miss Marina Phea
Field of Study   Environmental Engineering
Thesis Advisor   Professor PISUT PAINMANAKUL, Ph.D.
Thesis Co Advisor   Nattawin Chawaloesphonsiya, Ph.D.

        Accepted by the FACULTY OF ENGINEERING, Chulalongkorn University
in Partial Fulfillment of the Requirement for the Master of Engineering

                      -- Dean of the FACULTY OF
                                                                     ENGINEERING
                      (Professor SUPOT TEACHAVORASINSKUN, D.Eng.)

THESIS COMMITTEE
                      -- Chairman
                      (Associate Professor WIBOONLUK PUNGRASMI,
                      Ph.D.)
                      -- Thesis Advisor
                      (Professor PISUT PAINMANAKUL, Ph.D.)
                      -- Thesis Co-Advisor
                      (Nattawin Chawaloesphonsiya, Ph.D.)
                      -- Examiner
                      (Associate Professor VIBOON
                      SRICHAROENCHAIKUL, Ph.D.)
                      -- External Examiner
                      (Assistant Professor Marupatch Jamnongwong, Ph.D.)

                      จุฬาลงกรณ์มหาวิทยาลัย
                      CHULALONGKORN UNIVERSITY

มารีนา เพีย : การพัฒนาระบบบำบัดดินปนเปื้อนจากอุตสาหกรรมปิโตรเลียมโดยใช้ถังปฏิกรณ์แบบกวนร่วมกับกระบวนการทำให้ลอย. (Development of Flotation Enhanced Stirred Tank (FEST) Process for Petroleum Hydrocarbons Removal from Drill Cuttings) อ.ที่ปรึกษาหลัก : ศ. ดร.พิสุทธิ์ เพียรมนกุล, อ.ที่ปรึกษาร่วม : ณัฐวิญญ์ ชวเลิศพรศิยา

งานวิจัยนี้มุ่งเน้นในการศึกษาสภาวะที่เหมาะสมในการดำเนินงานและพัฒนากระบวนการบำบัดสำหรับการกำจัดสารประกอบไฮโดรคาร์บอนจากปิโตรเลียม (TPH) ออกจากดินปนเปื้อนโดยใช้ถังปฏิกรณ์แบบกวนร่วมกับกระบวนการทำให้ลอย (Flotation Enhanced Stirred Tank: FEST) โดยการศึกษาเริ่มแรกจะศึกษาประสิทธิภาพในการล้างดินปนเปื้อนของแต่ละกระบวนการประกอบด้วยกระบวนการกวน กระบวนการทำให้ลอยด้วยอากาศเหนี่ยวนำ (Induced air flotation: IAF) และกระบวนการทำให้ลอยด้วยอากาศละลาย (Dissolved air flotation: DAF) จากการทดลองพบว่าการล้างดินปนเปื้อนกระบวนการทำให้ลอยมีประสิทธิภาพในการบำบัดสูงกว่ากระบวนการกวน โดยมีประสิทธิภาพในการบำบัดสูงถึงร้อยละ 40 และ 30 สำหรับกระบวนการทำให้ลอยด้วยอากาศละลายที่ความดันอิ่มตัว 4 บาร์ ในขณะกระบวนการทำให้ลอยด้วยอากาศเหนี่ยวนำที่อัตราการไหลของอากาศเท่ากับ 3 ลิตรต่อนาทีและกระบวนการกวนที่ความเร็วในการกวนเท่ากับ 600 รอบต่อนาที มีประสิทธิภาพในการบำบัดเพียงร้อยละ 30 นั่นเป็นเพราะว่าฟองอากาศที่เกิดจากกระบวนการทำให้ลอยนั้นช่วยเพิ่มการกำจัดสารประกอบไฮโดรคาร์บอนที่ติดอยู่กับดินปนเปื้อน ทำให้ประสิทธิภาพในการบำบัดของกระบวนการทำให้ลอยนั้นสูงกว่ากระบวนการกวน อีกทั้งประสิทธิภาพในการบำบัดขึ้นอยู่กับค่าอุทกพลศาสตร์ของฟองอากาศในรูปอัตราส่วนระหว่างพื้นที่ผิวสัมผัสจำเพาะกับความเร็วเกรเดียนท์ (a/G) โดยอัตราส่วนระหว่างพื้นที่ผิวสัมผัสจำเพาะกับความเร็วเกรเดียนท์สูง จะทำให้ประสิทธิภาพการบำบัดสูงด้วย ดังนั้นประสิทธิภาพการบำบัดของกระบวนการทำให้ลอยด้วยอากาศละลายจึงมากกว่ากระบวนการอื่นๆ และเพื่อเพิ่มประสิทธิภาพในการบำบัดรวมทั้งศึกษาปฏิกิริยาระหว่างปัจจัยที่เกิดขึ้น จึงได้ทำการศึกษากระบวนการร่วมระหว่างกระบวนการกวนกับกระบวนการทำให้ลอยทั้งอากาศเหนี่ยวนำ (Stirring and IAF) และอากาศละลาย (Stirring and DAF) และกระบวนร่วมระหว่างกระบวนการกวน กระบวนการทำให้ลอยด้วยอากาศเหนี่ยวนำและกระบวนการทำให้ลอยด้วยอากาศละลาย (Stirring-IAF-DAF) ด้วยโปรแกรมออกแบบการทดลอง (Design of Experiment: DOE) โดยใช้วิธีการพื้นผิวตอบสนองแบบเซ็นทรัลคอมโพสิต (Central composite design-response surface methodology: CCD-RSM)) พบว่าสภาวะที่เหมาะสมในการล้างดินปนเปื้อนด้วยกระบวนการร่วมระหว่างกระบวนการกวนกับกระบวนการทำให้ลอยด้วยอากาศละลาย คือ ที่ความดันอิ่มตัว 4 บาร์ ความเร็วในการกวน 400 รอบต่อนาทีและเวลาในการบำบัด 70 นาทีนั้นโดยมีประสิทธิภาพในการบำบัดถึง 50% และเมื่อเพิ่มกระบวนการทำให้ลอยด้วยอากาศเหนี่ยวนำเข้าไป ทำให้ประสิทธิภาพในการบำบัดสูงขึ้น โดยมีประสิทธิภาพสูงสุดถึง 60% ที่อัตราการไหลของอากาศ 2 รอบต่อนาที ความดันอิ่มตัว 2 บาร์ ความเร็วในการกวน 800 รอบต่อนาทีและเวลาในการบำบัด 60 นาที

สาขาวิชา	วิศวกรรมสิ่งแวดล้อม	ลายมือชื่อนิสิต ....
ปีการศึกษา	2562	ลายมือชื่อ อ.ที่ปรึกษาหลัก ....
		ลายมือชื่อ อ.ที่ปรึกษาร่วม ....

6170425321 : MAJOR ENVIRONMENTAL ENGINEERING

Marina Phea : Development of Flotation Enhanced Stirred Tank (FEST) Process for Petroleum Hydrocarbons Removal from Drill Cuttings. Advisor: Prof. PISUT PAINMANAKUL, Ph.D. Co-advisor: Nattawin Chawaloesphonsiya, Ph.D.

This work aims to develop the treatment process for the removal of total petroleum hydrocarbons (TPH) from DC by using the combination of air floatation and stirring processes, called Flotation Enhanced Stirred Tank (FEST). Initially, stirring, induced air flotation (IAF), and dissolved air flotation (DAF) are individually investigated over DC washing. Afterward, the combination process between "stirring-DAF" and "stirring-IAF-DAF" are continuously observed for finding the better conditions of TPH removal efficiency. To optimize the operational terms of the treatment process, the Design of Experiment (DOE) is applied to design the experimental conditions within the central composite design-response surface methodology (CCD-RSM). Consequently, the result of the stirring process showed that the higher rotational speed represented a better result of removal efficiency, i.e., 200, 400, and 600 rpm could remove TPH around 20%, 25%, and 30%, respectively, for 1h of treatment time. In IAF treatment, the results indicated that the lowest airflow rate (1 LPM) gave the least treatment performance compared to the higher airflow rate (2-3 LPM). After 60 min of treatment time, the washing performance using 2 and 3 LPM was about 28% and 30% of the removal percentage, respectively, while it showed roughly 22% of TPH that eradicated by 1 LPM. Moreover, it was signified that almost 40% of that was removed by microbubbles generated by a saturated pressure 4 bars at the same time in the DAF unit. Hence, to obtain the improved TPH removal percentage, the studied DOE of the combination process between "stirring-DAF" and "stirring-IAF-DAF" were examined. The results demonstrated that the optimum removal percentage would achieve approximately 50% of TPH from DC when P_s was 4 bars, V_m was 400 rpm, and t was 70 min with a correlation $R^2 = 0.8691$. Then, in the three combination units that contained four variables (Q_g, P_s, V_m, and t) were analyzed by varying their studied levels in DOE as well. Similarly, the optimum elimination of TPH would receive approximately 60% with the conditions of Q_g was 2 LPM, P_s was 2 bars, V_m was 800 rpm, and the time t was 60 min.

Field of Study:	Environmental Engineering	Student's Signature ....
Academic Year:	2019	Advisor's Signature ....
		Co-advisor's Signature ....

ACKNOWLEDGEMENTS

TABLE OF CONTENTS

Page

LIST OF TABLES

LIST OF FIGURES

จุฬาลงกรณ์มหาวิทยาลัย
CHULALONGKORN UNIVERSITY

ABBREVIATIONS

CB: Cutting Boxes

CDS: Cuttings Dryer System

CMC: Critical Micelle Concentration

DAF: Dissolved Air Flotation

DC: Drill Cuttings

DPR: Director of Petroleum Resources

IAF: Induced Air Flotation

NAPLs: Non-Aqueous Phase Liquids

OBM: Oil-Based Muds

ODC: Oil-Based Drill Cuttings

PAC: Poly Aluminum Chloride

PAHs: Polycyclic Aromatic Hydrocarbons

PBT: Pitched-Blade Turbine

POME: Palm Oil Mill Effluent

SBM: Synthesis Based Muds

THC: Total Hydrocarbons

TPH: Total Petroleum Hydrocarbon

WBM: Water-Based Muds
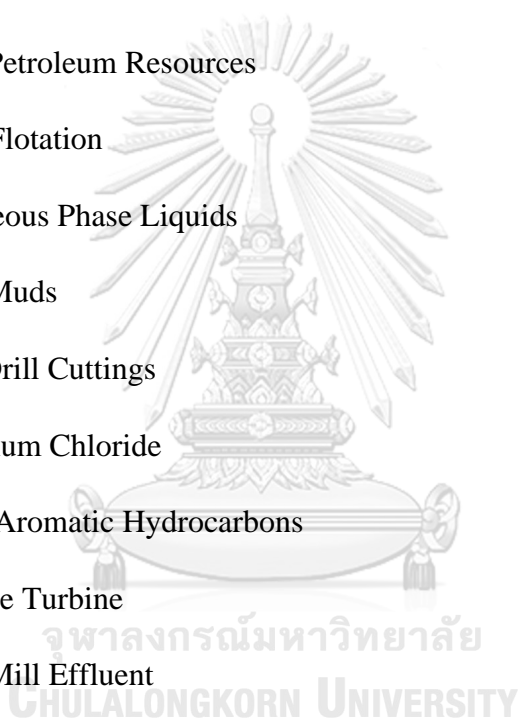
CHAPTER 1
INTRODUCTION

1.1 General Context

Petroleum is one of the significant sources of energy and economy for many countries in the world. As petroleum exploration and production have become an important industrial activity, there are also many investments happening in recent years. It is estimated that the daily petroleum consumption was around 85 million barrels in 2006 and increased to approximately 106.6 million barrels in 2030 in the world (Igunnu & Chen, 2012). For instance, the petroleum exploration and production in Nigeria's Niger Delta area had improved the economy of the nation a lot over the past five decades. These reasons cause many drilling wells are extracted and drilled into the ground in order to bring the accumulated hydrocarbons up to the platform for commercial and innovative petroleum products. Drill cuttings (DC) transport is an essential part of every drilling operation because it is necessary to avoid the cuttings accumulation in the borehole and the proceed drilling. In the system, drilling fluids are continuously pumped from the surface of the platform down through a drilling pipe to the drill string in order to enhance cuttings extraction; then, they bring the cuttings back to the rigs via annulus to store at the settling pit. Afterward, DC are separated from muds using vibrating screens, hydrocyclone, or centrifuges. The cuttings will be managed and remediated on the rigs in order to separate the adhered fluids as much as possible before either discharging to the ocean, transporting to the shore for land disposal, or re-injecting into a disposal well, depends on the local infrastructure and environmental regulations (IOGP, 2016).

Consequently, waste management is one issue facing the oil and gas industry because a large amount of drill cuttings and spent mud were produced during the drilling operations. This problem has frequently thrown the industries into numerous challenges and concerns of finding technological development for controlling the wastes and safe environment. When those wastes are not properly managed, the process can pose many significant impacts on the environment, such as soils and sediments, surface-water, ground-water, the atmosphere, the aquatic environment, and

the sustainable ecosystems due to the largely generated drill cuttings (DC) within drilling fluids throughout the operation (Ite, Ibok, Ite, & Petters, 2013). The reason is that these wastes contained not only organic materials but also inorganic constituents, including polychlorinated biphenyls, petroleum hydrocarbons, and heavy metals (Onwukwe, Nwakaudu, & Development, 2012; Yan, Lu, Guan, Zhang, & Zhang, 2011). For instance, the discharge of petroleum hydrocarbons and petroleum affects social and economic problems, human well-being, and impacts the host communities in the nine oil producing states in the Niger Delta. In a similar vein, soils and sediments are the most vulnerable petroleum contaminants. Precisely, they are easily contaminated with benzene, toluene, ethylbenzene, and xylenes, aliphatic, and polycyclic aromatic hydrocarbons (PAHs). Therefore, hydrocarbons contaminated soils and sediments are one of the discerning problems because its characteristics of aromatic components cause oxygen depletion (Ite et al., 2013). According to Kubo, Kido, Fuwa, Hoshino, and Development (2016), DC is easily contaminated by drilling muds due to their small size, which was fully coated by drilling muds during their transportation from the borehole to the platform. It is complicated to remove the drilling muds from DC, even after repeated washing. Therefore, most of DC needed to separate and decontaminate after drilling operation before being disposed of wastes back into the environment; otherwise, they will become the global concern because of their long-term toxicity (Ite et al., 2013; Xionghu, Fengchun, & Fluid, 2004).

So far, to deal with the disposal concerns, several treatment technologies have been explored, including physical treatment, chemical treatment, and biological methods to reach the effective treatment in terms of efficiency, affordable cost, non-hazard chemical use, and saving the environment (Agarwal, Zhou, Liu, & Research, 2016). However, some chemical methods are not so popular as the use of harsh chemical agents affected the environment. At the same time, bioremediation is another treatment method that offers advantages such as natural products from renewable resources, excellent biodegradability, less toxic, and good environmental compatibility. Nevertheless, this technique has known as a prolonged process and difficult to address with bio-refractory organic contaminations. Besides, other physical approaches, such as thermal desorption, microwave, supercritical fluid

extraction, and ultrasonication, etc., are also observed, yet they are extremely costly and high energy usage (Sun, Liu, Wang, & Liu, 2019). In the past, flotation technology has been commonly utilized in order to remove the hydrophobic contaminated minerals from hydrophilic constituents and to separate bitumen from sediments that were contaminated by oil in petroleum industries. This process has known as the effective one; however, it needed to observe under some studied parameters such as the viscosity, the adhesion forces between oil and the sediments, and the separation temperature consideration in the system. Unlike flotation separation method, sediment washing technology was another choice that required a large amount of surfactant. Surfactants reduced the hydrophobicity of the oil phase, so the oil could be wetted by the water phase easily; then, it could detach from the sediment phase and remove it. However, in most researches, the use of surfactants caused some problems owing to their toxicity and low biodegradability. Thus, surfactants of low toxicity and high biodegradability were further innovated in order to diminish the threat to the environment (Agarwal & Liu, 2015; Wang, Shammas, Selke, & Aulenbach, 2010).

Hence, this study aims to investigate and evaluate the effects of a potential treatment for TPH removal from DC washing by using the combination of two physical processes, including the flotation process and mechanical stirring, which can follow the environmentally friendly, economical, and less operational installation. The other methods and parameters using are further studied and detailed in Chapter 3 and 4.

1.2 Problem Statements

In general, DC brought from the deep well to the surface, which accompanies with drilling muds. The large volume of DC disposal became the most significant concern worldwide; hence, many industries were trying to find effective management and treatment.

There was evidence of various effects on the sea environment because of the operational discharge of DC and drilling fluids. This direct disposal could eradicate the benthic communities since the sedimentation and particles were released and suspended. Furthermore, the discharge that was related to some pollutants such as

heavy metals, total hydrocarbons (THC) etc., could have acute toxicity, long term impacts through the accumulation of sediments, which could contaminate or leak into the groundwaters (Aagaard-Sørensen, Junttila, & Dijkstra, 2018).

Untreated DC potentially posed pollution to the environment, known as hazardous waste. For example, oil-contaminated sand, which was contaminated by the oil spillage, threatened to aquatic habitats and severely affected to population residing nearby the shoreline. In 2017, 300 tons of oil spillage on Pasir Gudang beach in Singapore exposed the oil stick on sands and formed more sticky substances (i.e., tarballs). By the action of beach dynamics, the oil burial could spread up to several meters of the depth and cause serious decerning owing to its acute toxicity (Sun et al., 2019).

The remediation of oil-contaminated soils was one of the challenges for global environmental science and engineering, e.g., some pollution pathways, including polycyclic aromatic hydrocarbons (PAHs), may be complicated in treatment due to their complex properties such as toxicity and carcinogenetic (Kuppusamy et al., 2017).

During drilling, stimulation, and production of oil and gas processes, a lot of amount of produced water were produced daily worldwide. Thus, the water effluent has become one of the most concerning issues that resulted in environmental problems. Consequently, the treatment process requires specific regulatory standards or technical requirements. Similarly, the treated produced water could be re-injected in offshore production without consuming much freshwater and spending much money (Fakhru'l-Razi et al., 2009; Veil, 2011; Zheng et al., 2016).

1.3 Research Objectives

The objective of this research work was to propose a treatment process for petroleum hydrocarbon removal from drill cuttings by using the air flotation process to enhance the stirring process in a column reactor. Two specific objectives could express as below:

➢ To optimize experimental conditions by modifying the Induced Air Flotation (IAF) and the Dissolved Air Flotation (DAF) processes combining with mechanical stirring for the DC washing process.

➢ To observe the mechanism of bubble hydrodynamics in terms of interfacial area compared to velocity gradient (a/G) ratio as a function of TPH removal efficiency (%Eff) in the combination process (FEST).

1.4 Hypotheses

The hypotheses in the research study were:

1) The optimum conditions of the combination process (the air flotation combined with the stirring process) may enhance in TPH removal from drill cuttings.
2) Saline water (the fraction between NaCl and water that mix to represent as seawater) may be effective and assist in removing of TPH from drill cuttings.
3) The values of a/G may be useful and be able to predict for further TPH removal proficiency in the FEST process.

1.5 Scopes of the Study

This research study was conducted in the laboratory of the Department of Environmental Engineering, Chulalongkorn University. In this research work, several scopes covered as in the following parts:

➢ DC that was sampled in this study, was from the actual petroleum drilling process, which was located in an offshore site. These samples were taken to characterize for physicochemical properties that were very useful for a treatment analysis.

➢ Tap water and saline water (3-3.5% of NaCl concentration to represent the average salinity of seawater (Radzuan, Belope, Thorpe, & Design, 2016; Sun et al., 2019)) were selected as the washing reagents in the further experiments.

➢ Experimental conditions in the mechanical stirring process were also studied to test for some identified parameters, such as impeller screening, motor rotational speed (V_m), washing time (t), and solid to liquid (S/L) ratio.

➢ DC washing was studied by observing the different effects of every single unit, such as Induced Air Flotation (IAF), Dissolve Air Flotation (DAF), and Stirring process.

➢ The experimental conditions in combination process called flotation enhanced stirred tank (FEST) was varied between the combination of IAF with Stirring, DAF with Stirring, and IAF, DAF with Stirring process together.

➢ The acrylic column reactor (H = 25cm x ID = 6cm) was employed in this study.

➢ After drill cuttings treatment, the oily produced water was identified as its characteristics to compare with the produced water specifications, whether it could be reinjected back into the drilling operation or not.

จุฬาลงกรณ์มหาวิทยาลัย

CHULALONGKORN UNIVERSITY

CHAPTER 2
THEORY AND LITERATURE REVIEWS

2.1 Petroleum Resource Formation

Oil and gas were formed from the accumulations of plant and animal materials that were buried underground, especially under the water sources such as an ocean, river, or coral reef. A long time ago, these materials were accumulated with sediments, which could push deeper and deeper into the earth's surface by the mechanisms of the increase of pressure from the overlying weight if sediments and the rise of temperature from the ground were created as fossils fuel. Then, when the hydrocarbon pyrolysis occurred in a confined layer of porous reservoir material, oil and gas reservoirs were created. Oil finally existed inside the small void spaces in rock in the form of tiny droplets, as shown in **Figure 2.1** (Guerra, Dahm, & Dundorf, 2011). In other words, oil and gas formation could define as petroleum, which referred to a natural occurrence of many mixed compositions, which were made up of predominant hydrocarbon compounds. Petroleum normally contained nitrogen, sulfur, and oxygen together with minimal amounts of nickel, vanadium, and other trace elements. The compositions of petroleum mostly occurred in three forms, such as solid form (i.e., asphalt), liquid form (i.e., crude oil), and gaseous form (i.e., natural gas) existing in underground geology. Likewise, petroleum hydrocarbons could categorize into four classes including, (1) saturated hydrocarbons (pentane, hexadecane, octacosane, and cyclohexane), (2) aromatics (naphthalene, phenanthrene, benzene, and pyrene), (3) asphaltenes (phenols, fatty acids, ketones, esters, and porphyrins), and (4) resins (pyridines, quinolines, carbazoles, sulfoxides, and amides) (Ite et al., 2013). Thus, in order to obtain petroleum for supplementary uses, many oil and gas industries were invested over oil and gas drilling operations.
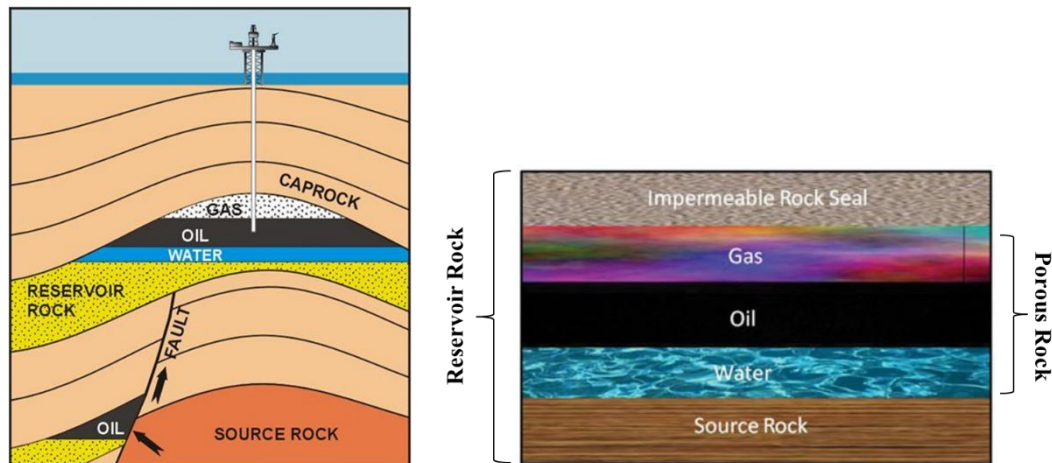
Figure 2.1 Typical reservoir of petroleum (Igunnu & Chen, 2012)

2.2 Drilling Operations of Oil and Gas Industries

Typically, the drilling operation was a significant activity in oil and gas exploration and productions as it could drill into extraction wells to take the accumulated hydrocarbons up to the platform for commercial petroleum products. The process of petroleum drilling wells produced two main kinds of wastes, including drilling fluids (muds) and drill cuttings. In the system, drilling muds were continuously circulated from the surface down to the drill string in order to enhance DC transportation, cool down the bit, and control the pressures of fluids (Ball, Stewart, Schliephake, & Research, 2012; Onwukwe et al., 2012). Then, these muds aided to carry the cuttings back to the rigs via annulus to store at the settling pit, as shown in **Figure 2.2.** As the drill bits milled the rocks into drill cuttings, these cuttings became entrapped with the fluids and were transported up to the surface (settling pit). At the settling pit station, the cuttings are separated from the fluids and other contaminants so that the cleaned drilling muds were used to reinject back in the system through the drilling pipe (Schaanning et al., 2008). The initial step of removing cuttings from fluids was the vibration screens called shale shaker. The cuttings, then, were collected and kept in a tank for further treatment or management. Additionally, other mechanisms such as hydro cyclone, centrifugation, and gravitational settling were processed for further removal of fine solids or particles that tended to interfere in drilling performance (US EPA 2000). Although shale shaker could assist a lot in solids separation, there were some limitations in separation treatment technologies, which often resulted in several

base fluids, mud constituents, and possibly crude oil that were ineffectively removed from the cuttings. Hence, the cuttings that adhered to drilling fluids were ending up as residuals in the solid waste stream (Sadiq et al. 2003).
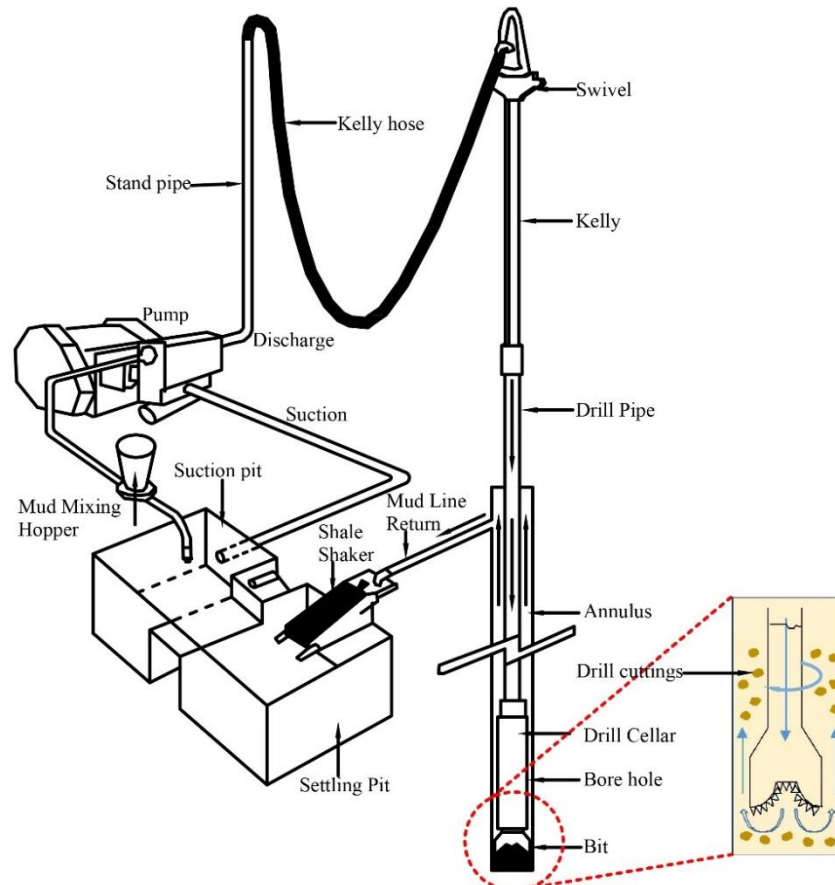
Figure 2.2 Circulating system of drilling process (Broni-Bediako, Amorin, & Technology, 2010)

2.2.1 Drilling Fluids Using in the System

According to Broni-Bediako et al. (2010), drilling muds or fluids were known as any fluids that circulate in a well to extract cuttings from a wellbore. As mentioned before, these fluids were commonly used on drilling rigs in the oil and gas industry because they could ensure a safe and productive oil or gas well. To obtain a well to be drilled successfully, safely, and economically, drilling fluids contained their essential functions:

➢ To remove drill cuttings from the bottom of the bits;

> ➢ To carry those cuttings to the surface;
> ➢ To make cuttings suspend in the fluids when circulation stops working;
> ➢ To prevent the borehole from collapsing;
> ➢ To protect formations hole from damage; and
> ➢ To clean, to lubricate, and to cool down the drill bits, etc.

There were three classes of drilling muds using in drilling procedures consist of (1) water-based muds (WBM), (2) oil-based muds (OBM), and (3) synthetic-based muds (SBM) as described below:

Water-based muds (WBM): usually contained seawater as the base liquid mixed with bentonite, clay, and barium sulfate (barite) to control mud density. Besides, some additives, including thinners, filtration control agents, lubrication agents, and other compounds for specific functions, were added to gain the desired drilling properties. In drilling procedures, the water-based muds could contain in drill cuttings around **10** to **20%** depends on their grain size (Broni-Bediako et al., 2010; Neff & Management, 2008).

Oil-based muds (OBM): referred to the muds that based on hydrocarbon distillation (diesel oil or mineral oil) and the other formations, namely polynuclear aromatic hydrocarbons. They may consist of barites ($BaSO_4$), which were used to control hydrostatic pressure inside the formation hole. A case in the Gulf of Mexico, the cutting wastes were carried up to the platform at the north of the sea by using oil-based muds (OBM), which contained **5** to **15%** of oil (Breuer, Stevenson, Howe, Carroll, & Shimmield, 2004). Thus, the management of wastes involving this OBM was more complicated owing to its high containment of diesel, the polyaromatic hydrocarbons, and mineral oil (Ball et al., 2012).

Synthetic based muds (SBM): were from the emulsion of "pseudo-oil," organic liquids such as ethers, esters, olefins or vegetable oils, and the synthetic base and water, with additives. SBM had been widely used in drilling procedures due to its more considerable advantages and less environmental toxicity compared to other types of fluids. Because of the high cost and presence of the organic substances, drill cuttings with synthetic-based drilling fluids had to separate in the solid control

system. Necessarily, there were two steps in this separation; firstly, all the recovered drilling fluid was re-injected into the well for continuously drilling operation; secondly, all cuttings were removed from the pit for further treatment (Júnior, Martins, Ataíde, & Duarte, 2017).

2.2.2 Drill Cuttings (DC)

In general terms, drill cuttings were described as the mixture between drilling fluids and soils, sediments, or rock fragments, particularly with chemicals that produce and use during the operations. After transportation from the hollow drill string, drill cuttings were collected and stored in a pit or tank for further disposal or management. Moreover, they could contain various toxic substances that were associated with oil and gas during drilling activities, and their components potentially impact the environment, as listed in **Table 2.1** (Bakke, Klungsøyr, & Sanni, 2013; Stuckman, Lopano, Berry, Hakala, & Engineering, 2019). Hence, the amount of generated shale drill cuttings was notified according to a well pad that varies mostly based on the typical depth of drilling well. For instance, approximately **4.30 million tons** of Marcellus Shale drill cuttings were generated in the state of Pennsylvania, and around **113 million tons** of shale drill cuttings were generated in the U.S (Stuckman et al., 2019).

Table 2.1 Waste components and environmentally significant constituents

Waste types	Components	Environmentally Significant Constituents
1). The waste of lubricants	Lube oil, grease	Heavy metals, organics
2). Spacers	Mineral oil, detergents, surfactants	Hydrocarbons, alcohol, aromatics
3). Spent or contaminated water-based muds (include brine)	Whole muds, mineral oil, biodegradable matters	Heavy metals, inorganic salt, biocides, hydrocarbons, solids/ cuttings, BOD, organics
4). Water-based muds cutting	Formation solids, water-based muds, mineral oil	Heavy metals, inorganic salt, biocides, hydrocarbons, solids/ cuttings

Waste types	Components	Environmentally Significant Constituents
5). Spent/contaminated oil-based muds	Whole muds, mineral oil	Hydrocarbons, heavy metals, inorganic salts, solids, BOD, organics, surfactants
6). Oil-based muds cuttings	Formation solids, oil-based muds	Heavy metals, inorganic salt, hydrocarbons, solid/cutting
7). Spent bulk chemical	Cement, bentonite, barites, viscosities, thinners, fluid loss, reducers, specialty product	Heavy metals, hydrocarbons, organics, solids
8). Spent-special products	H_2S scavengers, defoamers, tracers	Zinc carbonates, iron oxides, hydrocarbons, silicone oils, potassium salts, radioactive material

Source: (Bashat, 2002)

2.3 Drilling Wastes Management

Drilling waste management was one of the challenging processes facing the oil and gas industry because drilling wastes had known as the second-largest amount of waste after produced water was generated by the industry. For example, around **150 million barrels** of drilling waste had been produced from onshore wells in the United States (Onwukwe et al., 2012). This reason caused the operators to use a variety of methods to handle those wastes depending on the required regulations, and how expensive those options were as listed below.

2.3.1 Alternative Managements for DC

From the past until now, oil and gas operators had utilized many approaches to minimize as well as to reduce the toxicity of generated wastes and disposal techniques to offer environmental protection and public safety. There were three waste management hierarchies that are widely used to control and manage drilling wastes, including (1) waste minimization, (2) treatments and disposal, (3) recycle or reuse the wastes as described below (Onwukwe et al., 2012).

Waste minimization: one crucial thing that was used for minimizing waste was to reduce toxic materials in various operations. For example, drilling companies used new types of drilling fluids that consisted of non-aqueous fluids as their bases like olefins, esters, linear alpha-olefins, and paraffin. Synthetic-based muds (SBM) were one of the most desirable choices since their properties were free of poly-nuclear aromatic hydrocarbons, less toxic, and biodegradable. Besides, drilling industries could improve some drilling technology such as the "slim hole technique," which used slim hole drillings to minimize the volume of drilling fluids and cuttings generation.

Treatment and disposal: treatment was a method used to decrease the number of toxic wastes and placed them in another appropriate position before the ultimate disposal. For oil and gas industries, drilling wastes were managed in different ways, including onsite burial, land spreading or farming, thermal treatments, injection, and bioremediation processes.

Recycle or reuse the wastes: for this method, there were various ways of drilling waste recycling or reusing such as road spreading applications, filling or covering materials, restoration of wetlands with clean cuttings, and recovering for thermal treatments.

According to de Almeida, Araújo, and de Medeiros (2017), to minimize its effects on the environment, different technical scenarios of managing offshore drill cuttings waste for improved sustainability had been implemented, as mentioned in **Figure 2.3** and detailed below:

a) Offshore Discharge: drill cuttings could discharge at the operation site if they were treated at Cuttings Dryer System (CDS) in accordance with environmental regulations;

b) Onshore Disposal: drill cuttings from CDS were temporarily stored in cutting boxes (CB). After that, these drill cuttings were transported to a waste treatment facility for further treatment and finally, disposal in an industrial waste landfill;

c) Offshore Re-injection: re-injection of drill cuttings at the place was necessary since it could save much amount of water usage;

d) Microwave Treatment: drill cuttings are treated in pilot-scale by microwave equipment. The result of dry waste was transported for final disposal in the landfill.
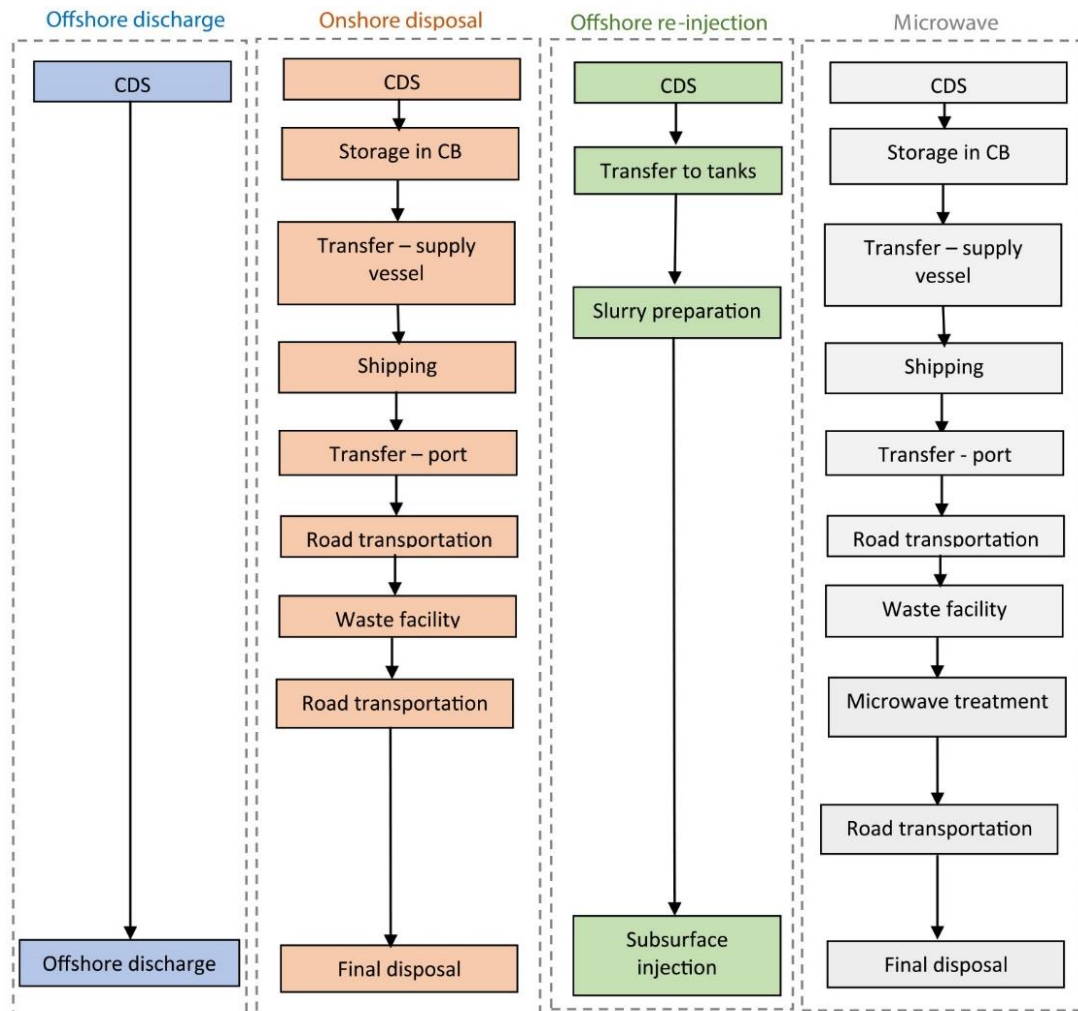
Figure 2.3 Processing stages of drill cutting management

2.3.2 Regulations for Discharge of Drilling Wastes

Water-based drilling fluids and cuttings: before discharging the cuttings adhered WBM, industries must submit evidence of muds with low toxicity to the Director of Petroleum Resources (DPR) with a permit application. Then, the discharges needed to determine how hazardous and toxic waste was. Besides, the cuttings contaminated with WBM could discharge offshore or to the deep-water without treatment.

Oil-based drilling fluid cuttings: OBM must treat to meet DPR's satisfaction with permit application by proving the low toxicity, so that it could be disposed of, recovered, reconditioned, and recycled. The percentage of oil remaining on cuttings must define as only **1%** for the disposal goal.

Synthetic based drilling fluid cuttings: SBM must recover, recondition, and recycle. However, SBM cuttings must contain **5%** drilling fluid or less than for discharging. Besides, **10%** of esters specially provides for higher retention limits for some deep-water wells.

2.3.3 Current Treatment Techniques

It was crucial to find out the new development and sustainable practice for drill cuttings management. So, many research works had been explored in drill cuttings treatment regarding environmental safety, effectiveness, and economical methods. **Table 2.2** described the different approaches and the limitations using to remove the toxic hydrocarbons.

Table 2.2 Drill cuttings treatment techniques

Treatment Methods	Limitations
1. Landfill disposal	Air pollutant emissions, leakage of leachate, and groundwater contamination
2. Stabilization/ Solidification	Potential leaching and short-term stability
3. Bioremediation	Time constraint in the process which is very slow
4. Supercritical fluid oxidation	Intensive energy process due to high temperature and pressure requirement
5. Microwave drying/ Heating	Massive heat energy using and costly operation
6. Soil washing/ Extraction	The leftover of toxic species in the treated soil and high chemical cost

Source: (Poyai, 2018)

2.4 Soil Washing Techniques

Soil washing or solvent extraction was a process that use to wash soil contaminants with water or solvents such as surfactants, weak acid solution, or mild alkaline solution. It was a process that involved high shear energy for the solid-liquid separation (Von Lau, Gan, Ng, & Poh, 2014). The primary washing mechanism was to apply aqueous-based solutions with physical processes. There are several methods that have proven to be the better options, as listed in **Table 2.2**. Amongst these methods, soil extraction has known as a practical way due to some reasons: (1) fast process, (2) low energy consumption, (3) long-term stability, (4) less installation footprint, and (5) possible reusing the washing solution (Poyai, 2018). Thus, it is vital to study the extracting agents, which plays an essential role in that process as depicted underneath:

2.4.1 Organic Solvents

In previous studies, the organic solvents were the reagents used for extracting oil-contaminated soil. There were several kinds of organic solvents, including hexane, propane, methanol, butane, dimethyl ether, and acetone. These kinds of solvents were usually used to extract hydrophobic contaminants, especially PAHs, due to their lipophilic characteristics (Von Lau et al., 2014).

Although the organic solvents above indicated the high efficiency of oil extraction from contaminated soil, they were costly and extremely flammable owing to their high volatility. Therefore, they were undesirable for use in the soil washing process. According to Yap, Gan, and Ng (2012), the author utilizes ethyl lactate/water, which was one of the organic solvents. Since it was a kind of green solvents, it was recommended to use it nowadays due to its ability for biodegradability and non-toxicity to the environment.

2.4.2 Surfactants

Regarding Urum and Pekdemir (2004), surface-active agents or surfactants were defined as the amphiphilic molecules that contained a hydrophobic tail and hydrophilic head. They were the active ingredients that could concentrate at the air-

water interface. These active ingredients were found in soaps and detergents and mostly used to separate oily emulsions in liquids. When the solubility of surfactants in non-aqueous phase liquids (NAPLs) increased, surfactants began to deduct their surface or interfacial tension in air-water and oil-water interfaces. These phenomena made monomer aggregation form as micelles. The concentration that micelles first began to form as aggregation was known as the critical micelle concentration (CMC). The surfactants were characterized by physical properties depending on the CMC, such as emulsion formation, oil solubilization, foams and detergents, interfacial, and surface tensions, as shown in **Figure 2.4**.

Accordingly, Von Lau et al. (2014) had studied the types of surfactants for PAHs extraction. Some typical **non-ionic surfactants** were reviewed and listed as follows: Tyloxapol, Brij 30, Brij 35, Tergitol NP-10, Tween 40, and Tween 80. **Anionic surfactants** contain alkylated diphenyl oxide, di-sulfonates, Alkylbenzene mono-sulfonates, Alkyl sulfates, Steol 330, Sodium dodecylbenzene sulfonate, SDS, and Dowfax 8390, which had also been considered according to their hydrophobicity. **Cationic surfactants** had studied too. They were dodecyl pyridinium bromide and alkyl-benzyl dimethylammonium chloride. However, for industrial applications, surfactants were classified based on the charge; they carried in the water at their neutral pH, namely anionic, cationic, and zwitterionic or amphoteric. Four main classes were briefly described as in the following:

a. **Anionic surfactant**: referred to surfactants that contain a negative charge and quickly adsorbed onto the positive charge hydrophilic surface. These kinds of surfactants were commonly used in industrial applications because of their low cost. Anionic surfactants could be listed as follows: soaps, sulfate surfactants, and sulfonate surfactants.

b. **Cationic surfactant**: referred to surfactants that contain positive charge and tended to adsorb onto the negative charge hydrophilic surface. These kinds of surfactants were used at site remediation due to their specific properties that strongly absorbed onto most surfaces.

c. Nonionic surfactant: referred to surfactants that contained no charge and tended to adsorb onto either hydrophilic or hydrophobic surfaces. Nonionic surfactants were mostly based on ethylene oxide or ethoxylated surfactants.

d. Zwitterionic surfactant: referred to surfactants that consisted of both positive and negative shape without changing the charge of their surfaces significantly, as shown in figure beneath (Lersjintanakarn, 2008).
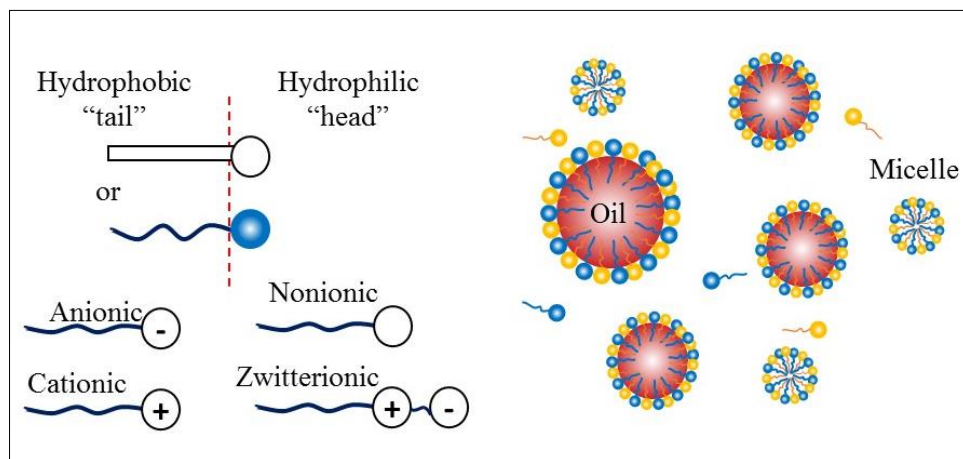
Figure 2.4 Surfactants (left) and oil destabilization by surfactants (right)

(Lersjintanakarn, 2008)

2.4.3 Biosurfactants

Biosurfactants were kinds of surfactants that produce from biologically based materials, which sometimes could be synthesized by many different microorganisms. They were grouped into six major classes based on the producing microorganism, including cross-linked fatty acids, glycolipids, polysaccharide-lipid complexes, phospholipids, lipoproteins–lipopeptides, and the entire cell surface (Urum & Pekdemir, 2004).

2.5 Design Concepts and Theories

2.5.1 Design of Experiment (DOE)

DOE was from the term Design of Experiment, which indicated to the experimental methods. In the experiment, DOE was beneficial for researchers since it helped to minimize the total amount of the experiment and varied all investigated factors

simultaneously for experimental activities. In applications, DOE aimed to facilitate researchers in experimenting, such as defining factor screening, study influent factor, study factor optimization, and model prediction, etc. The experimental design consisted of two comparison techniques like factor at a time design (OFAT) and statistically designed experiments, which will discuss below:

1)Ics One Factor at a Time Design (OFAT)

This experiment was varied only one factor at a time. In contrast, other independent factors kept constant due to some reasons: 1) it required fewer resources, less obtained information, and mostly uses in industries, where the experiments were costly and spent a long time, 2) predict the effects of each factor, and required less variability, 3) improve the prediction of the response of factor in the bigger region. For instance, an experiment (y) was affected by three factors, temperature (x_1), pressure (x_2), and reaction time (x_3). The levels of the varied factors were 2 (p=2), so the trailed experiment was 4 (N=4) by presenting in **Eq. 2.1** and **Table 2.3** below.

$$N = k (P - 1) + 1 \qquad\qquad Eq\ 2.1$$

Table 2.3 Experimental conditions of classical design with 3 factors, 2 levels

Number of experiments	y	Factor level			Other References
		x1	x2	x3	
1	y1	P1	P1	P1	
2	y2	P2	P1	P1	
3	y3	P1	P2	P1	
4	y4	P1	P1	P2	

Usually, this classical method was not preferred to apply for estimation of how much it influenced the experimental response due to all the factors are considered as independent factors.

2) Statistically Designed Experiments

There were several techniques that were frequently designed for static experiments, including Factorial design, Response surface design, Mixture Design, and Taguchi

design. Factorial design and Response surface design were favorable in this study; hence, they were illustrated as follows:

1) Factorial Design

A factorial design was the most effective method for studying the effects of two or more factors. For factorial design, two factors with different levels were combined after arranging. If the level of the factors were changed, the response would be affected, called the main effect. But in some cases, the difference in response of factor levels was not the same for all levels of other factors, and it was called interaction of the factors. The regression model represents two factorial experiments that were shown in the **Eq. 2.2**, while y was the response, β was the determined parameter, x was the variable of factor, and ϵ was the random error.

$$y = \beta_0 + \beta_1 x_1 + \beta_2 x_2 + \beta_{12} x_{12} + \in \qquad Eq\ 2.2$$

This factorial design was more advantageous than OFAT because it was easy to illustrate and avoid misleading conclusions. There were four different methods of factorial design, including Two-factor factorial design, Two-level (2^k) Factorial Design, Single Replicate of 2^k Factorial Design, and One-half Fraction of 2^k Factorial.

2) Response Surface Design

Response surface design or response surface methodology (RSM) was one kind of statistical techniques, which were influenced by several variables and tried to optimize the response. It was an essence for modeling analysis. For example, to obtain the maximum yield (y), the level of temperature (x_1) and pressure (x_2) were determined in the process. The yield (y) was written in the function of factors' level of temperature and pressure by **Eq. 2.3,** where ϵ was an error in response (y). If E(y) was the expected response and η was the response surface; then, the surface represented by **Eq. 2.4**.

$$y = f\left(x_1, x_2\right) + \in \qquad Eq\ 2.3$$
$$\eta = f\left(x_1, x_2\right) \qquad Eq\ 2.4$$

Since we did not know the relationship between the variations and the response in RSM, the low-order polynomial was firstly determined. If it was well in linear

function, the first-order model was constructed as in **Eq. 2.5**. The response surface showed graphically, as in **Figure 2.5,** with the contours plot for better visualization.
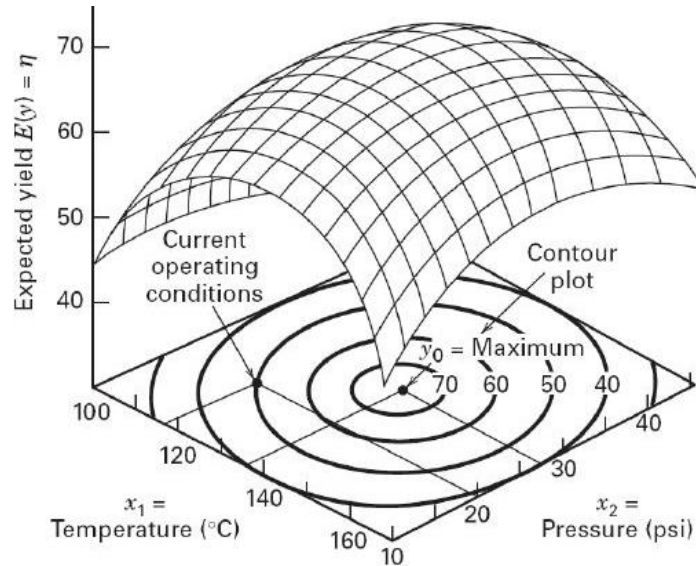
Figure 2.5 The response surface with the contour plot

The second-order model was also employed in **Eq. 2.6** if it was in curvature and a higher degree of the polynomial. The fitted surface was an analysis method for RSM, called response surface designs, which was designed for the determination of the optimum operations conditions and satisfaction region.

$$y = \beta_0 + \beta_1 x_1 + \beta_2 x_2 + ... + \beta_k x_k + \in \qquad Eq\ 2.5$$

$$y = \beta_0 + \sum_{i=1}^{k} \beta_i x_i + \sum_{i=1}^{k} \beta_{ii} x_{ii}^2 + \sum_{i<1} \beta_{ij} x_i x_j + \in \qquad Eq\ 2.6$$

❖ **Central Composite Design (CCD)**

CCD or Second-order rotatable design or Box-Wilson design was generally used for fitting the second-order model as well as for response surface design. The comparison between simplex design and central composite design was illustrated, as shown in **Figure 2.6** with k = 3 factors.
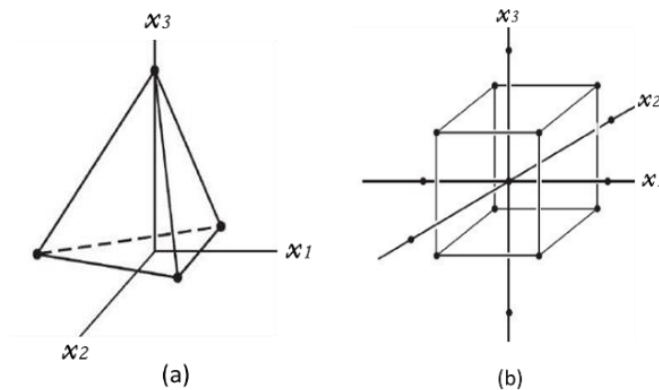
Figure 2.6 (a) Simplex design and (b) Central composite design for k = 3

2.5.2 Bubble Hydrodynamic

Bubble hydrodynamic was important to study in the flotation process because some parameters represent the performance of bubbles and particles inside the process. The studied parameters contained the rising velocity of the bubble, the diameter of the bubble, the formation frequency, the spreading coefficient, and the interfacial area, which were discussed for understanding the performance of the bubble that was generated in the flotation.

3) Stoke Law and Bubble Rising Velocity

In the flotation system, stoke law was applicable for particles (bubbles, droplets, or bubble-droplet aggregation), which mostly had a spherical shape. Moreover, the smaller diameter of bubbles (the larger surface area) caused the velocity to rise more slowly than the bigger gas bubbles in the same liquid. Hence, the slower rising rate contributed to a higher collision rate with oil droplets, which made the flotation efficiency to increase as described in **Eq. 2.7** (Wang et al., 2010). However, the rising rate calculated from stoke law was different according to real conditions due to some reasons such as (i) particles may exist in many various shape, (ii) particles may exist in different size (diameter) due to their coalescence, (iii) the presence of turbulent flow regime is difficult to maintain compared to laminar flow (Saththasivam, Loganathan, & Sarp, 2016).

$$V_T = \frac{g(d_W - d_B)D^2}{18v} \qquad\qquad Eq\ 2.7$$

Where D was the diameter of a spherical bubble (m); V_T was the terminal velocity of a spherical bubble (m/s); d_W was the density of water (kg/m^3); d_B was the density of gas bubble (kg/m^3); v was the water viscosity (Pa-s), and g was the gravitational acceleration (g = 9.81 m/s^2).

As mentioned earlier, particle size (bubbles and oil droplets) played a vital role in the flotation process. Small bubbles were useful for droplet aggregation due to their large surface areas. In contrast, large bubbles tended to rise rapidly, which resulted in lower collision efficiency. Also, oil droplets, which were bigger than 20µm, were suitable for flotation purposes. Those that were smaller than 10µm were not rise based on Brownian motion. Thus, it emphasized that using the smallest possible bubbles led to optimum flotation efficiency (Saththasivam et al., 2016).

4) **Spreading Coefficient**

Since bubble-droplet attachment was preliminary controlled by the interface tension between the water, oil, and gas bubbles, the different interface tension between water-gas (γ_{wg}), oil-water (γ_{ow}), and oil-gas (γ_{og}) was shown to calculate the spreading coefficient, S_0. This coefficient indicated the strength of the bubble-droplet attachment and entailed with the equation below (Saththasivam et al., 2016).

$$S_0 = \gamma_{wg} - (\gamma_{ow} + \gamma_{og}) \qquad\qquad Eq\ 2.8$$
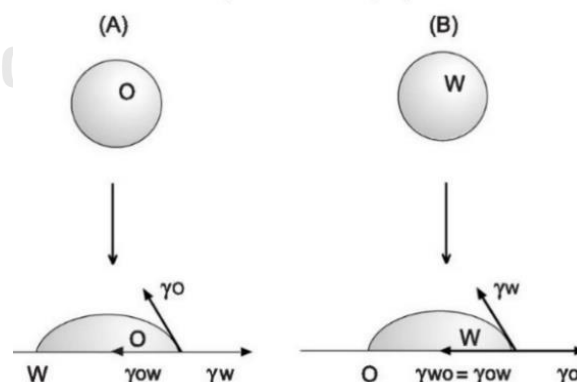
Figure 2.7 (A) Oil Spreads on the water phase, (B) Water spreads on the oil phase

5) **Interfacial area**

The interfacial area was the function of the bubble formation frequency, the terminal bubble rising velocity, and the generated bubble diameter. It expressed as followed:

$$a = N_B \times \frac{S_B}{V_{Total}} = f_B \times \frac{H_L}{U_B} \times \frac{S_B}{V_{Total}} \qquad\qquad Eq\ 2.9$$

Where N_B was the number of bubbles, S_B was the surface area of the air bubble (m^2), V_{total} was the total volume of water and air in the reactor (m^3), H_L was the depth of water above the aeration point (m), and U_B was floating velocity (m/s) (Painmanakul, Sastaravet, Lersjintanakarn, Khaodhiar, & Design, 2010).

2.5.3 Conventional Treatment Methods for Oily Wastewater

Currently, a dramatic increase in petroleum refinery caused a large volume of oily wastewater; then, discharged to the environment without treatment properly. Hence, many challenging treatment techniques have become an urgent problem and must explore to resolve every oilfield and petroleum industry. From research, there were different ways of treatment methods which applied following the different kinds of oily wastewater, consist of adsorption, coagulation/flocculation, flotation, coagulation, and flotation, etc. (Ahmad, Sumathi, & Hameed, 2006; Yu, Han, & He, 2017). So these methods were briefly described in the following parts.

6) **Floatation Process**

The flotation process was a physical separation process that used bubbles to separate particles that had a density lower than water, such as oil and grease, algae, plastic, etc. In this operational unit, the bubbles were introduced into the system for making as bubbles attachment with the particles, which form as agglomeration. After that, agglomeration was rising to the water surface due to the different density between particles and bubbles, so that particles could separate by using a skimmer.

Table 2.4 Advantages and its applications of the flotation process

Advantages	Applications
1). High efficiency	Mineral ore recovery
2). Rapid separation	Pre-treatment process
3). Small footprint (conventional process)	Resources separation and recovery
4). Tailor-made design and operation	Water supply production
5). Potential for materials recovery	Wastewater treatment
6). Compatible with other processes	Sludge thickening

In the flotation process, four steps have been raised in studying, such as (1) bubbles generation, (2) bubbles-particles contact, (3) separation, and (4) sludge/foam removal (Hendricks, 2006). Step (2) bubbles-particles contact was the most important one because it showed how much efficiency which bubbles could attach to the particles. **Figure 2.8** showed about how bubbles were working in bubbles-particle contact.
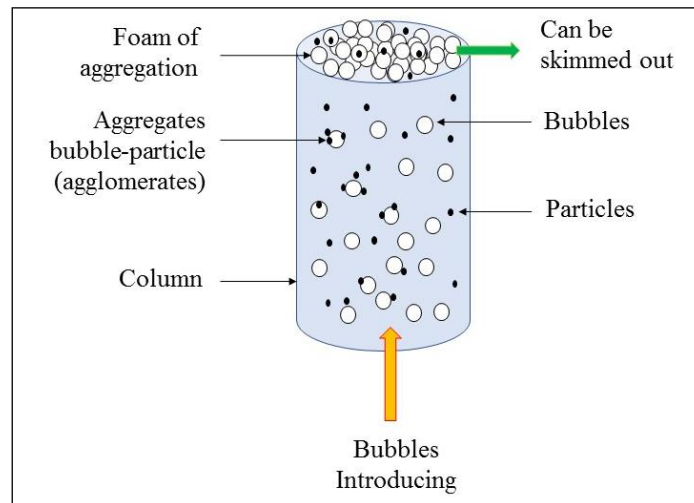
Figure 2.8 Bubbles-particles contact

1) **Mechanisms of Flotation Process**

Chawaloesphonsiya (2014) revised the mechanisms of the flotation process. Particle captured in flotation was theoretically discussed by three sub-efficiencies, including (1) collision efficiency, (2) attachment efficiency, and (3) stability efficiency, which could be defined as captured efficiency (E_{capt}) as described in **Eq. 2.10**.

$$E_{capt} = E_{collision}.E_{attachment}.E_{stability} \qquad\qquad Eq\ 2.10$$

Bubbles attached the particles and form as flocs called bubbles-floc attachment, which consist of four mechanisms, as shown in **Figure 2.9** below.
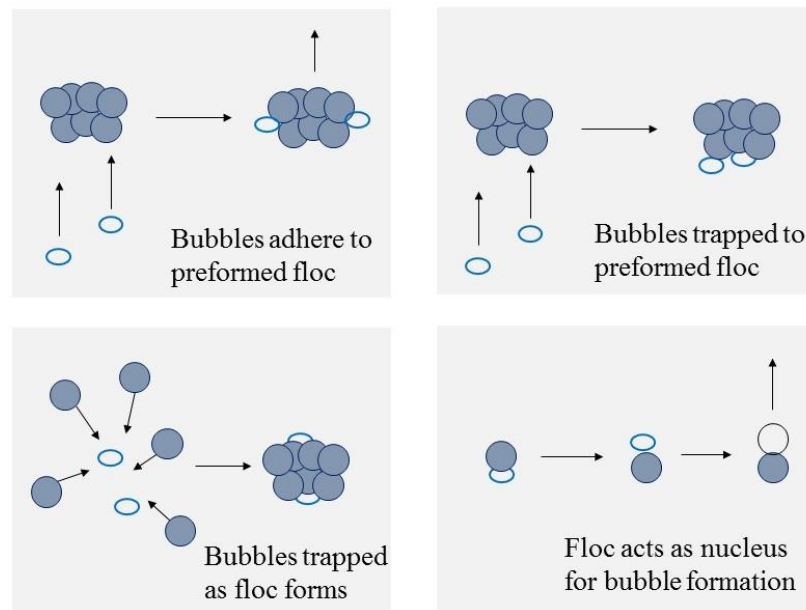
Figure 2.9 Mechanisms of bubbles formation and adhesion

In order to enhance the treatment process, the flotation process played an essential role in removing especially oil, suspended solids, small particles, and other particles in different phases; for instance, oil emulsion in water. The flotation process was divided into three main types based on bubbles generation methods such as induced air flotation (IAF), dissolved air flotation (DAF), and Electrolytic flotation (EF).

2) Dispersed Air Flotation or Induced Air Flotation (IAF)

IAF was a process that bubbles are generated by diffusers, spargers, and other mechanical methods. This process was suitable for the bubbles with a size range from 700 to 1500 µm in diameter (Rubio, Souza, & Smith, 2002). Here were some advantages and disadvantages of IAF to be considered, as shown in **Table 2.5**.

Table 2.5 Advantages and disadvantages of IAF

Advantages	Disadvantages
Simple and fast process	Usually needed frothing
Suitable for large size of particles separation, such as mineral processing, oil-water separation, and industrial wastewater	Chemicals are needed to add to flocculate the oil and SS in wastewater treatment
Low maintenance	Inefficient for water treatment

Figure 2.10 Bubbles creation by diffusers in millimeter range
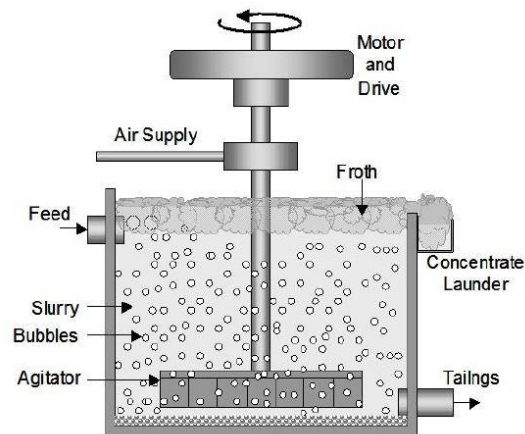
Figure 2.11 Dispersed air flotation with an agitator (Bui, 2017)

3) **Dissolved Air Flotation (DAF)**

DAF was a process that bubbles are generated by the reduction in two different pressure (30 and 65 psi) of the supersaturated water in the air. Bubbles were formed by the precipitation of the air within the range of 30 to 100 micrometers (*μm*) in diameter. In the DAF process, the liquid flowed through a pressure reduction valve into the flotation cell when the pressure was reduced; then, small bubbles were formed from the supersaturated solution (Rubio et al., 2002; Wang et al., 2010). Figure 2.12 below represented the typical operation of the DAF unit. The water inlet and air compressor were introduced into the air contact tank, then the pressurized air (tiny bubbles) were generated and flowed into the treatment system.
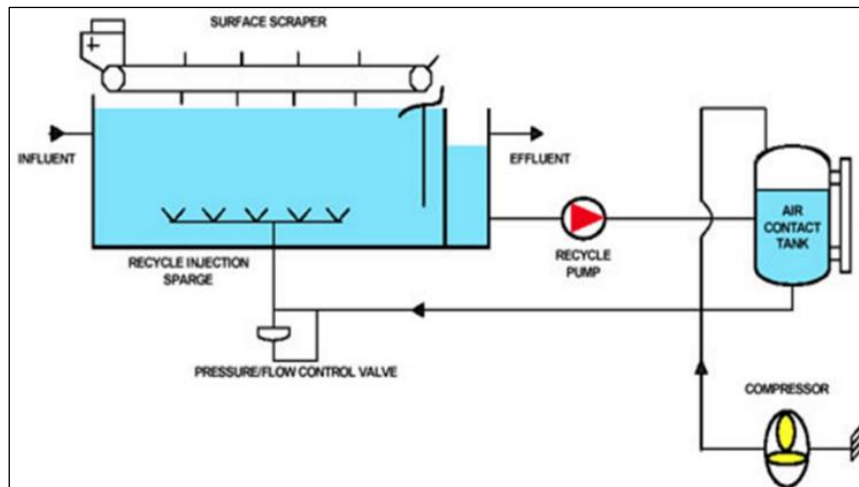
Figure 2.12 Typical dissolved air flotation system

> **Tank Shape Design**

In the air flotation system, tank design was favorable in two main figures, such as the rectangular shape and the circular shape. Due to the studies, the circular tank was the most interesting choice for designing; however, these two kinds were described different advantages that gave ideas to the next researchers for considering (Wang et al., 2010). The **circular shape tank** was financial in terms of construction and beneficial for maintenance. However, the rectangular shape tank was easy for the construction and easy to follow the standard size as well as to scale up from the lab scale.

4) **Coagulation/ Flocculation Process**

Coagulation referred to the addition of coagulants or chemical coagulants to create conditions for the suspended, colloidal, and dissolved matter for subsequent processing such as flocculation, which was allowed for the subsequent removal of particulate and dissolved matter. **Flocculation** referred to the destabilization of the particle aggregations that their electrical surface charge had been reduced. They were formed by the addition of coagulants into larger particles known as flocculant particles or ''floc''. Then, the aggregated floc was removed by gravity sedimentation or filtration. The differences between coagulation and flocculation were depended on the time required of their processes. Typically, coagulation occurred in less than 10

seconds, while flocculation occurred for 20 to 45 minutes (Crittenden, Trussell, Hand, Howe, & Tchobanoglous, 2012).

1) Coagulation Process

In the coagulation process, the common coagulant usage contained alum, ferric chloride, and ferric sulfate hydrolyze, which used in rapidly mixing with the water that was treated to

- Destabilize small suspended and colloidal particulate matter;
- Adsorb or react the colloidal and dissolved NOM to particles;
- Create flocculant particles that can sweep through the water to be treated, enmeshing small suspended, colloidal, and dissolved material so that they can settle down and remove (Crittenden et al., 2012).

Coagulation destabilized particles by adsorbing to particles' surface, neutralizing their charge (reducing the repulsive forces), and forming bridges between them. There was the number of different mechanisms involved in a coagulation process, including (1) ionic layer compression, (2) adsorption and charge neutralization, (3) inter-particle bridging, and (4) sweep coagulation. These mechanisms were essential in forming flocs of residue oil and suspended solid, which could be quickly settled and finally removed.

2) Flocculation Process

Flocculation was a process that produces aggregations that could be removed by subsequent particle separation procedures such as gravity sedimentation and filtration. Two general types of flocculation were identified: (1) micro-flocculation (known as perikinetic flocculation) in which particle aggregation was randomly brought by the thermal motion of fluid molecules, frequently called Brownian motion, and (2) macro-flocculation (known as orthokinetic flocculation) in which particle aggregation was brought by inducing velocity gradients and mixing in the fluid. Macro-flocculation was delivered in different forms by differential settling, in which large particles overtook the small particles to form the larger ones. The particles in water could be classified as suspended, colloidal, and dissolved constituents. Due to the small size of these constituents, they did not settle down in a reasonable time; thus,

chemicals must be used to assist their removal (Crittenden et al., 2012). **Figure 2.13** below showed the different sizes of various particles.
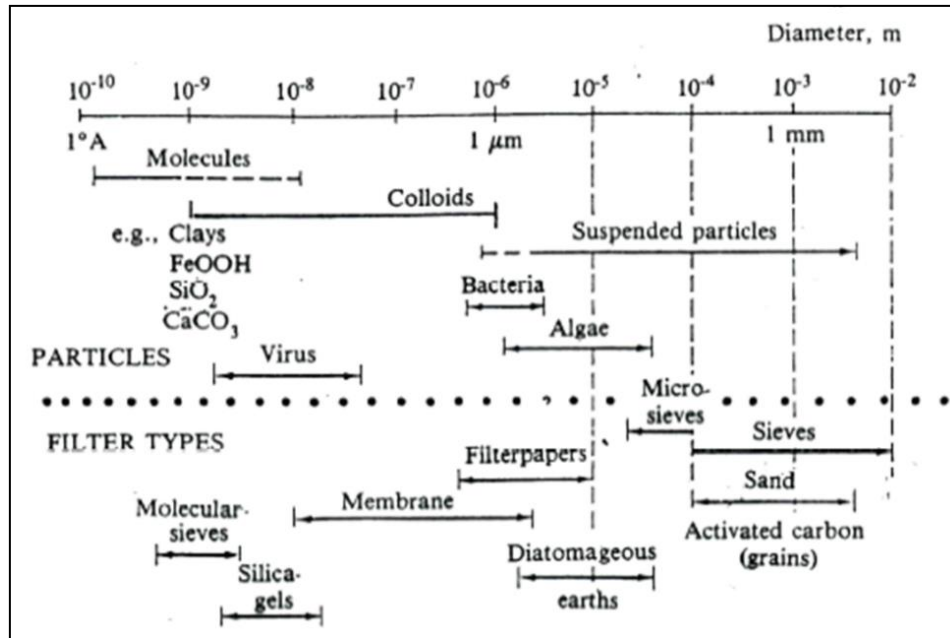
Figure 2.13 Diameter of various colloidal particles

5) Jar Test Experiment

Jar-test was a common conventional method that uses for the physic-chemical treatment of water and wastewater. The jar test simulates for coagulation/flocculation process in a series of batch mode which tested and varied for finding the optimum of pH, coagulant type, and coagulant dosage, using in the treatment process. In general, coagulation and flocculation are performed in standard jar-test apparatus, using a jar tester comprises six paddle motors, which were equipped with six beakers of 1-liter volume. To be tested, the ranges of coagulant dosage were prepared and specified by using a magnetic stirrer before adding into sample volume. One of the six beakers of samples was needed to be blank. Afterward, the pH value of the sample was adjusted to pH 7 by using 1.0 M H_2SO_4 or 1.0 M NaOH. Then, after adding the selected coagulant or possibly coagulant aid into sample beakers, "flashed mixed or rapid mixing" was performed immediately around 4 minutes and using a speed about 150 rpm. Subsequently, the stirrer speed was needed to be reduced into "slow mixing" in order to simulate a flocculation basin. The flocculation mode was performed by

slowdown the mixing after rapid mixing for approximately 20 minutes at 20 rpm. Eventually, the stirrers were turned off and allowed the liquid to settle down for 30 min. After the sedimentation period, the supernatant was withdrawn form a point located about 2 cm below the top of the liquid level of the beaker. It was to determine the turbidity or suspended solids, COD, oil and grease (O&G) by using standard methods, so that the effect of coagulant dosage in treatment could be studied (Daud et al., 2015).

Figure 2.14 Jar test apparatus with 6 beakers

(source: https://www.indiamart.com/proddetail/jar-test-apparatus-9398163130.html)

2.5.4 Oily Wastewater Treatments

1. Emulsion

The emulsion referred to colloidal systems containing a liquid, which normally ranged from 2 up to a homogeneous mixture such as oil and water mix homogeneously without separation. The emulsion was divided into two main types (1) the oil-in-water emulsion (O-W emulsion), which has oil as an internal phase, and (2) the water-in-oil emulsion (W-O emulsion), which had water as an internal phase such as mayonnaise salad, sausage (*foodnetworksolution.com/wiki/word/0674/emulsion-อิมัลชัน, 2019*). **Figure 2.16** illustrated about the summary of the classification of oily wastewater and the oil and water emulsion classification.
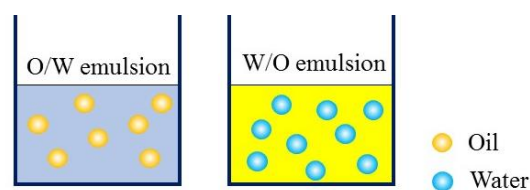
Figure 2.15 The differences between oil and water emulsion
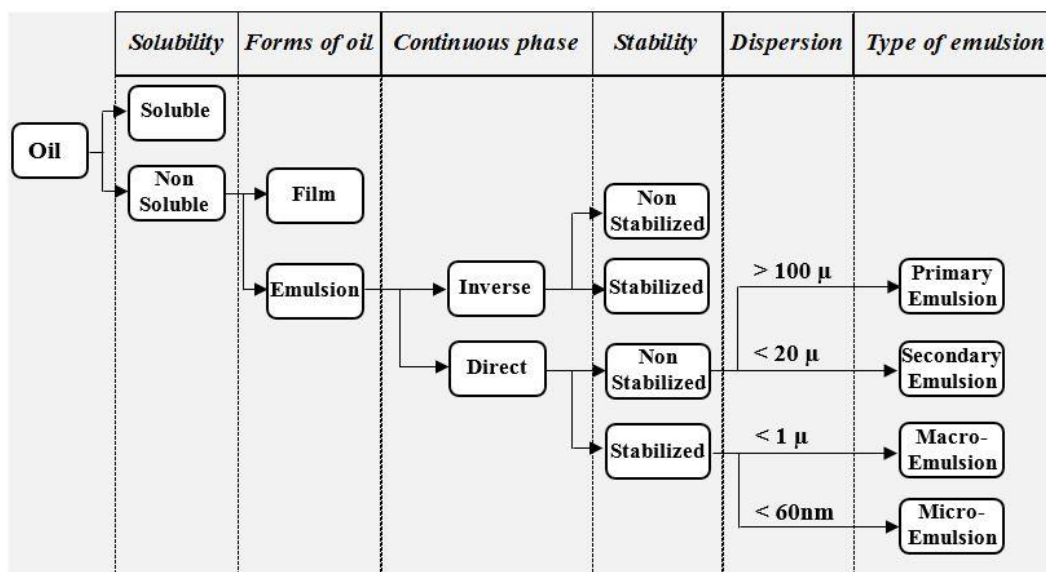
Figure 2.16 Summary of oily wastewater classification (Chawaloesphonsiya, 2014)

2. Stable Emulsion Properties

Mechanisms of emulsification were involved with two processes called stable emulsion and unstable emulsion. Oily wastewater, which contained stable emulsion was very difficult for treatment; thus, the stable emulsion needed to destabilize. Normally, the interfacial tension of oil was positive. When surfactants were added, it was lower, so the stability of oil droplets increased, and the surface area of oil droplets was then increased. Thus, the droplets' diameter was decreased. The dynamic stability of the oil was listed into two mechanisms, as exhibited below.

2.1. The electrical barrier: in this case, some mechanisms were explained based on the charge of particles. Oil droplets generally had a negative charge due to the adsorption of negative ions, which attracted a positive charge to attach the surrounding of droplets. Two layers were occurring during the attachment, namely, (1) stern layer that was in the inner layer of bubbles, and (2) diffused layer: the counter ions stayed surrounding the stern layer, as shown in **Fig. 2.17**.

2.2. Mechanical barrier: or the dynamic barrier, that caused by a film of surfactants on the surface of droplets, prevented the coalescence of droplets. The mechanical barrier made some emulsions became very stable. Hence, to obtain the stability of cutting-oil emulsion in some products, multi-surfactants were added to create a dynamic barrier.
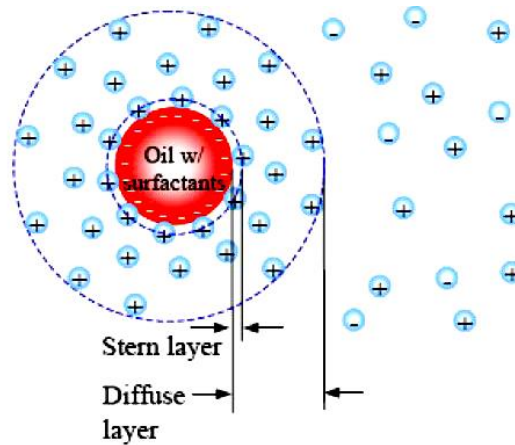
Figure 2.17 Diagram of the electrical double layer

2.5.5 How to Destabilize the Stable Emulsion

To destabilize the emulsion is to eliminate or minimize the stabilized properties of the emulsion by various methods. They were (1) the increase of interfacial tension to get rid of thermodynamic stability, (2) the removal of surfactant films around the droplets, and (3) reducing the charge of the droplets to remove the electrical barriers.
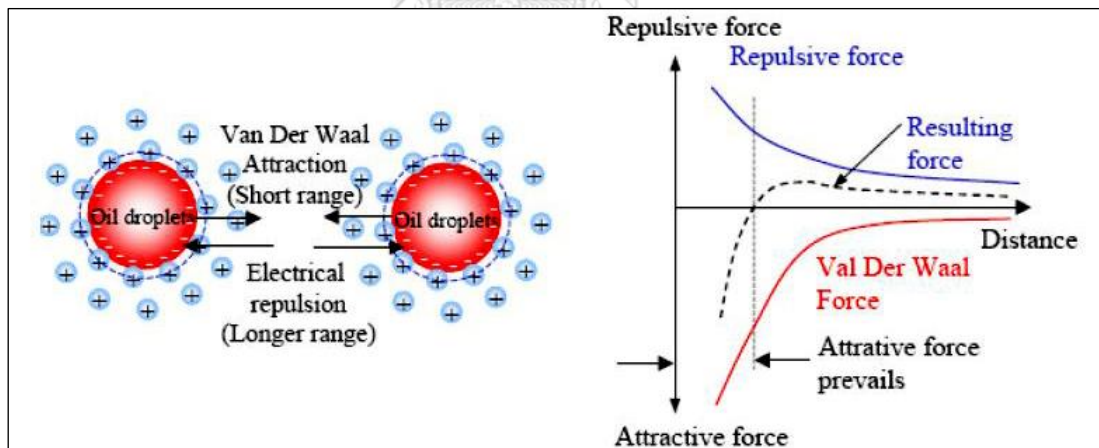
Figure 2.18 The effect of the repulsive, and attractive force of oil droplets

1. Mechanisms for Destabilization of Oily Emulsion

Concerning Chawaloesphonsiya (2014), the mechanisms for the destabilization of the oily emulsion applied as follows:

a) Diffuse layer thickness reduction: usually, oil droplets were negative charges. The counterions (opposite charge or positive charge) were attached to the surrounding

droplet's surface. The ions reduced the diffused layer of the droplet; therefore, the droplets moved closely and possibly agglomerate.

b) Sweep coagulation: some metal salt, which formed with the other ion in water, such as hydroxide ion (OH^-), could catch the oil droplets. Thus, they were separated from the stable mixture.

c) Adsorption and charge neutralization: adding surfactants was one of the methods that use for adsorbing and neutralizing the charge of droplets since some surfactants had a different charge from them.

d) Bridging: oil was trapped by some chemicals that had bridging properties so that oil was absorbed on the surface of chemicals.

e) Precipitation of surfactants: after adding the surfactants, the valence of salts usage was to precipitate with them. It was noted that the higher valence of salts would precipitate with surfactants better than the smaller ones with the minimum dosage. A jar test was used to vary and find the better one.

2. Chemicals for Destabilization

Chemicals or coagulants were the common methods used for destabilizing the stable oily emulsion. There were some coagulants, which are frequent usage as follows:

a) Monovalent electrolytes
b) Bivalent electrolytes
c) Multivalent electrolytes
d) Surfactants with opposite charge

2.6 Previous Research Study Reviews

2.6.1 The Different Treatment Technologies for Soil Contaminants

Sun et al. (2019) investigated the sand contaminated by oil spills by using microbubbles (Mbs) that were generated in a column reactor with tap and saline water. The study was analyzed some affected parameters such as **Mbs size, Mbs flowrate, washing time,** and the comparison between tap and saline water in the treatment process. The result was found that the self-collapsing Mbs-based method had been explored as a chemical-free approach in this remediation. Moreover, Mbs with a size of less than 50 µm was applied in this work because smaller bubbles

contained huge interfacial area and lowered rising speed in the liquid phase. So, Mbs could attach with particles and remove them out effectively. After experiments, the flow rate of 150 ml/min and washing time of 40 min were found to be the better conditions in getting rid of the oil spill from the sands. Finally, it was shown that more than 90% of oil removal was achieved within tap water rather than saline water due to some reasons. Mbs usually had negative charges with a zeta potential of -35 mV, which could be reduced by sodium chloride of saline water. So, reducing the zeta potential of MBs caused electrostatic repulsion decreased, which made the removal efficiency was lower than tap water. The removal mechanism was shown beneath.
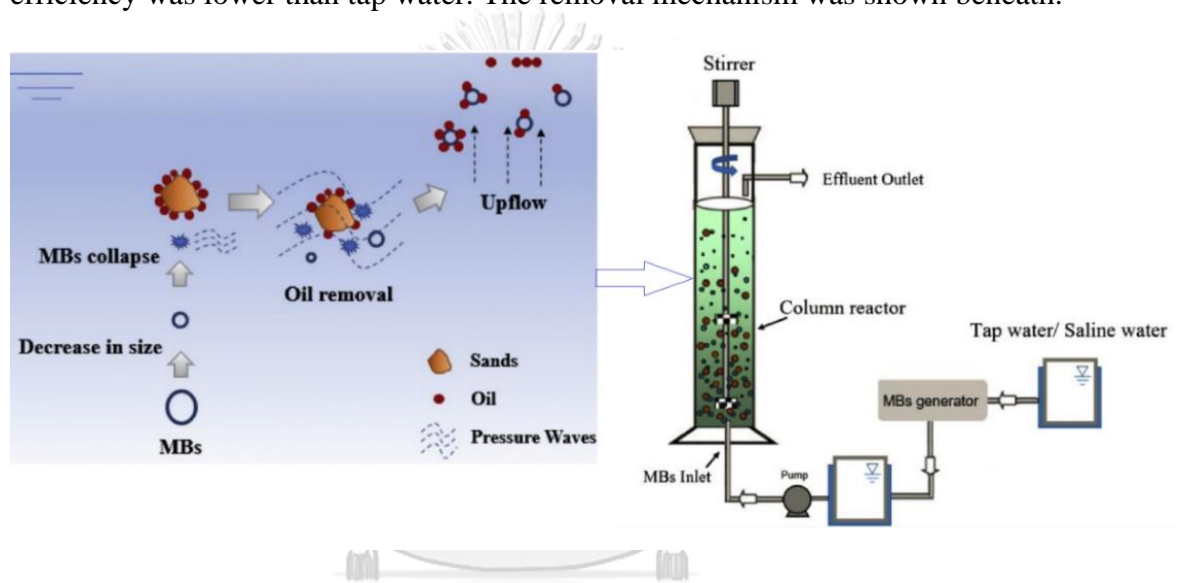
Figure 2.19 Treatment by chemical-free self-collapsing microbubbles

Regarding Ahmadkalaei, Gan, Ng, Talib, and Research (2016), the investigation about the green solvent (ethyl lactate, EL) for desorption of total petroleum hydrocarbons (TPH) from contaminated soil was determined. Artificially contaminated soil was carried out in batch desorption experiments at different EL solvent percentages. The effected EL percentage, TPH, and liquid to solid ratio (L/S (v/w)) on initial desorption were evaluated to observe the potential desorption performance of EL. As a result, EL had been demonstrated that it was fast in desorbing and had high efficiency. The result was represented by the Pseudo-second order rate, in which R^2 is between 0.9219 and 0.9999.

Urum, Pekdemir, Ross, and Grigson (2005) worked on the investigation of the removal of crude oil from contaminated soil by using a washing technique with air

sparging assisted stirred tank reactors. In experiment procedures, two surfactants were used, including rhamnolipid and sodium dodecyl sulfate (SDS) with different studied parameters such as temperature, surfactant concentrations, washing time, and volume/mass ratio. There were three washing modes, which were used to investigate in this study, namely, **stirring only**, **air sparging only,** and **the combination of stirring and air sparging,** as shown in **Figure 2.20**. This work was studied, two prepared rinse solutions consisted of the seawater prepared solutions and distilled water. The result showed that greater than 80% of crude oil was removed from the non-weathered soils by using SDS, while rhamnolipid showed similar oil removal at the third and fourth levels of the tested parameters. The authors suggested that only dependent on the physicochemical characteristics of the washing media was not effective; thus, adding air sparging into the reactor was a better choice to enhance crude oil removal. Moreover, the oil removal was more significant with seawater prepared solutions rather than distilled water prepared solutions at the first and second parameter levels tested. Therefore, the approach of soil washing was noted to be effective when it assessed are sparging and surfactants.
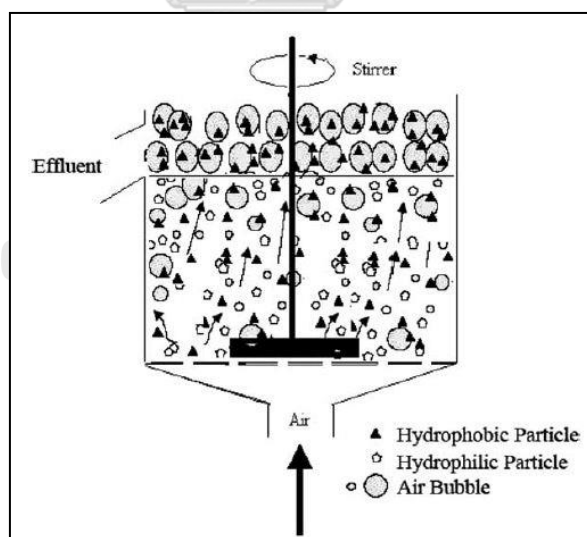
Figure 2.20 Schematic illustration of air sparging assisted stirred tank reactor

Zhang et al. (2001) applied a flotation method using a conventional mechanically agitated machine (Denver cell) and a flotation column to remove hydrophobic compounds from soils. Owing to most organic contaminants were hydrophobic, it was possible to separate these organic materials from the soils by using the flotation

technique, which known as an inexpensive but effective technology. According to the characteristics of soil contaminants in this study, flotation was selected. There were some effected parameters required to investigate, such as reagent type, conditioning time, flotation time, surfactant dosage, pulp pH, pulp temperature, and solid to liquid ratio. The soil sample was artificially contaminated by mixing with solvent, which refined paraffin oil dissolved in hexane and the hexane then removed by evaporation. It was found that 74% of the contaminant removal was reached from soil particles range from 75 to 830 µm in conventional flotation, whereas up to 80% of oil could be removed from 250 to 830 µm of soil fraction in column flotation. However, the soil in the range of 75-830 µm was shown 65% of oil removal. Therefore, the author had been considered flotation as the potential and desirable method for cleaning up contaminated soils.

With regard to Torres et al. (2007), the characterization and treatability of soil contaminants from the oil exploration zone were studied. There were three main purposes in this study including (1) characterizing a soil highly contaminated with crude oil, TPH, and metals level at different fractions, (2) evaluating the surfactants for soil washing by modifying single and mixture surfactants, and (3) evaluating the surfactants for different soil particle sizes washing. The samples were taken from the real exploration zone in Tabasco, Mexico, and characterized by determining the particle size, TPH range, and 6 containing metals (Cd, Cu, Cr, Ni, V, and Zn). In initial characterization, soil samples were taken from an oil exploration site and kept at 4 ℃ before analyzing. Afterward, the soil was taken to dry at environmental temperature and mill in order to sieve in different meshes such as mesh 10 (1,700 μm) until mesh 100 (150 μm). **For soils that were bigger than mesh 10, they were separated due to big hydrocarbon agglomerates covered by thin layers of sand. These particles were kept apart since they were plastic and not be able to break in this kind of mill.** The treatability test was employed in order to remove TPH from contaminated soil by using surfactants. As a result, the applied treatments were capable of getting rid of TPH only 9.1 to 20.5 %; however, using sodium dodecyl sulfate (SDS) 1% solution could remove TPH 35.4% while the combination between sodium dodecyl sulfate and salts gave the removal efficiency up to 49.5%.

Yan et al. (2011) had investigated about remediation of oil-based drill cuttings through a biosurfactant-based washing followed by a biodegradation treatment. The oil removal from drill cuttings was tested by the washing process, which used a Rhamnolipid as a washing solution and sawdust as a bulking agent. The experiments were carried out to determine the effected parameters such as (1) biosurfactant concentration, (2) L/S ratio; (3) washing time; (4) stirring speed; and (5) temperature. **The pH of the biosurfactant-ODC mixture was neglected because it varied between 7.3 to 7.5 in each tested concentration.** For liquid to solid ratio (L/S), the experiment was tested by varying ODC samples 20g to vary with the volume of 20, 40, 60, 80, and 100 mL, respectively, while the concentration of the rhamnolipid solution was 10, 30, 60, 120, 240, 360, 480 and 600 mg/L was added into a 250 mL flask. The biosurfactants were prepared by shaking the flask with different speeds 100, 150, 200, 250, 300, and 350 rpm respectively, over a period 5 to 50 min with the allowable settlement time 2 hours. After biosurfactant washing pretreatment, the biological treatment was performed later by using sawdust in individual stainless-steel boxes (30 cm length, 20 cm width, and 10 cm height). As a result, it was observed that oil removal from oil-based drill cuttings was achieved at 83% with the biosurfactant washing. However, the second step of bioremediation was reduced concentrations of saturated and aromatic hydrocarbons and decreased to 2140 and 1290 mg/kg after 120 days, respectively. This study was mentioned that these two-stage remedial systems could reduce treatment time and increase treatment efficiency as compared with single bioremediation or washing treatment.

Corresponding to soil washing process, Urum and Pekdemir (2004) had been studying about the selection of biosurfactants, which were the most suitable in crude oil contaminated soil treatment. Five biosurfactants were used to analyze for the better efficiency in washing: Aescin, L-a-Phosphatidylcholine (L-a-Lecithin), Rhamnolipid (microbial), Saponin, and Tannin compared with a well-known chemical surfactant Sodium dodecyl sulphate (SDS). The results showed the ability of surfactants to reduce air-water surface tension, which indicated the reduction of the interfacial force of oil and soil (the interfacial tension between crude oil and distilled water was measured as $25 mNm^{-1}$). Critical micelle concentration (CMC) was the aqueous

concentration of surfactants, in which the surface tension of the solutions first showed the smallest tensional force. The reduction of interfacial tension indicated the ability of surfactants to remove oil from the soil. Since the CMC value of rhamnolipid and tannin were the lowest and the interfacial tension reduced to the lower value too, $4.5mNm^{-1}$. It was indicated that rhamnolipid and tannin were able to remove oil from the soil rather than the other surfactants. As a result, Rhamnolipid and SDS removed up to 80% oil, followed by 42% of Lecithin. The evaluation of biosurfactant solutions for possible applications in removing crude oil from soil was studied by measuring surface and interfacial tension, foaming and emulsification ability, sorption to the soil, and solubilization. Meanwhile, biosurfactants with low CMC values and a high degree of sorption to soil may have stronger abilities to eliminate oil, whereas the low solubilization and low interfacial tension of crude oil caused the effects of emulsification and solubilization to become negligible in oil removal effectiveness.

Poyai (2018) had studied the development of a treatment process for petroleum drill cuttings via the soil washing technique. The author used impellers in creating a mixing condition between soil samples and washing reagent (Ethyl Lactate), so the effects of impeller types were very important to the study. Three types of axial flow impellers were compared, including pitched 4-blades turbine (PBT−4), hydrofoil, and propeller impeller, which were typically applied for horizontal mixing, blending, and solid suspension in water or wastewater treatment. However, in order to achieve better results, the characteristics and further experiments were carried out, as shown in **Figure 2.21**, **Figure 2.22**, and **Table 2.6**. The mixing performance of different impellers was visually observed through the transparent vessel, which fitted with the designed impellers of a thickness W = D/5 and diameter D = T/3 for creating the turbulent flow where T is the vessel's diameter. Eventually, the results showed that the propeller impeller gave the worst mixing performance as it had no suspension of oil droplets and drill cuttings particles inside the vessel. On the other hand, hydrofoil and PBT-4 had similar mixing potential, which revealed the better conditions for drill cuttings washing, whereas the PBT-4 impeller was concerned about higher energy input than hydrofoil. Thus, the **hydrofoil impeller** was selected for further

investigation due to its acceptable properties in terms of mixing potential and low energy consumption.

Table 2.6 Properties of the impellers

Impeller Type	Share	Power Number (N_P)	Pumping Number (N_Q)
PBT-4	Moderate	0.9-1.6	0.7-0.9
Hydrofoil	Low	0.3-0.9	0.6-0.7
Propeller	Very low	0.3-0.6	0.5-0.7
Source: Metcalf and Eddy (2004)			
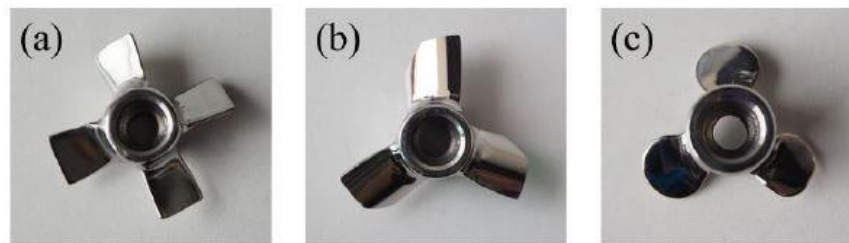
Figure 2.21 (a) PBT−4, (b) Hydrofoil, and (c) Propeller
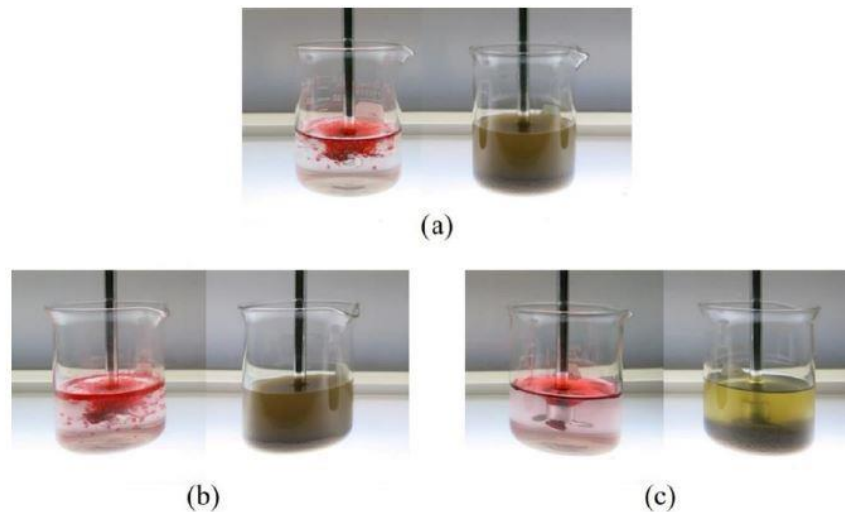
Figure 2.22 Performance of (a) Hydrofoil, (b) PBT−4, and (c) Propeller on the suspension of oil layer (left) and drill cuttings particles (right)

Similarly, Ayranci, Kresta, Derksen, and Technology (2013) had mentioned the experiments and simulations of solids suspension in the mixing tank. In batch processes, to generate the flow in a tank under turbulent conditions and assist in the entrainment of solids suspension in the liquid, impellers are crucial involving. So that

the author had studied the role of baffles and the effects of impeller types on the suspension process including, the Lightnin A310 and Pitched-blade turbine (PBT) impeller, which played a vital role in the mixing process. A cylindrical tank was designed with the inner diameter of T=24 cm, height H =T, and the baffle's width was W = T/10 (**Figure 2.23**). The tank was filled with water and solids by using a test with these two different types of impellers. A Lightnin A310 was the impeller that has diameter D= T/3 and a four-blade, 45°-pitched-blade turbine (PBT), which also had diameter D= T/3. The off-bottom clearance C had been set to two values: C = 0.25T, and 0.20T, as summarized in **Table 2.7**.

Table 2.7 Liquid flow characteristics

Cases (#)	Impeller Type	Clearness C/T	N [rev/s]	v_{tip} [m/s]	Rey.
1	A310	0.25	15	3.77	9.6×10^4
2	A310	0.2	15	3.77	9.6×10^4
3	PBT	0.25	15	3.77	9.6×10^4
4	PBT	0.25	10.8	2.71	7.0×10^4
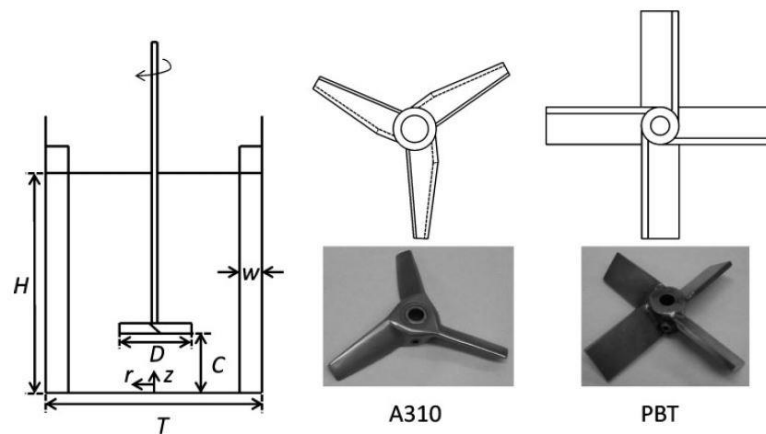
Figure 2.23 Schematic of tank geometry and impellers A320 (left) and PBT (right)

The direct relation between turbulence and solids distribution was demonstrated through a comparison between A310 impeller and PBT. The results showed that PBT had stronger turbulence due to its higher power number, the role of baffles in directing the liquid flow, and the upward direction of particles that were highlighted. In Case #4 (C/T = 0.25), PBT rose quicker than other cases due to the flow field. However, the flow speed in case #4 had the most significant impact (N = 10.8 rev s⁻¹).

2.6.2 Oily Wastewater Treatments by Flotation Process

Based on Chawaloesphonsiya, Wongwailikhit, Bun, and Painmanakul (2019), the authors were studied about the treatment of stabilized oily wastewater using modified induced air flotation (MIAF), which referred to the combination between the IAF and coagulation process. The stabilized oily wastewater was synthesized by using three different types of oil, including palm oil, lubricating oil, and cuttings oil. Oil concentration was measured in terms of chemical oxygen demand (COD). To perform coagulation process within the IAF system, different alum concentrations were required to vary in order to obtain the better ones in the separation process. However, the column reactor, which had a diameter of 5 cm with 2 m height, was set up for this experiment, as shown in **Figure 2.24**. As a result, the maximum efficiency was higher than 85% by using airflow rate 0.3 LPM for 10 minutes. Furthermore, the mixing in the flotation unit of bubbles motion was defined by a velocity gradient (G), which was obtained by the impart power (P) of water in mixing conditions that accounted for bubble flocculator as shown in **Eq. 2.11** and **2.12**.
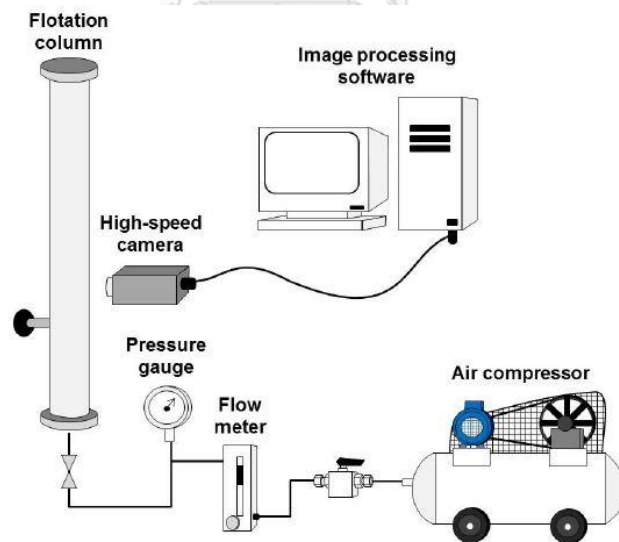
Figure 2.24 The experimental operation of the IAF unit

$$G = \sqrt{\frac{P}{\mu V}} \qquad\qquad Eq\ 2.11$$

$$P = C_1 Q_g \log\left(\frac{h + C_2}{C_2}\right) \qquad\qquad Eq\ 2.12$$

Regarding Daud et al. (2015), suspended solids (SS), color, COD, and oil and grease were removed from biodiesel wastewater by using coagulation and flocculation processes. The characteristics of biodiesel wastewater showed that the total amount of SS was 348 mg/l, COD was 5900 mg/l, the color was 95 PtCo, and O&G was 2680 mg/l. The author investigated the removal efficiency by using different coagulants such as aluminum sulfate, poly aluminum chloride, ferric chloride, and ferric sulfate. A standard jar-test apparatus was performed in this process in order to optimize the amount of coagulant dosage using. Jar Tester Model CZ150 comprised of six paddle motors (24.5mm x 63.5mm), equipped with six beakers of 1L volume. The pH value of the 500-milliliter biodiesel wastewater sample was adjusted to pH 7, respectively, by using 1.0 M H_2SO_4 or 1.0 M NaOH. Different concentrations of coagulant were prepared as 50,100,150, 200, 250, 300, 350, 400, 450, 500, 550 and 600 mg/l and added into 500 milliliter of biodiesel wastewater sample. Moreover, the system was fixed as rapid mixing for 4 min at 150 rpm and slow mixing for 20 min at 20 rpm, the liquid was clarified for 30 min. As a result, the experiment showed that PAC was found to be superior coagulant to remove suspended solids (SS), color, COD, and oil and grease, 97%, 95%, 75%, and 97% followed by alum, 92%, 92%, 53%, and 99%, respectively. Therefore, this research study indicated that coagulation and flocculation were a useful method. PAC was considered as the most effective in SS, color, COD, oil, and grease removal.

Ahmad et al. (2006) investigated the comparative efficiency of aluminum sulphate (alum), poly aluminum chloride (PAC), and chitosan, which used as the coagulant to remove residue oil and suspended solid in palm oil mill effluent (POME). In this research work, the coagulation process was used due to its capability of destabilizing and aggregating colloids and oil droplets as well as destroying emulsions. The reason to compare the efficiency between alum, PAC, and chitosan was that using alum or PAC as coagulants created hazardous activated sludge, which contained residual aluminum and may cause side effects when discharged into the open water body. Thus, it has become a necessity to develop a more efficient, environmentally friendly coagulant, which has similar potential as aluminum coagulants with an enhanced economic profile such as a natural polyelectrolyte called chitosan. Jar apparatus was

used to find the better conditions of this coagulant in the coagulation process in this work. POME contains about 10,000 mg/l of suspended solids and 2000 mg/l of residue oil. The results proved that chitosan was comparatively more efficient and economical to alum and PAC. After the experiment, the optimum conditions were defined that dosage of chitosan 0.5 g/L consumed only 15 min of contact time, mixing speed 100 rpm, sedimentation time 20 min and pH 4, and had more efficient (95% SS and residue oil removal) and economical compare to alum and PAC (dosages 8.0 and 6.0 g/l, 50 and 60 min of settling, respectively, 30 min of mixing time at 100 rpm, and pH of 4.5).

Regarding Meyssami and Kasaeian (2005), the author mentioned about one natural polyelectrolyte called chitosan, which was better in treatment because of its safety for both human beings and the environment. Some coagulants such as chitosan, starch, alum, and ferric chloride had been determined on the coagulation of oil droplets by using jar test apparatus and turbidimetric measurements. Olive oil emulsion samples were prepared in this study using surfactants and other agents that could form stable oil-water emulsions. In the jar experiments, chitosan and alum used together at concentrations of 15 and 25 ppm, respectively, at pH 6 to produce the lowest turbidity values. In the meantime, a concentration of 100 ppm of chitosan, an airflow rate of 3 LPM, aeration time of 45s, a temperature of 20 ºC, and pH 6 were used in air flotation experiments to produce optimum levels. Finally, at optimum conditions of coagulation and flotation stages, the COD of the olive oil emulsion could be removed by 95%.

Irfan et al. (2017) were examined about the removal of COD, TSS, and color of black liquor by the coagulation-flocculation process at optimized pH, settling, and dosing rate. The author preferred to modify different coagulants in a coagulation-flocculation process like alum, ferric chloride, aluminum chloride, ferrous sulphate, poly aluminum chloride (PAC), cationic and anionic polyacrylamide polymers in individual form as well as in different combination forms. They found that coagulants used in combinations were more effective in reducing COD, TSS, and color than using an individual form. The most effective results were found by using cationic and

anionic polyacrylamide combination with ferric chloride and aluminum chloride and reduced 76% of COD, 95% of TSS, and 95% of color were observed at pH <3.

Indeed, Bensadok, Belkacem, and Nezzal (2007) had identified about cutting oils treatment by using coupling coagulation and dissolved air flotation (DAF). The treatment process was carried throughout the combine process between chemical destabilization and physical treatments. First, this study was mentioned about three different kinds of chemical groups of neutralization, with or without combined thermal action such as metal salts, acids, and synthetics polyelectrolytes. Then, the oil emulsion was separated by a flotation application. DAF was selected due to its effect to create the small size of gas bubbles and the formation of the agglomerates between bubbles-particulates. For the DAF application, the average diameter of the generated bubbles is inversely proportional to the saturation pressure, as shown in **Eq. 2.13**.

$$d_b = 382.52 P_S^{-1.09} \qquad \qquad Eq\ 2.13$$

Eventually, the formulation of oil has destabilized by $CaCl_2$ in terms of kinetic separation, which can decrease the oil concentration from 8% up to 10%. The average diameter of air micro-bubbles (50 µm) was considering the saturation pressure of 6.5 bars.

From Etchepare, Oliveira, Azevedo, Rubio, and Technology (2017), separation of emulsified crude oil in saline water by dissolved air flotation (DAF) with micro and nanobubbles was carried out. This work investigated the separation of emulsified crude oil in saline water, which contained 30 g /L of NaCl and employed with microbubbles (MBs) within diameter D_{32}: 30-40 µm, and nanobubbles (NBs) within diameter D_{32}:150-350 nm. The bubbles were generated simultaneously by the depressurization of air-saturated water by adjusting the relief valve. There are three steps in this studying including i) Flotation with MBs and NBs, ii) ''Floatation" by NBs only, and iii) Flotation with MBs and NBs following floc conditioning by nanobubbles. These three conditions provided the best result of 99% efficiency, which was obtained at 5 bar and 5 mg/L of Dismulgan. The study was mentioned about the use of low saturation pressure (Psat = 3.5 bar) could result in lower oil concentration in treated water (29 mg/L). The floatation process resulted in oil removal efficiencies

from 75 and 90% with and without NaCl 30g/L. It is observed that the NBs entrap and adhere inside the flocculated oil droplets and form the aerated oily flocs, which could subsequently assist the MBs in the flotation application. This summarizes that the flotation process appears to have the potential to improve oil separation.

2.7 The Reasons for Selecting Stirring/ IAF/ DAF Processes for This Study

The application of flotation was widely studied for various purposes, including water treatments, wastewater treatments, especially for the elimination of hydrophobic composites from particles. It was possible to separate the organic contaminants from soils by using the flotation technique since flotation can remove hydrophobic and organic materials from the soil effectively (Zhang et al., 2001).

Base on several kinds of research, flotation had been modified and applied to various types, including Induced Air Flotation (IAF), Dissolved Air Flotation (DAF), and other advanced techniques. In general, the DAF process could provide the highest treatment efficiency since the tiny bubbles were generated (from 30 to 100 µm in diameter), while the IAF process was formed by a combination of a high-speed mechanical agitator or an air injection system (700 to 1500 µm in diameter) (Painmanakul et al., 2010). For instance, hydrophobic particles were selectively adsorbed on the gas bubble surface, normally on air, and float to the surface, where those particles were concentrated and removed along with the foam. This operation was known as a simple, able to use medium and high flowrates, effective, and economical method (Syllos S. da Silva 2012). Mostly, dissolved air flotation (DAF) had been remarkably applied in many industries for many processes such as pre-treatment in the desalination process, preparation the raw water at wastewater treatment plants in order to remove particles in the mining and mineral processing, and the removal of crude oil in refinery industries. The reduction of rapid pressure in the DAF tank created the formation of various microbubbles, which could attach the oil droplets to form as agglomerations. The agglomeration had an average density that was different from the oil droplet in water. So that, buoyant force and rising velocity had been applied in this system that caused the flotation was very successful in

creating oil droplets as a layer on the surface of the DAF tank and removed (Radzuan et al., 2016).
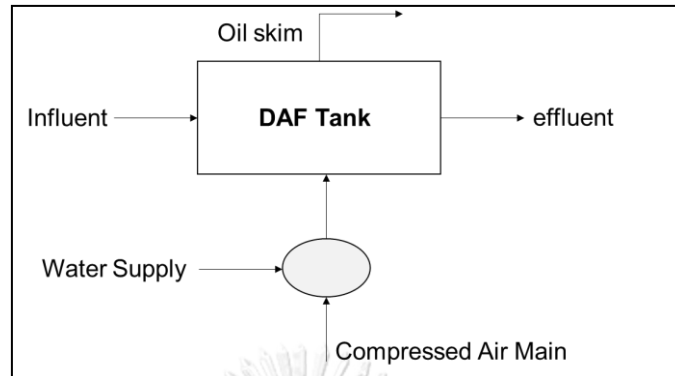
Figure 2.25 Full flow pressure of the DAF system

Anyway, the soils that polluted by petroleum hydrocarbons have become the worldwide environmental and health concerns, which led to further attention and investigation for its remediation (Lai, Huang, Wei, & Chang, 2009). Therefore, many novelty methodologies had been investigated toward petroleum hydrocarbons contaminated soils/sediments/and drill cuttings remediations such as the combination of two processes between flotation and mechanical stirring. Related to the previous studies, microbubbles and mechanical stirring had been applied and were very useful for the removal of the oil spillage from the sand. (Agarwal et al., 2016; Sun et al., 2019). The soil contaminated by crude oil was remediated by using air sparging, which assisted by stirring. This process significantly showed the result in removing crude oil from the soil (Urum et al., 2005). Another study was investigated the evaluation of the separation efficiency of oil-contaminated soil by bubble bursting energy and the remediation of oil-contaminated soil by using microbubbles (Kim, Kim, & Han, 2012). Hence, air flotation was modifying within the stirring process in order to observe the mechanical removing and the percentage of TPH removal from drill cuttings.

2.8 Research Gap

Operational discharges of drill cuttings from offshore oil and gas platforms had created public concern because they represented an extensive input of contaminants entering the sea from many widely dispersed point sources. Until now, drill cuttings

claimed to be treated by conducting many types of research for better and practical treatments before disposal or reusing. Using extracting agents to enhance soil washing had known as the common treatment method; however, some of them were toxic to the environment and costly too. Although there were various researches on petroleum wastes washing, it still has some gaps and limitations of treatment technologies, which required further studies. The summary table below was from some previous learnings on soil washing techniques, which we can compare and considered.

Table 2.8 Summary of oil-contaminated soil washing methods

Contaminant Types	Processes	Chemical Reagents	Removal Efficiency	Ref.
1). Oil spill-contaminated sands	Flotation Stirring	Chemical-free	> 90%	Sun et al. (2019)
2). TPH contaminated soil	Desorption	Ethyl lactate	> 80%	Ahmadkalaei et al. (2016)
3). Crude oil contaminated soil	Air sparging Stirring	SDS and Rhamnolipid	> 80%	Urum et al. (2005)
4). Hydrophobic compounds contaminated soils	Flotation Agitation	SDS and DTAB	> 70%	Zhang et al. (2001)
5). Oil contaminated soils	Desorption	SDS Salts	> 35%	Torres et at. (2007)
6). Oil-based drill cuttings	Adsorption	Rhamnolipid Sawdust	> 80%	Yan et al. (2011)
7). Crude oil contaminated soil	Shaking	Rhamnolipid SDS	> 80%	Urum and Pekdemir (2004)

Furthermore, cutting fluids, which were considered as the oily wastewater containing loads of hydrocarbons, and fine particles, were needed to study its properties to find out the alternative usage. After drill cuttings washing, oily wastewater somehow happened from the oil emulsions, which also caused problems to the environment; hence, some different techniques were investigated in oily wastewater removal, which indicated in some former studies as shown in the tables below:

Table 2.9 Summary of some potential treatment methods

Pollutant Removal	Processes	Chemical Reagents	Removal Efficiency (%)	References
SS, Color, COD, O & G	Coagulation Flocculation	PAC Alum Ferric chloride Ferric sulfate	97%, 95%, 75%, 97% 92%, 92%, 53%, 99% 95%, 93%, 63%, 97% 88%, 88%, 54%, 94%	Daud et al. (2015)
COD TSS Color	Coagulation Flocculation	Ferric chloride and PAC and Cationic polymer	76%-COD 95%-TSS 95%-Color	Irfan et al. (2017)
SS and Residual oil	Coagulation	Chitosan	> 95% - Oil & SS	A. Ahmad et al. (2006)
Oil in water	Induced Air Flotation Coagulation	Alum	> 60%	Romphophak et al. (2016)

From the gaps and limitations of literature reviews, it was observed that the design of the flotation process that uses tiny bubbles (micro-size and nano-size) was very useful for oily wastewater treatment. On the other hand, for soils or drill cuttings washing, flotation application required further studies in order to notify whether it was effective in this kind of treatment or not. Furthermore, if chemical substances were expected to reject from soil treatment systems, other washing media were also required in the study too, such as Saline water, Distilled water, and Tap water.

In overall, from the previous studies, it could be drawn into some gaps as followed:

➢ The process was mostly used with chemicals or surfactants, which has known as very costly and not environmentally friendly.

➢ The process of air flotation, such as IAF and DAF, was mostly studied with oily wastewater with better results but not mainly studied with DC washing, which was contaminated by the petroleum hydrocarbons based.

➢ The combination of the physical process was not mainly studied over DC washing; even these modifications has known as the beneficial methods that do not harm the environment and economic saving.

CHAPTER 3
RESEARCH METHODOLOGY

3.1 Study Overviews

This chapter summarized the materials and methods using in the research work. In this study, TPH removal from DC was the main identification; therefore, the physicochemical properties of DC were firstly studied. The washing processes were investigated in both single and combination processes, as represented in **Figure 3.1**. Moreover, the oily produced water that remained after the soil washing process was investigated for its properties to examine whether it could use back in the reinjection system or not. The methods used for TPH removal (%) and all equations used to calculate in flotation and stirring process were included in the analytical methods section.
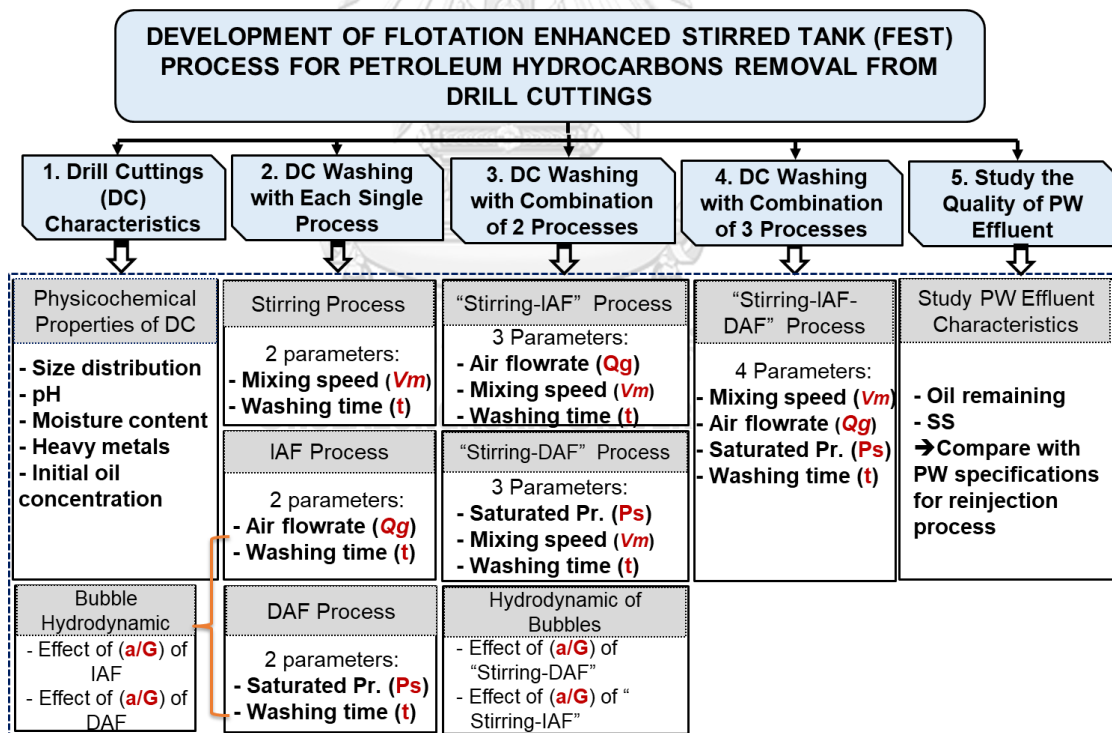
Figure 3.1 Overview of the framework

3.2 Experimental Set-up

3.2.1 Experimental Set-up with Induced Air Flotation (IAF) Process

The column reactor was constructed by a transparent acrylic material with **6 cm** of inner diameter and **25 cm** of height, respectively, as illustrated in Figure 3.2 below.
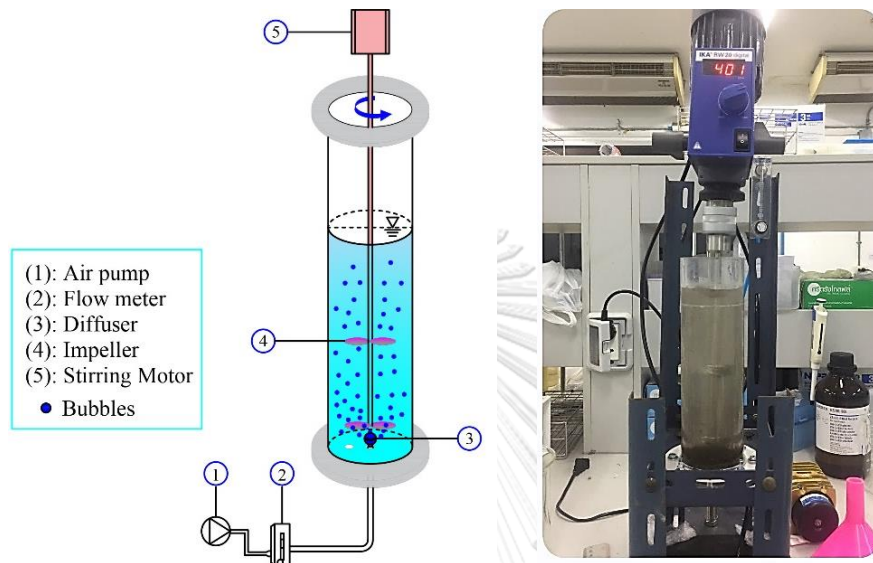
Figure 3.2 Experimental set-up of stirring with induced air flotation (IAF)

This experimental set-up was equipped with the stirred motor and impeller(s). At the same time, an air diffuser was installed at the bottom of the reactor and connected to the air compressor that was installed for the IAF process. The airflow rate of IAF was regulated by the airflow meter (see **Figure 3.2**).

3.2.2 Experimental Set-up with Dissolved Air Flotation (DAF) Process

(1): Air compressor
(2): Gate valve
(3): Pressure gauge
(4): Submersible pump
(5): PVC ball valve
(6): Relief valve
(7): Impeller
(8): Stirred Motor
(9): Pressure vessel

• Oil droplets
• Microbubbles
• Cuttings
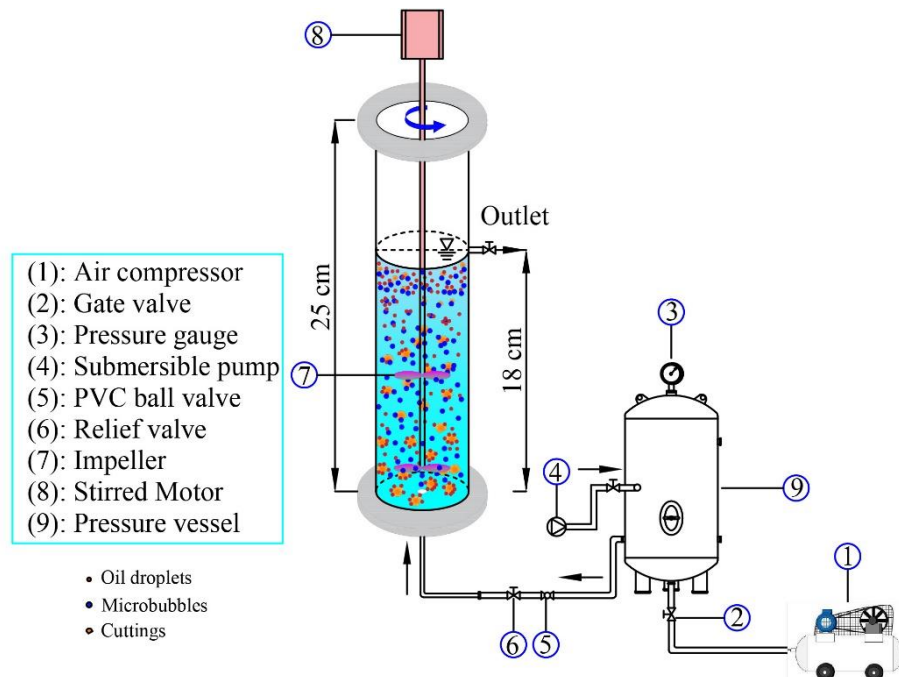
Figure 3.3 Schematic of stirring with dissolve air flotation (DAF)

Figure 3.4 Experimental set-up of stirring with dissolved air flotation (DAF)

Similarly, this experimental set-up was equipped with the stirred motor and impeller(s). Yet, the air compressor and pressure vessel were connected at the bottom

of the reactor, as represented in **Figure 3.3**. Then, the tiny bubbles were produced under the differences of saturation pressure inside the tank. All experiments were conducted under the ambient temperature (~28°C).

3.3 Materials and Chemicals

3.3.1 Experimental Equipment

❖ Stirred motor: is a kind of overhead mixing motor that suitable for mixture with high viscosity liquid or solid-liquid. It is widely used in the laboratory for physical and chemical analysis, petrochemical analysis, and others.

❖ Air compressor: is one instrument that can store pressurized air more and more in its storage. It is used to convert air to create microbubbles in this work.

❖ Pressure Vessel: is a kind of cylinder with a piston of the open-end vessel, whereas a tank can create as pressurized fluids or store liquid vapors and gases under pressure.

❖ Flowmeter: is necessary to control gas or liquid flow before allowing to flow to the inlet of the tank.

❖ Pressure gauge: is one equipment that use to maintain pressure during operation.

❖ pH-meter: is needed to measure pH in various liquids. METTLER-TOLEDO model is used in this study.

❖ Gas chromatography equipped with a flame ionization detector (GC-FID): GC-Gas chromatography is used to separate or detect small particles in either gas or liquid phase. Flame-ionization detection (FID) is typically used for organic compounds detection in GC; especially, it can characterize the carbon range of hydrocarbon samples.

3.3.2 Chemicals and Washing Reagents

❖ Tap water: is employed to be the washing reagent in the soil washing process because it is simple and beneficial for bursting microbubble in the reactor.

❖ Saline water: is employed to be one of the washing regents in soil washing and oily produced water treatment compared to tap water.

❖ <u>Hexane (C_4H_{16}) and Acetone</u>: use to extract oil in the soil to find the oil concentration in Gas Chromatography (GC-FID).

3.4 Experimental Procedures

As briefly mentioned, three main parts, including the individual investigation of each process, a combination of two processes with stirring, and optimization of the efficient combined process previously found by using statistical DOE. In the stirring experiment, impeller selection criteria including type of impeller (pitch 4-blades and hydrofoil impellers) and the number of the impeller (1-3 impellers) were firstly studied through adding 50 g of DC in 500 mL tap water under the operation of 300 rpm rotational speed and 30 minutes washing time. For impeller operation, the variation of rotational speed (200 - 600 rpm) and washing time (0-60 minutes) were investigated in terms of TPH removal efficiency. In the IAF experiment, it was conducted by varying air flow rate (1.0 - 3.0 LPM) and washing time (0-60 minutes), while saturated pressure (2 - 4 bar) and washing time (0 - 60 minutes) were varied in the DAF experiment. The DC was also prepared the same as in the stirring experiment.

Stirring combined with IAF was designed at three different conditions of rotational speed, airflow rate, and washing time, i.e., low level (200 rpm, 1 LPM, and 20 min), middle level (400 rpm, 2 LPM, and 40 min), and high level (600 rpm, 3 LPM, 60 min). Plus, stirring combined with DAF was also designed at three conditions of saturated pressure, airflow rate, and washing time, i.e., low level (2 bar, 200 rpm, 20 min), middle level (3 bar, 400 rpm, 40 min), and high level (4 bar, 600 rpm, 60 min). Both combined processes were comparably analyzed for optimizing investigation.

The optimization process was studied at three levels of each factor by utilizing the central composite design of response surface design. The empirical correlation was lastly constructed in terms of TPH removal efficiency and independent variables by using the experimental results. Then, the study of bubbles hydrodynamics of each flotation and FEST process was conducted.

3.4.1 Samples Characteristics

A 10 kg of a soil sample that was taken from an oil extraction platform was received and kept at 4ºC before its characterization. Samples were obtained and used to characterize their physicochemical compositions. In the soil distribution step, the sample was dried at environmental temperature and milled. After that, the soil was sieved by using sieve analysis which has the size from 3mm to the smallest (< 2 µm) and can recognize as three classes called (1) sand (50-3000 µm), (2) silt (2-50 µm), (3) clay (< 2 µm) as depicted in **Figure 3.5**. The larger particles that were retained on mesh 7 (2,830 µm) are separated due to their bigger properties such as soil grains, gravels, etc.

Figure 3.5 Cuttings sample distribution procedures

For moisture content, 100 g of soil will take to bake for 16 hours to calculate for moisture content by the following formula:

$$MC(\%) = \frac{M_W - M_d}{M_d} \times 100 \qquad\qquad Eq\ 3.1$$

Where M_w is the weight of wet soil (g), and M_d is the weight of dry soil after baking (g) (ASTM D2216).

For pH measurement, the soil will triplicate shake with the deionized water by a magnetic stirrer for 30 seconds, then measure by using a pH-meter. The overall pH will calculate to find the average one. **Table 3.1** shows the overall characteristics of drill cutting using in the experiments.

Table 3.1 Physicochemical characteristics of cutting samples

No	Parameters	Unit	Analytical Methods
1	Size distribution		Sieve analysis
	Sand (50-2000µm)	%	-
	Silt (2-50 µm)	%	-
	Clay (< 2 µm)	%	-
2	pH	-	pH-meter
3	Moisture Content	%	ASTM D2216
6	Initial TPH Concentration	mg/kg	GC-FID

3.4.2 Drill Cuttings (DC) Washing with the Individual Process

1. Preliminary Experiments

➢ **S/L ratio:** the experiment was conducted four ratios between soil to tap water volumes such as 1:2.5, 1:5, 1:10, and 1:15. Mixing speed and time was fixed as 300 rpm and 30 min, respectively. This part expects to find a better ratio between soil and tape water using in the washing process for further steps.

➢ **Impeller screening:** impellers were very common in the conventional mixing process because they could provide better contact between cutting particles and washing liquid like water. Two types of axial flow impeller were the most use in mixing conditions containing pitched-4 blades impeller and hydrofoil impeller, as shown in Figure 3.6. Each impeller diameter was defined by 50% of tank diameter in order to create turbulent flow and well mixing (Tom D. Reynolds, 1996).

Figure 3.6 Pitched-4 blades impeller (left), Hydrofoil impeller (right)

2. DC Washing with Stirring Process

In the stirring process, a mechanical stirred motor model IKA RW20 digital was used in this study. There were 2 main parameters, mixing speed (V_m) and washing time (t), which would be considered and conducted the experiments by varying in the time

interval 10min for 1 hour (10min, 20min, 30min, 40min, 50min, and 60min) in order to find the better results of mixing speed and time as shown in the table below.

Table 3.2 Factors optimization in the stirring process

No	Parameters	Unit	Factor Levels		
			1	2	3
1	Mixing speed (V_m)	rpm	200	400	600
2	Washing time (t)	min	10 min-time intervals (1 hour)		

(speed 600 rpm (Urum et al., 2005), speed > 100 rpm (Lai et al., 2009))

3. DC Washing with IAF Process

In this process, a rigid stone diffuser (see **Figure 3.7**) was used to create air bubbles inside the reactor. Two parameters were considered, such as air flowrate (Q_g) and washing time (t). Similarly, the experiments were conducted in the time interval of 10 min for 1 hour (10min, 20min, 30min, 40min, 50min, and 60min), as shown below:

Table 3.3 Factors optimization in IAF process

No	Parameters	Unit	Factor Levels		
			1	2	3
1	Air Flowrate (Q_g)	LPM	1	2	3
2	Washing time (t)	min	10 min-time intervals (1 hour)		

(Q_g: 0.1-1 LPM (Chawaloesphonsiya et al., 2019), Q_g: 3 LPM (Meyssami & Kasaeian, 2005))
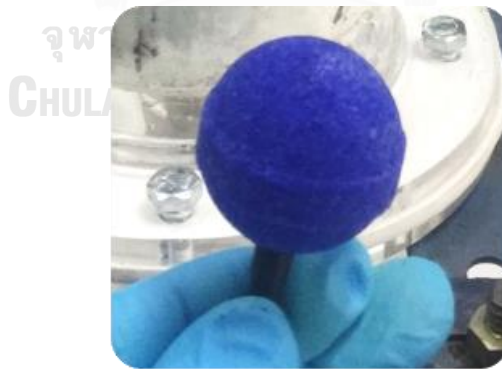
Figure 3.7 Rigid stone diffuser

4. DC Washing with DAF Process

Likewise, the Dissolved Air Flotation process was a process that used saturated air that dissolves in water to create small tiny bubbles. In this process, saturated pressure (P_s) and washing time were crucial to study for DC washing in the DAF system. Thus,

the factor levels would find out by varying each pressure saturation within 10 min time intervals for 1 hour, as revealed in **Table 3.4**.

Table 3.4 Factors optimization in DAF process

No	Parameters	Unit	Factor Levels		
			1	2	3
1	Saturated Pressure (P_s)	Bar	2	3	4
2	Washing time (t)	min	10 min-time intervals (1 hour)		

(Ps: 2-4 bars (Bensadok et al., 2007; Rubio et al., 2002; Wang et al., 2010))

3.4.3 DC Washing with the 2 Combination Processes

The objective of this part was to find the maximum experimental conditions from each combination process. "Stirring-IAF" and "Stirring-DAF" had compared each other in order to define one combination process that will offer a better percentage of TPH washing from DC. The tables below were listed and studied.

1. Stirring Combined with IAF Process

Table 3.5 Factors optimization in stirring combine with IAF process

No.	Parameters	Unit	Min. Levels	Max. levels
1	Air Flowrate (Q_g)	LPM	1	3
2	Mixing speed (V_m)	rpm	200	600
3	Washing time (t)	min	20	60

2. Stirring Combined with DAF Process

Table 3.6 Factors optimization in stirring combine with the DAF process

No.	Parameters	Unit	Min. Levels	Max. levels
1	Saturated Pressure (P_s)	Bar	2	4
2	Mixing speed (V_m)	rpm	200	600
3	Washing time (t)	min	20	60

3.4.4 DC Washing with the 3 Combination Processes

Meanwhiles, Stirring, IAF, and DAF will be observed together to examine the effective conditions for DC washing. This step, four parameters will be investigated through DOE (CCD-RSM), as shown in the table below.

Table 3.7 Factors optimization in the combination of "Stirring-IAF-DAF" processes

No.	Parameters	Unit	Min. Levels	Max. levels
1	Air Flowrate (Q_g)	LPM	1	3
2	Mixing Speed (V_m)	rpm	200	600
3	Saturated Pressure (P_s)	Bar	2	4
4	Washing Time (t)	min	20	60

After obtaining the optimum conditions, these three combined processes will compare with the two combined processes in terms of treatment efficacy, economic saving, and operational conditions. Then, the best one will be selected.

3.4.5 Water Treatment Studying

The oily produced water characteristics: this water was characterized by measuring the oil remaining, suspended solids, pH in water in order to understand its properties in purpose using water recovery instead of using fresh water. Table 3.8 lists all the required components of water effluent.

Table 3.8 Produced oily water characteristics

No	Parameters	Unit	Analytical Methods
1	pH	-	pH meter
2	Oil Concentration	mg/L	FastHEX methods
3	Suspended Solids (SS)	mg/L	Evaporated at 103-105°C for 1 hr

3.5 Analytical Methods

3.5.1 Removal Efficiency

The removal efficiency was illustrated by determining the percentage between the initial and final concentrations of oil in terms of total petroleum hydrocarbon (TPH).

$$TPH \; removal \, (\%) = \frac{Initial \, TPH - Residual \, TPH}{Initial \, TPH} \times 100 \qquad Eq \; 3.2$$

3.5.2 Gas Chromatography (GC) Analysis

Gas chromatography was used to analyze the oil containing in the soils. Because TPH could be classified into different groups consists of gasoline range organics (GROs),

diesel range organics (DROs), and oil range organics (OROs), GC could characterize an n-alkanes group of exact oil containing in drill cuttings. In this work, GC was equipped using a flame ionization detector (GC-FID), as shown in **Figure 3.8**. According to EPA method 8015B, after the treatment within processes, a certain amount of oil spill-contaminated soils was collected and air-dried. 1g of soil will be extracted by 60 ml of hexane and shake for 90 min before analyzing with GC-FID.

Figure 3.8 Gas chromatography (GC-FID) instrument

The operating conditions of GC-FID was conducted following the table below.

Table 3.9 GC-FID conditions for the TPH analysis

No.	Parameters	Operating Conditions
1	Inlet	Splitless
2	Injection Volume	1 μl
3	Column	HP-1 (capillary: 30m x 0.32mm x 0.25μm)
4	Carrier gas	2 mL/min Helium (He)
5	Temperature	Inject: 300 °C; Detector: 330 °C
6	Oven Program	45 °C for 3 min, and 15 °C/min to 300 °C
7	Low Concentration	2,000 mg/l
8	High Concentration	10,000 mg/l
9	Calibration Solution	Diesel oil-Hexane

3.5.3 Design of Experiment (DOE)

DOE was used throughout a computer software program called Minitab 17® to study and analyze the experimental parameters statistically. **The central composite response surface design** (CCD-RSD) was selected for factor optimization and analysis in order to seek the most influential responses of design criteria operating in laboratory experiments. In this study, the DOE technique was used in the combination processes such as "Stirring and IAF process," "Stirring and DAF process," and "IAF and DAF process" in the purpose of:

✓ Statistically minimizing the numbers of the experiment which generated by many factors

✓ Optimizing the best value obtained by the experiments by showing the reliable plotted graphs and analysis of variance (ANOVA)

After experimental works, the results could analyze in TPH removal efficiency (%) and explain as the following steps:

1) Residual plot of model adequacy analysis;

2) Analysis of variance (ANOVA);

3) Main effects plot of the fitted mean value in terms of TPH % analysis;

4) Surface plot of two factors a time for factor optimization analysis;

5) And Summary of the appropriate parameters using in the experiment.
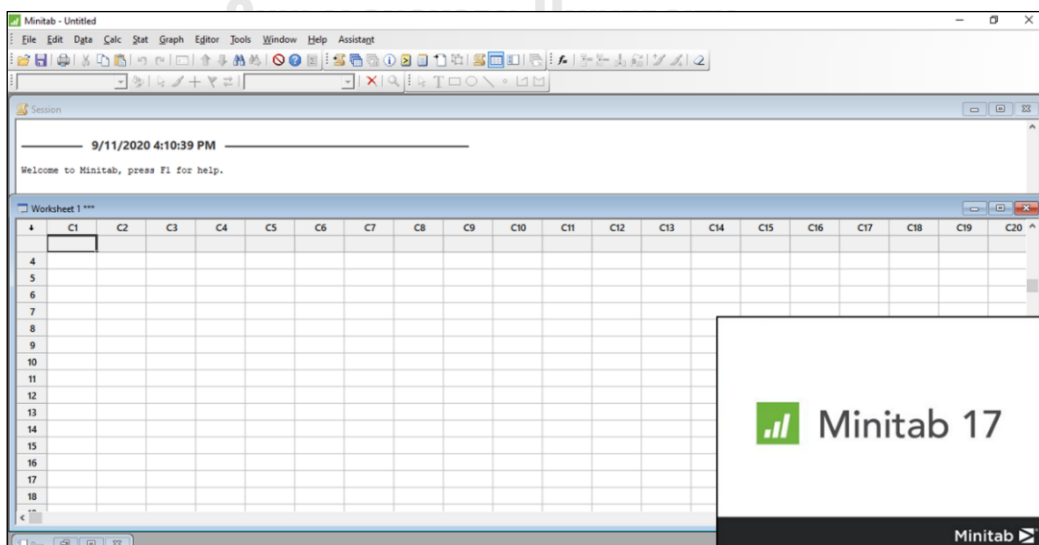
Figure 3.9 Computer software program, Minitab 17®

3.5.4 Velocity Gradient

1) Velocity Gradient in Rapid Mixing

Gradient Velocity (G) was the difference in velocity between adjacent layers of the fluid, which represents in a turbulent flow. In order to understand the mixing condition in the column reactor, the velocity gradient (G) could calculate in the following formulas:

$$G = \left(\frac{P}{\mu_L V_L} \right)^{0.5} \qquad\qquad Eq\ 3.3$$

$$P = N_P \rho n^3 d^5 \qquad\qquad Eq\ 3.4$$

μ_L was the dynamic viscosity of the fluid (kg/m.s), V_L was the volume of using reactor (m³), **P** was power imparted to water from mixing (Watt), N_p was the Power number of the impeller, **ρ** was the density of the fluid (kg/m³), **n** was impeller speed (rps), and **d** was Impeller diameter (m) (Crittenden et al., 2012).

2) Velocity Gradient of Bubbles

The gradient Velocity of Bubbles was determined when pneumatic mixing was employed in tanks with aeration devices. The gradient velocity and detention times were similar to magnitude and range as those used for the rapid mixing. For velocity gradient, **G** was defined by the determination of the required power, as shown in **Eq 3.5**.

$$G = \left(\frac{P_C}{\mu_L V_L} \right)^{0.5} \qquad\qquad Eq\ 3.5$$

$$P_C = C_1 Q_g \log\left(\frac{h+10.4}{10.4} \right) \qquad\qquad Eq\ 3.6$$

Where **G** was the velocity gradient of Bubbles (S⁻¹), V_L was water volume (m³), P_C was the rate of power (watts), C_1 was constant = 3,904, μ_L was the viscosity of the liquid (kg/ m.s), Q_g was air flow rate (m³ /min), and **h** was the depth to the diffuser (m) (Reynolds & Richards, 1996).

3.5.5 Bubbles Hydrodynamic Analysis

1) Bubbles Diameter (D_B) in IAF:

The bubble diameter (D_B) was determined through the equivalent diameter (d) and the Sauter Mean diameter of bubbles (D32) as followed.

$$d = \sqrt[3]{E^2 e}; \qquad D_{avg} = D_{32} = \frac{\sum_i n_i d_i^3}{\sum_i n_i d_i^2} \qquad\qquad Eq\ 3.7$$
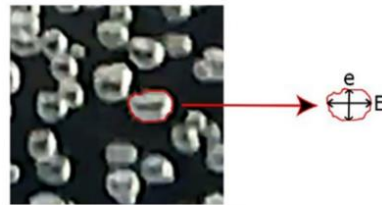
Bubbles that captured by ImageJ

Where n_i was the number of bubbles which derived from an equivalent diameter d_i

Bubble rising velocity: $\qquad\qquad U_B = \frac{\Delta D}{T_{frame}} \qquad\qquad\qquad Eq\ 3.8$

Where, ΔD was the bubble displacement between times t = 0 and t, T_{frame} was the time between frames (Wongwailikhit et al., 2018).

2) Bubbles Hydrodynamic Analysis in DAF:

The average diameter of the generated bubbles was calculated by:

$$d_b = 382.52 P_S^{-1.09} \qquad\qquad\qquad Eq\ 3.9$$

Where P_s was Saturated Pressure (Bar) (Bensadok et al., 2007).

From Stoke's law, Bubble rising velocity was calculated by:

$$U_B = \frac{gd^2}{18\upsilon} \qquad\qquad\qquad Eq\ 3.10$$

Where d was the diameter of MBs (m), and ϑ was kinetic viscosity of water (m^2/s), (Takahashi, 2005).

3) Interfacial area of Bubbles (a)

The interfacial area of bubbles (a) in the IAF Process was examined through several parameters such as bubble formation frequency (f_B), bubble size (D_B), the velocity of rising of bubbles (U_B) that analyzed from samples of 50 to 100 numbers of the bubble by photography using 240 frames per second of slow-motion of iPhone 6 plus camera. The bubbles size was measured in image processing software (ImageJ).

$$a = f_B \times \frac{H_L}{U_B} \times \frac{S_B}{V_{total}} = f_B \times \frac{H_L}{U_B} \times \frac{\pi D_B^2}{AH_L + N_B V_B} \qquad Eq\ 3.11$$

CHAPTER 4
RESULTS AND DISCUSSION

4.1 Drill Cuttings Characteristics

4.1.1 Size Distribution

The particle size was one important factor that contributed to the removal efficiency because the particle fractions could represent the treatment capability. All samples were kept at 4ºC before processing for characterization. In experiments, the larger particles that retained on mesh 7 (2,830 μm) were separated due to their bigger properties such as soil grains, gravels, etc. Since these grand particles contained a limited surface area and hardly reacted with other constituents, they were assumed not to be significantly polluted by total petroleum hydrocarbon (TPH). With this regard, the cuttings were dried at room temperature and screened by using sieve analysis from 2 mm to the smallest (< 2 μm), classifying into three classes, i.e., sand, silt, and clay. Then, the particle size was also confirmed by the analysis of size distribution. It was observed that the samples were mostly in the silt class (2-50 µm), which was shown as 82% in size classification. Besides, the samples were 14.43% in the sand range (50-2000 μm), and only 3.56% in the clay range (< 2 μm), as represented in **Figure 4.1**. Most DC samples had a mean diameter (D_{50}) of 21.6 µm with a specific surface area of 387.6 m^2/kg.
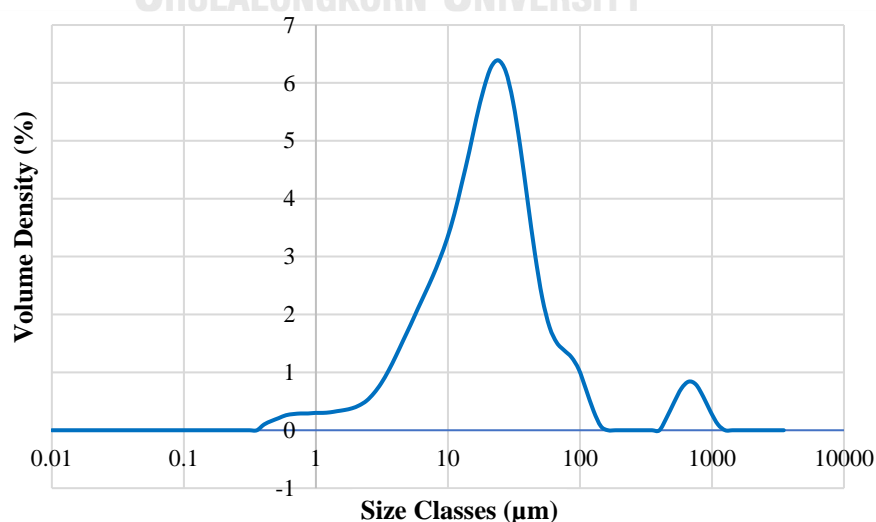
Figure 4.1 Size distribution of DC samples

4.1.2 Moisture Contents

The moisture contents were obtained from the calculation by weight loss after oven drying following the standard method of ASTM D2216. 100 g of samples were taken to bake for 16 hours for moisture content like the following calculation:

$$MC(\%) = \frac{20g - 19g}{19g} \times 100 = 5.26\%$$

It was noted that the higher moisture contents in the surface of soil containing oils could be contributed to insufficient aeration of the soil that might have the displacement of air in the soils, which could encourage waterlogged and reduced rate of evaporation. However, the coated soil surface by the hydrocarbons could diminish the water capacity contained in the soil owing to some significant reductions in clay (Osuji & Nwoye, 2007). In general, some parts of coats could cause the soil structure breakdown, and the soil particles disperse, then the percolation and retention of water reduced when the soils were contaminated with crude oil. Therefore, the moisture contents in the samples of this study showed a lower percentage (5.26%), which represented the reduction of water inside these samples and the contamination of petroleum hydrocarbon.

4.1.3 Initial TPH Concentration

In this work, in order to measure the concentration of petroleum containing in drill cuttings, the soil extraction method was used following the standard approach of EPA 8015B (U.S. EPA, 1996), which was measured by Gas Chromatography which equipped by a Flame Ionization Detector (GC-FID) machine. A certain amount of cutting was collected and air-dried at room temperature. 1g of soil was extracted by 60 ml of hexane and shake for 90 min before analyzing with GC-FID. It was necessary to prepare a standard calibration curve by using the most related hydrocarbons, which contain in the soil sample. Diesel oil was the best commercial oil, which can use to represent the contained oil in drill cuttings because the functional group of diesel oil was frequently found in drill cuttings in Thailand. Five solutions of diesel oil, such as 2,000 mg/L, 4,000 mg/L, 6,000 mg/L, 8,000 mg/L, and

10,000 mg/L, were prepared to experiment with GC-FID under the operating conditions, as represented in **Figure 4.2** beneath.
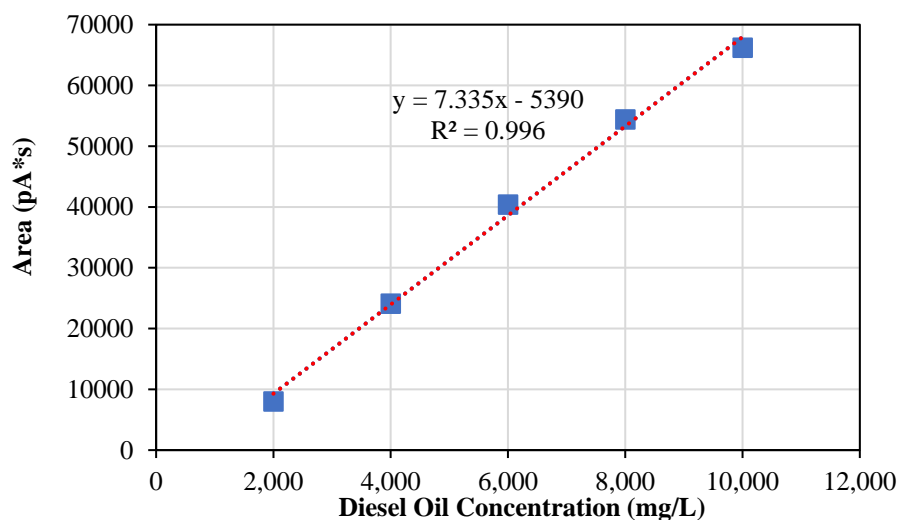
Figure 4.2 Standard calibration curve

After measuring TPH via the machine, we found that diesel oil had the peaks, which represented the carbon range from C_8 to C_{24}, as shown in **Figure 4.3**. Consequently, we could identify the concentration of oil in contaminated soil by comparing the retention time of the carbons range from drill cuttings to the calibration curve of commercial diesel oil. From the graph, the most relevant carbon range of the soil sample was on the retention time between 14 and 19 minutes, so that the TPH in drill cuttings held the atoms of carbon ranging from C_{14} to C_{22}, which was in the group of diesel engine fuel (C_{16}-C_{23}) (Liu, Wang, Wang, & He, 2016). Therefore, using commercial diesel oil as the calibration curve was very suitable for these DC. The cuttings were measured throughout this calibration curve, and their area was found to be 30,800 p*A, which represented in 4,934 mg/L of diesel oil concentration.

Table 4.1 Initial TPH concentration

No	Hexane and Time Extract	Y = 7.335x-5390		DC (mg/kg)
		x (mg/L)	Y (pA)	
1	1 g of DC was extracted by 60 ml of Hexane for 90 min	4,934	30,800	296,000
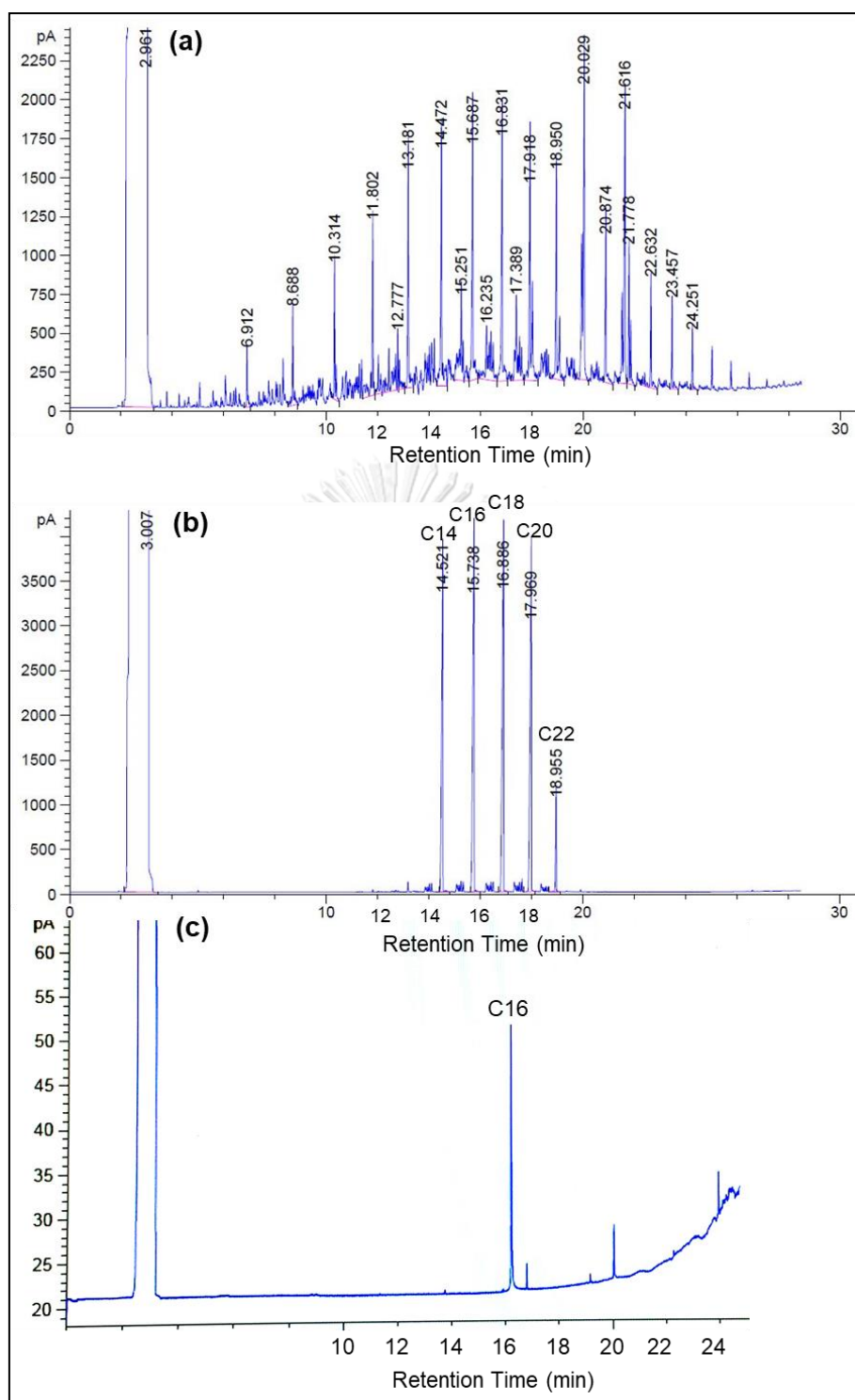
Figure 4.3 Chromatogram of commercial diesel oil (a), TPH on DC (b), and TPH

standard of C$_{16}$

The table below was about the summary of the cuttings' characteristics.

Table 4.2 Physic-chemical characteristics of cutting samples

Parameters	Values
Size Distribution	
Sand (50-2000μm)	14.43%
Silt (2-50 μm)	82%
Clay (< 2 μm)	3.56%
pH	7.74
Moisture Content	5.26%
TPH Concentration	296,000 mg/kg

4.2 Preliminary Experiments

4.2.1 Reasons for Selecting Impeller Types

The **Pitched 4-blades** and **Hydrofoil** impeller were selected to compare each other since these two types created the axial flow patterns, which could solve two main challenges mixings such as solid suspension and stratification (**Figure 4.4**). In terms of impeller geometries, hydrofoil had the ability to create the same velocity and generate the flow in an axial-flow. In addition, they were not complicated for the installation inside the vessel since they could be supplied as a hub and blades inside the tanks and considered to be "low-shear." Then, they had the ability to maximize pumping capacity for fluids by reducing the power number of impellers. In the meantime, PBT-4 blades could generate both axial and radial flow velocity by just adjusting the impeller diameter to the vessel diameter ratio. Moreover, PBT could create the balance of flow and shear in the mixing vessel; especially, they were useful for mixing viscosity of fluids at the lower bottom clearance or at the shallow submersion.

In terms of hydraulic efficiency, both hydrofoil and PBT-4 blades were considered based on the mechanical power input, which could be calculated by **Equation 3.4** (Chapter 3). The power input was important to represent for hydraulic efficiency of pumps that were used by a different type of impeller. Moreover, PBT-4 was known to generate higher shear than the hydrofoil impeller, so that the velocity gradient that produced by PBT-4 was higher than hydrofoil (Machado, Nunhez, Nobes, & Kresta,

2012). Because PBT-4 and Hydrofoil were capable of providing better contact between drill cuttings particles and washing liquids in the treatment system; therefore, these 2 types were chosen to compare each other.

(A) Hydrofoil   **(B) PBT**
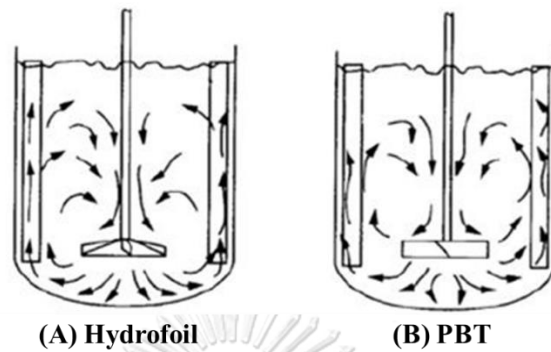
Figure 4.4 Flow patterns for Hydrofoil (A) and PBT-4 (B)

4.2.2 Effect of Agitation Type and Its Number Using in Stirring

In the impeller type screening, PBT-4 and hydrofoil impellers were compared in terms of TPH removal efficiency. Each type was varied its number (one, two, and three impellers) in a reactor to find out its effects on solid suspending. 50 g of DC had been washed with tap water 500 ml in the reactor with a rotational speed of 300 rpm for 30 min. The number of impellers of these two types was varied between one, two, and three per experiment. The result showed that using 1 impeller of PBT-4 provided the preferable percentage compared to 2 and 3 impellers of itself and hydrofoil in a reactor (**Figure 4.5**). It was noted that one impeller of PBT-4 had enough ability to suspend the soil matrix within the studied ratio of solid to liquid (1:10). From the experimental observation, since the second and the third impellers located far from the soil at the bottom of the tank, they were not significant effect on the mixing of this condition. This reason could explain based on the off-bottom clearance C, which is the height from the bottom of the reactor to the impeller located in the tank. C was studied to be 0.25 of tank diameter.
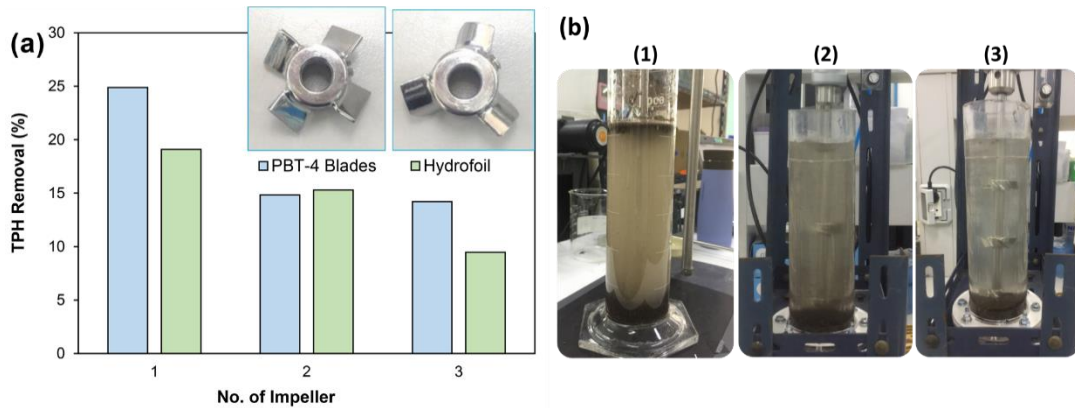
Figure 4.5 Effect of impeller design and operation on TPH removal efficiency

4.3 TPH Removal by Every Single Process

4.3.1 TPH Removal by Mechanical Stirring, IAF, and DAF Processes

Three different rotational speeds: 200, 400, and 600 rpm were employed for an hour with 10 minutes sampling time step in the stirring process. As seen in **Figure 4.7 (A)**, when the impeller speed increased to the higher level, it was remarkably showed that the values of response (TPH removal) were transforming to increase within the treatment time set. Regarding the rotational speed, 600 rpm provided the highest performance, followed by 400 rpm and 200 rpm. It was concluded that for one hour of washing time, 600 rpm of rotational speed resulted in almost 30%, which was higher than 25% and 20% by other rotational speeds 400 rpm and 200 rpm, respectively. This phenomenon could explain based on the turbulence in mixing conditions generated by rotational speed. The turbulence conditions might break the attraction between the TPH and the soils; hence, the TPH molecules detached from the soil and resulted in greater removal efficiency.
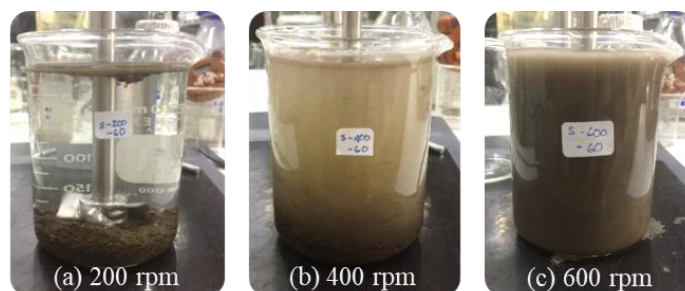
Figure 4.6 The DC washed by different rotational speeds of the mechanical stirring
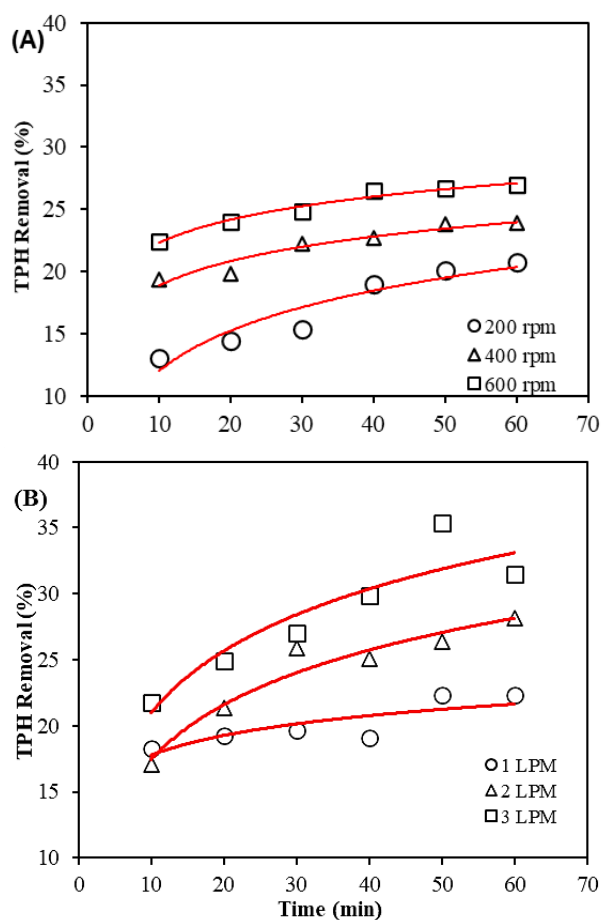
Figure 4.7 (A) Effect of different rotational speeds in stirring and (B) airflow rates in IAF processes

Moreover, in the IAF process, three airflow rate conditions: 1, 2, and 3 LPM were investigated on TPH removal as well. In **Figure 4.7 (B)**, the graph showed that 1 LPM provided the lowest treatment performance compared to the other two conditions (2 and 3 LPM), whereas 2 LPM and 3 LPM resulted in sharper treatment since the first 30 min. At the longest time for 1 hour in washing, approximately 20% of TPH was eliminated by IAF using Q_g = 1 LPM, and roughly 30% was eliminated by Q_g = 2 and 3 LPM. It was observed that the bubbles generated by IAF alone created the turbulent mixing inside the reactor when Q_g was increased. Similar to mechanical stirring, the more turbulent conditions, the more TPH eradication. Therefore, it could be stated that better treatment performance was achieved at the elevated airflow rate and time set.
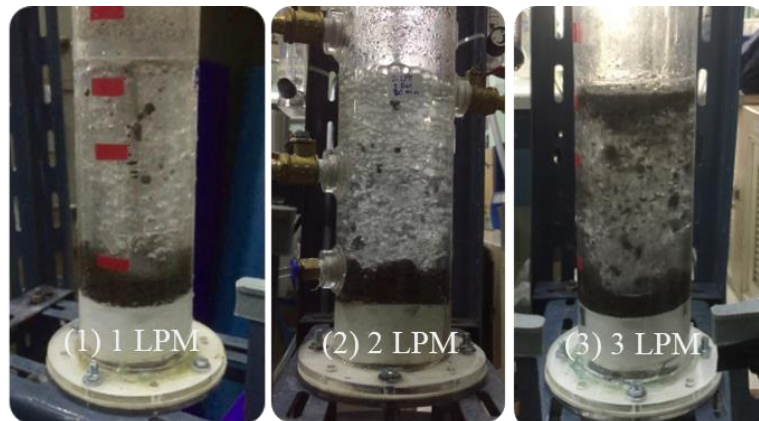
Figure 4.8 The DC washed by different airflow rates in IAF

Additionally, in the DAF process, three saturated pressures (P_s) of 2, 3, 4 bars were explored in the same washing time. The result was exhibited that almost 40% of removal proficiency was observed at the P_s of 4 bars with a washing time of 60 min, as seen in **Figure 4.9**. From the observation, there were not many of the bubbles produced in the flotation cell for the saturated pressure of 2 bars, which caused TPH removal efficiency from DC was less (roughly 26% after 1 hour of washing time). However, there were many tiny bubbles produced at the saturated pressure of 4 bars, which resulted in the TPH removal percentage higher than other pressures (see **Figure 4.10**). These results evidently demonstrated the applicability of microbubbles for effectively cleaning TPH from DC base on the increasing of the saturated pressure (P_s).
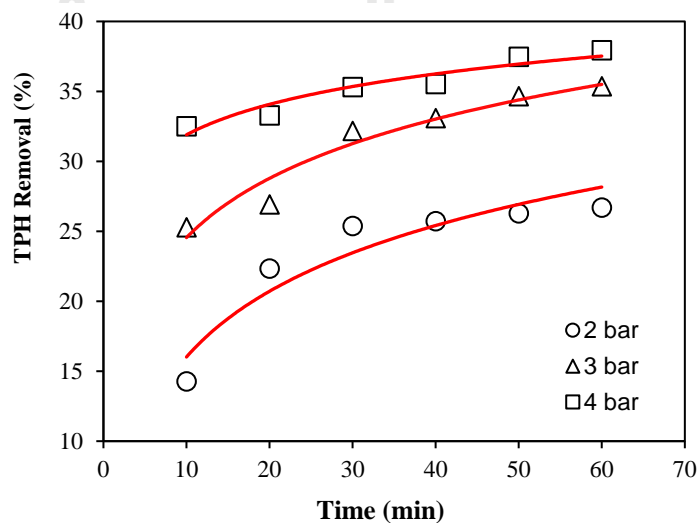
Figure 4.9 Effect of different saturated pressures in the DAF process
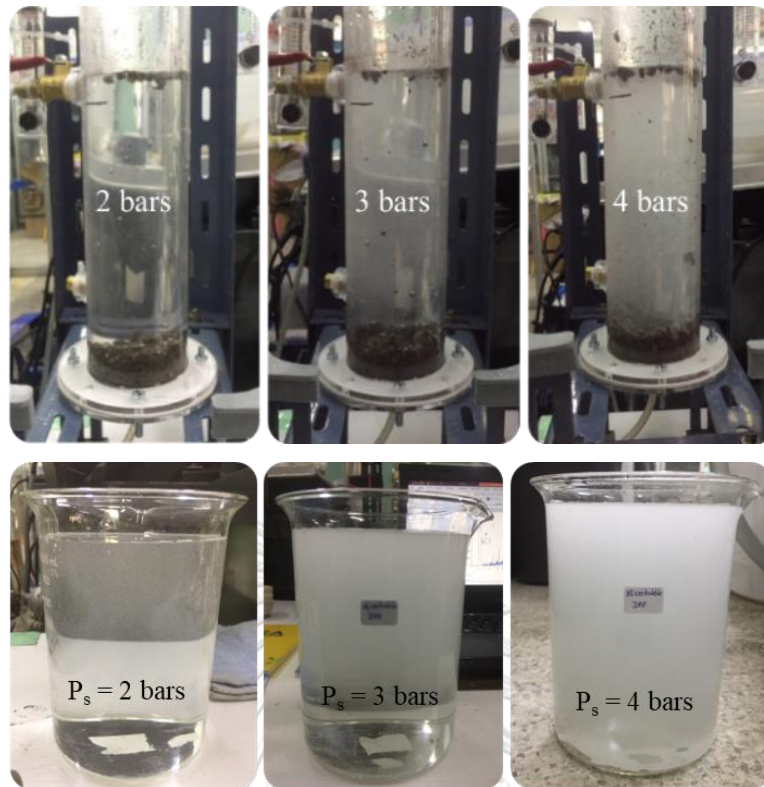
Figure 4.10 The generated microbubbles by saturated pressure from the DAF tank

4.3.2 Velocity Gradient in Mechanical Stirring

Table 4.3 was illustrated about the calculation of the velocity gradient base on equation 3.3 and 3.4 (Chapter 3). The results showed the gradients increased according to the rational speed (n: 200, 400, 600 rpm). These rationalizations revealed the more mixing speed using, the more turbulent of mixing inside the reactor was, as represented in Reynold numbers that were greater than 10,000, known as the turbulent conditions in the mixing system. Then, when the impeller speed **n** was operated greater such as 200 rpm, 400 rpm, to 600 rpm, the high turbulent flow inside the tank would increase and represent as the velocity gradient from 25, 560 s^{-1}, 72, 295 s^{-1}, to 132, 814 s^{-1}, respectively.

$$G = \left(\frac{P}{\mu_L V_L} \right)^{0.5} \qquad \text{(Eq. 3.3)}$$

$$P = N_P \rho n^3 d^5 \qquad \text{(Eq. 3.4)}$$

Table 4.3 Velocity gradient calculation in the stirring process

N_p	ρ (kg/m³)	n (rpm)	n (rps)	d (m)	P (w)	μ_L (kg/m.s)	Reynold Number (N_R)	G (s⁻¹)
		Rapid Mixing in Mechanical Stirring						
0.9	997	200	3.333	0.03	0.0008	0.00089	3,361	55
		400	6.667		0.0065		6,721	156
		600	10.00		0.0218		10,082	286
Np = 0.9 for PBT-4 (Metcalf and Eddy., 2004)								

4.3.3 Velocity Gradient and Interfacial Area of Bubbles

Table 4.4 illustrated the calculation of the velocity gradient in the induced air flotation process that showed how bubbles made the turbulent flow inside the reactor compared to rotational speed (n) in the stirring process. It was observed that in different Q_g of 1, 2, and 3 l/min exemplified the higher velocity gradient as well, such as 254, 359, 440 s⁻¹, respectively. Yet, these values were low compared to the velocity gradient of the stirring process. However, the high G values of bubbles indicated the effectiveness of the removal efficiency of TPH since the collision probability between air bubbles and oil droplets rose according to G values (Hoseini, Salarirad, Alavi Moghaddam, & Treatment, 2015).

$$G = \left(\frac{P_C}{\mu_L V_L} \right)^{0.5} \qquad (Eq.3.5)$$

$$P_C = C_1 Q_g \log\left(\frac{h+10.4}{10.4} \right) \qquad (Eq.3.6)$$

Table 4.4 Velocity gradient calculation in IAF process

Q_g (lpm)	Q_g (m³/min)	C_1	h (m)	V (m³)	P_c (w)	μ (kg/m.s)	U_B (mm/s)	G (s⁻¹)
		Induced Air Flotation (IAF)						
1	0.001	3904	0.106	0.0003	0.0172	0.00089	240	254
2	0.002				0.0344		267	359
3	0.003				0.0516		300	440

❖ **Bubbles Diameter (D$_B$)**

The bubble diameter (D$_B$) was determined through the equivalent diameter (d) and the Sauter Mean diameter of bubbles (D$_{32}$) as followed.

$$D_{32} = \frac{\sum_{i=1}^{N} d_1^3}{\sum_{i=1}^{N} d_1^2} \quad ; \quad d = \sqrt[3]{E^2 e}$$

Table 4.5 Interfacial area (a) and a/G ratio in IAF unit

Induced Air Flotation (IAF)					
Q$_g$ (lpm)	D$_{32}$ (mm)	U$_B$ (mm/s)	a (m^{-1})	G (s^{-1})	a/G (s/m)
1	3.42	240	42.96	254	0.169
2	4.09	267	64.50	359	0.180
3	4.27	300	82.31	440	0.187

Likewise, **Table 4.6** demonstrated how the bubbles generated in the DAF system to create turbulent conditions inside the tank. It was seen that the G values of bubbles created by the DAF system were lower than that in IAF, which showed only 113, 146, and 155 s^{-1} of saturated pressure 2, 3, 4 bars, respectively. These values represented the turbulent flow inside the reactor were less compared to the IAF and mechanical stirring unit. However, the small sides of bubbles and their rising velocity (U$_B$) represented the higher efficacy of TPH removal due to the collision between small bubbles and hydrocarbons droplets in DC. As mentioned by Wang et al. (2010), the smaller diameter of small bubbles provided a bigger surface area and caused the velocity to rise gradually than the bigger bubbles. So, the slower rising velocity contributed to the increase in flotation efficiency. Then, the effect of a-value and G-value of bubbles in the DAF system were studied in the next section as well.

Table 4.6 Velocity gradient (G) calculation in the DAF unit

Dissolve Air Flotation (DAF)								
P$_s$ (bar)	Q$_g$ (m^3/min)	C$_1$	h (m)	V (m^3)	P$_c$ (w)	μ (m^2/s)	U$_B$ (mm/s)	G (s^{-1})
2	0.00020				0.0034		19.774	113
3	0.00033	3904	0.106	0.0003	0.0057	8.9 x 10^{-7}	8.170	146
4	0.00037				0.0065		4.364	155

Table 4.7 The interfacial area (a) and a/G ratio in the DAF unit

Dissolved Air Flotation (DAF)					
P_s (bar)	D_B (μm)	U_B (mm/s)	a (m^{-1})	G (s^{-1})	a/G (s/m)
2	179.7	19.774	0.196E+12	113	0.173E+10
2.5	140.9	12.157	1.057E+12	127	0.833E+10
3	115.5	8.170	4.596E+12	146	3.153E+10
4	84.42	4.364	34.28E+12	155	22.06E+10

4.3.4 Effect of a/G in IAF process

In this part, the interfacial area (a) and the rotational parameter (G) were analyzed to offer a better understanding of the TPH reduction productivity from the flotation unit. First of all, **Figure 4.11** illustrated the relationship between the bubble diameter (D_B) and the airflow rate (Q_g) for the IAF process that applied in the experiments. Since this work used a rigid stone diffuser (see **Figure 3.7** in Chapter 3), It was remarked that the bubble diameters varied between 3.42 mm to almost 4.27 mm while the airflow rates were changed between 1.0 to 3.0 l/min, respectively. Moreover, the bubble dimensions almost remained stable at a higher airflow rate of 2 to 3 l/min in the IAF process. It indicated that when Q_g rose, the size of the bubbles formed by the rigid stone diffuser was slightly increased too. As mentioned by Painmanakul et al. (2010), the changes in bubble diameters were related to the buoyancy forces and surface tension. It was noted that the rising velocity that was obtained and calculated were based on the bubble sizes and the airflow rates, as repeated in **Table 4.5**.
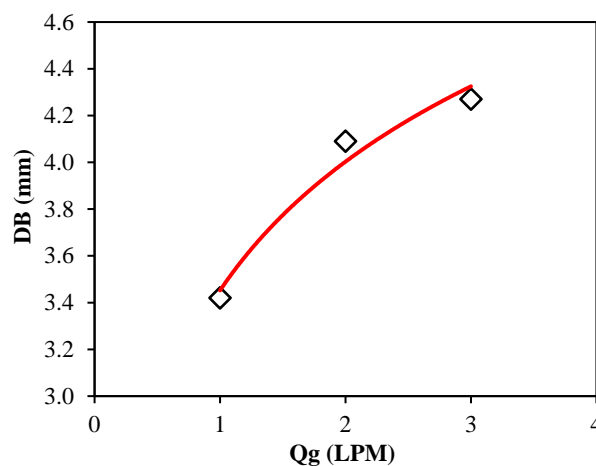
Figure 4.11 Bubbles size (D_B) vs. Airflow rate (Q_g) in the IAF process

As shown in **Figure 4.12 (A)**, the interfacial areas (a) of bubbles from IAF varied from approximately 43 to 82 m$^{-1,}$ while airflow rates altered from 1.0 to 3.0 l/min. It was noticed that the values corresponded to the number of bubbles formed in the system. Therefore, the values of (a) increased steadily with the injection airflow rate. Moreover, the G-vales rose gradually with the airflow rate as well. Their values were between almost 250 to 450 s^{-1}, whereas the airflow rates changed between 1.0 and 3.0 l/min. This information was revealed the characteristics of more turbulent mixing conditions created by the higher airflow rate (**Figure 4.12 (B)**).
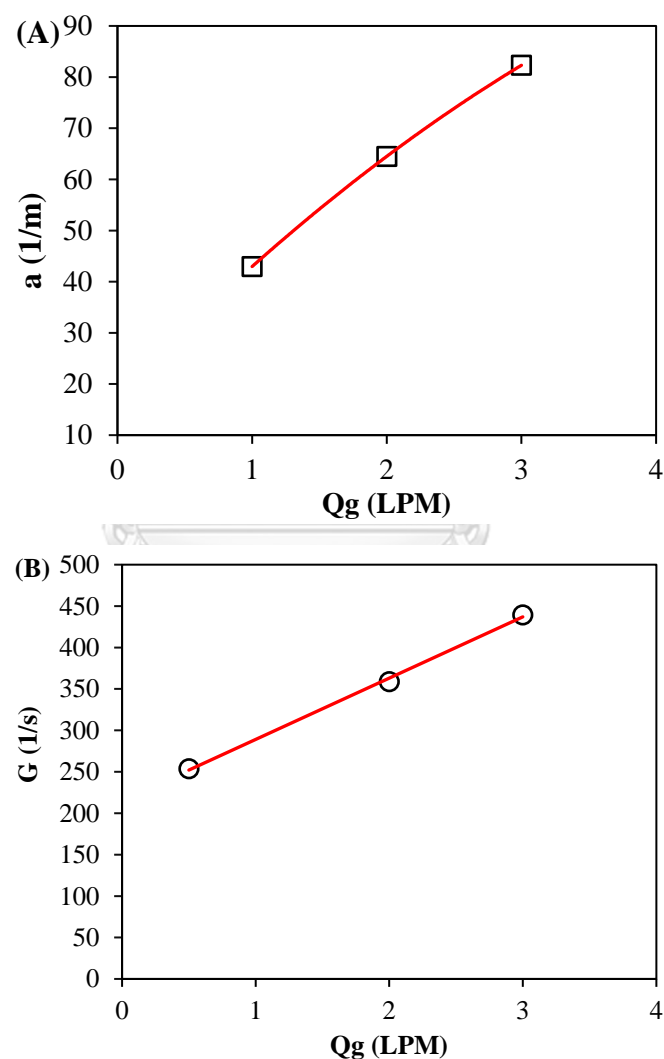
Figure 4.12 Bubbles interfacial area (a), and Gradient velocity (G) comparing to Airflow rate (Q$_g$) in IAF

In order to clarify the available surface of the bubbles area and the mixing conditions that happened in the flotation cell, the proportion between the interfacial area and the

velocity gradient was determined in **Figure 4.13**. As presented in the graph, the proportion of a to G changed between almost 0.17 and 0.19 s/m, while airflow rates could vary between 1.0 and 3.0 l/min. Furthermore, the supreme values of the a/G could receive at the airflow rate of 3.0 l/min, which corresponded to the Q_g that provided the highest removal proficiency obtained in the IAF process (see **Figure 4.13 (B)**). Therefore, the a/G portions could use in order to observe the maximum conditions of removal eff (%) in IAF. It was noted that the greater a/G indicated the higher contact probability between bubbles and oils with the high interfacial area of the bubble. Thus, the Oils preferably attached to the bubbles, which accelerated the flotation of oils to the liquid surface, resulted in more significant TPH removal.
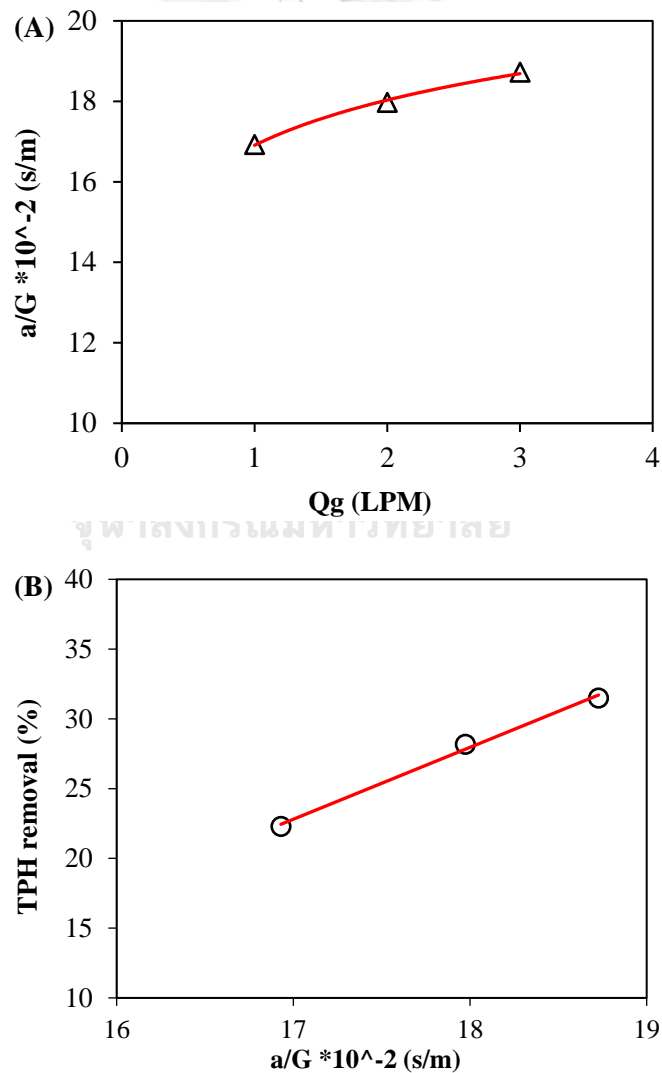
Figure 4.13 Effect of a/G value to airflow rate (A), and Effect of a/G value on TPH removal efficiency in IAF process (B)

4.3.5 Effect of a/G in DAF process

In general, the diameter of bubbles generated by the DAF system was tiny and could not measure directly. As suggested by Bensadok et al. (2007), the size of the bubbles could be calculated in theory based on the equation that showed in **Figure 4.14**. Due to the pressure limitation in the laboratory experiment, the pressures were operated between 2, 3, and 4 bars in the DAF tank. Although the number of bubbles would increase and the size of them would be smaller than the bubbles that created by 4 bars, the greater pressure than 5 bars were not likely to recommend for using in the DAF system, so the greater pressure than 5 bars was not considered in this study (Radzuan et al., 2016). As proved in **Figure 4.14**, it was observed that at P_s of 4 bars was represented the D_B of approximately 80 µm, while other P_s of 3 and 2 bars made the size of bubbles to be around 100 and 180 µm, respectively. It could identify that higher saturated pressure formed the smaller microbubbles and the greater amount of generated bubbles. In theory, the smaller diameter of air bubbles size had a critical surface area. Furthermore, the rising velocity was more slowly than the bigger air bubbles in the same liquid, so that the slower rising velocity could contribute to a higher collision rate with oil droplets, which made the flotation efficiency increased (see the results of TPH removal efficiency **Figure 4.9**).
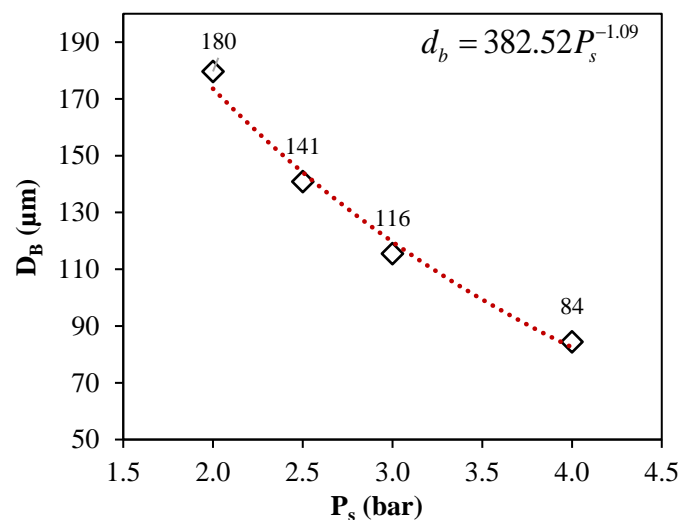
Figure 4.14 Bubbles size (D_B) vs. Saturated pressure (P_s) in the DAF process

As shown in **Figure 4.15**, the velocity gradient ranges generated by saturated pressures were showing the contrast values compared to bubbles diameters. It was

indicated that higher pressure would elevate velocity gradient (G) slightly, which was from around 110 s^{-1} to 150 s^{-1} by P$_s$ of 2 bars to 4 bars, individually. This marginally rise of G exhibited the low mixing conditions in the washing column; hence, it meant that the particles would not suspend enough inside the tank. However, when the saturated pressure increased, it was noticed that the diameters of the bubbles were smaller, which caused the rising velocity (U$_B$) of bubbles to become slower as well. In theory, the slower rising rate of bubbles was acquired since it would provide a long time for bubbles to attach with oil droplets. Thus, even though P$_s$ was regulated to 4 bars or higher than that and the velocity gradient (G) was rising, it still kept the rising velocity being slow in the system (see **Table 4.5**).
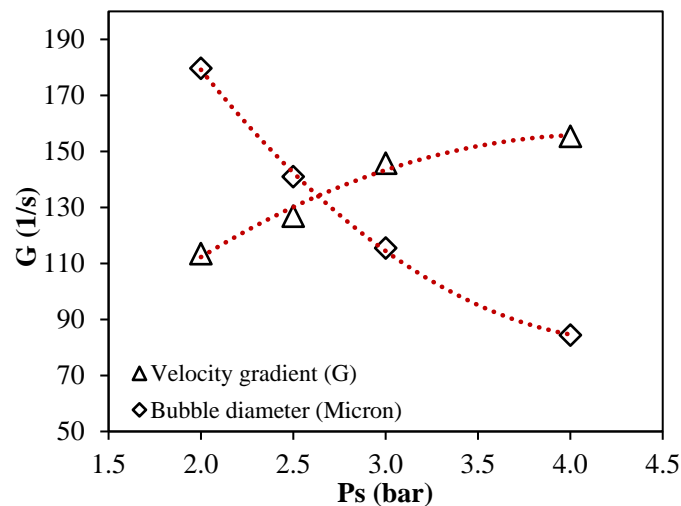
Figure 4.15 Bubbles diameter (DB) vs. Velocity gradient (G) in the DAF process

Similar to the IAF process, the interfacial area, **a** with velocity gradient, **G** were studied in the DAF process. According to the differences between the air bubble diameter produced in different processes, the diameter of the air bubble in the DAF was much smaller (roughly from 80 to 180 µm) than that in the IAF process (3.42 to 4.27 mm). So, the a and G values in DAF operation was also represented in much smaller values. As shown in **Figure 4.16** below, the four points were the a/G data that determined from the bubbles generated by pressure 2, 2.5, 3, and 4 bars, correspondingly. It was noticed that the a/G ratio rose within the increase of P$_s$ (2 to 4 bars), and it started to be almost constant at P$_s$ of 3 to 4 bars. This phenomenon was

explained the great a/G corresponded to the great TPH removal efficiency from DC in the single process itself.
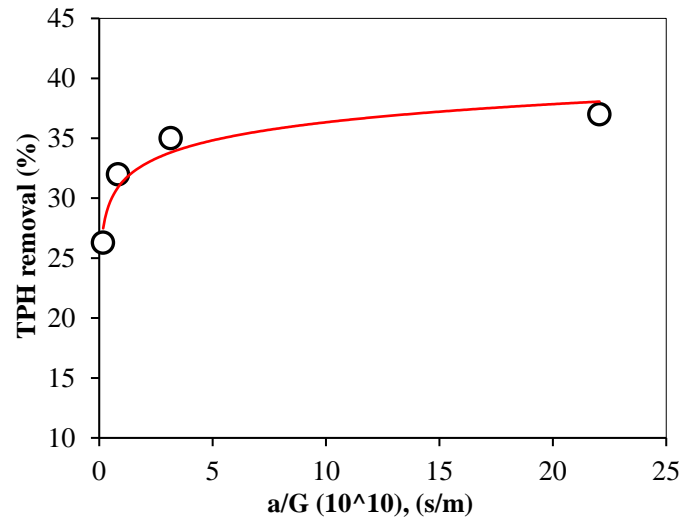
Figure 4.16 The consequence of a/G over TPH removal eff. in the DAF process

4.4 TPH Removal by Mechanical Stirring Combined with IAF/DAF

The effect of rotational speed (V_m) was accounted for the main factor for mechanical stirring, while the airflow rate (Q_g) was given as the considered factor in the IAF process. Then, these two parameters, including rotational speed and airflow rate, were also considered comparing to the washing time. The three conditions of V_m, Q_g, and time t ranked from the smallest to the highest range, including the first condition (200 rpm, 1 LPM, 20 min), second condition (400 rpm, 2 LPM, 40 min), and the third condition (600 rpm, 3 LPM, 60 min), respectively were studied. The results showed that the first and the second conditions gave a similar proportion of TPH removal, which were relatively 30%. However, the third condition that was considered as the high value of each parameter provided a high percentage, which showed roughly 37%, as illustrated in **Figure 4.18**.

Afterward, the combinations of stirring combined with DAF were examined in order to maximize TPH removal efficiency. The three designed parameters, such as saturated pressure (P_s), rotational speed (V_m), and the washing time (t), were observed. The three conditions of P_s, V_m, and t ranked from the smallest to the highest values including the first condition (2 bar, 200 rpm, 20 min), 2nd condition (3 bar, 400

rpm, 40 min), and the 3rd condition (4 bar, 600 rpm, 60 min), were determined and compared to the IAF. The results showed that stirring combined with DAF that used the condition, i.e., 4 bars, 600 rpm, and 60 min of treatment time was more effective (nearly 45% removal efficiency) compared to the other conditions, and the stirring combined with IAF, as represented in **Figure 4.18**. It was because microbubbles generated by DAF provided a high interfacial area, which enhanced the attachment between TPH and bubbles, then accelerated the flotation of oil molecules up to the liquid surface and resulted in high TPH removal capacity. Additionally, operating at high rotational speed (600 rpm) provided high turbulence that caused the DC particles suspended, so that the bubbles could carry the TPH up to the surface and removed.

Therefore, as the combination of "Stirring-DAF" provided a positive effect on TPH removal, this process was selected for detailed studying through the Design of Experiment (DOE) in order to define the factor optimization throughout the combination process, as described in the next section (Part 4.5).
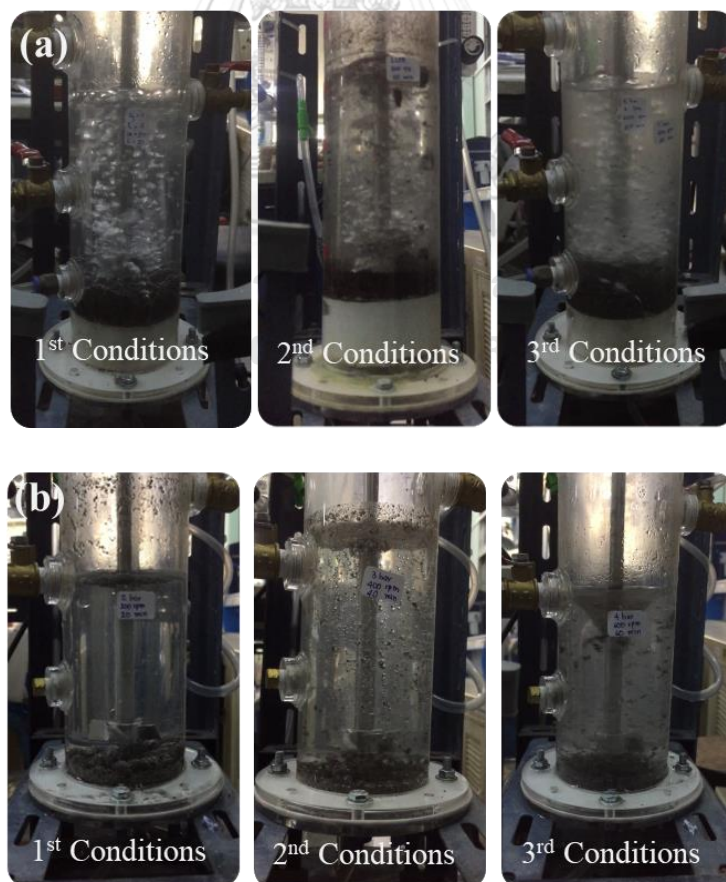
Figure 4.17 Three washing conditions of stirring with IAF (a), stirring with DAF (b)
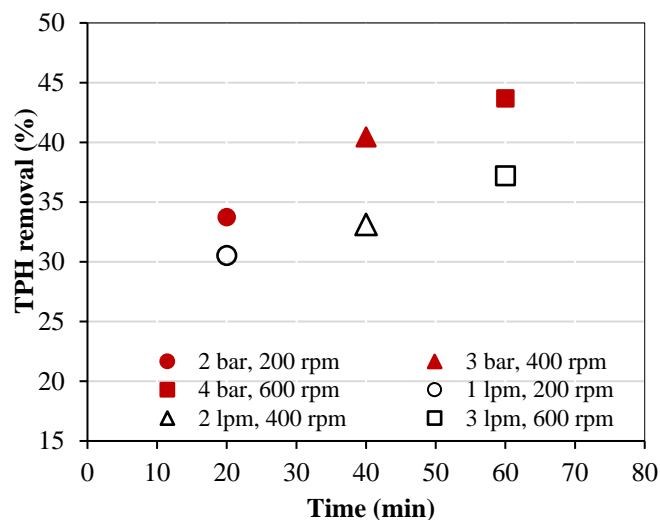
Figure 4.18 The comparison between stirring with IAF and stirring with DAF

4.5 Study Factor Optimization of Stirring Combined with DAF Process Using the Design of Experiments (DOE)

4.5.1 Experimental Design

DOE is a function that is used in the computer software named Minitab 17®. The three parameters that influence hydrocarbons removal in this process are investigated, including saturated pressure (P_s in DAF unit), mixing speed (V_m in stirring process), and washing time (t). The factor levels below were selected according to their effective ranges that were studied and obtained from the preliminary experiment. Hence, the three levels as designed by central composite deign-response surface methodology (CCD-RSM) were depicted in **Table 4.8**.

Table 4.8 Variables and factor levels using to design in CCD-RSD

No.	Parameters	Unit	Level		
			-1	**0**	1
1	Saturated Pressure (P_s)	bar	2	3	4
2	Mixing speed (V_m)	rpm	200	400	600
3	Washing time (t)	min	20	40	60

Experimental Results for TPH removal of "Stirring-DAF."

From CCD-RSD, the experimental conditions were generated as a single replication and showed the codes of design for 20 experiments, as listed in **Table 4.9**. TPH

removal efficiency was the response variable that was defined by the minimum and maximum values of saturated pressure (P_s), rotational speed (V_m), and washing time (t) using in stirring combined with the DAF system. The results were analyzed by statistical analysis (ANOVA) and explained based on F-test with P-value to verify the confidential level of factors optimization. A P-value of 0.05 or smaller than that for each factor was indicated the statistical significance at a 95% confidence level that selected in the study. Moreover, every result was checked by the main effect plots for each parameter, and by the contour plots for the interaction between two parameters.

Table 4.9 Experimental results for factors optimization

No.	P_s (bar)	V_m (rpm)	t (min)	TPH Removal (%)
1	2	200	20	33.73
2	4	200	20	41.45
3	2	600	20	42.17
4	4	600	20	42.43
5	2	200	60	30.35
6	4	200	60	42.89
7	2	600	60	42.56
8	4	600	60	43.68
9	1.32	400	40	29.43
10	4.68	400	40	43.46
11	3	63.64	40	27.09
12	3	736.4	40	40.29
13	3	400	6.36	38.13
14	3	400	73.64	40.90
15	3	400	40	40.46
16	3	400	40	39.45
17	3	400	40	38.77
18	3	400	40	38.77
19	3	400	40	38.77
20	3	400	40	38.77

4.5.2 Main Effect Plot of Line-Level and Interaction Parameters

From Minitab 17®, the model adequacy checking examined and revealed the reliability of the factor optimization. According to **Figure 4.19**, it was concluded that the data was reliable because the normal probability plot steadily followed a straight

line, while the versus fits were randomly scatted around zero lines, and the versus order fluctuated around the centerline as well (Minitab., 2000; Yotto., 2015).
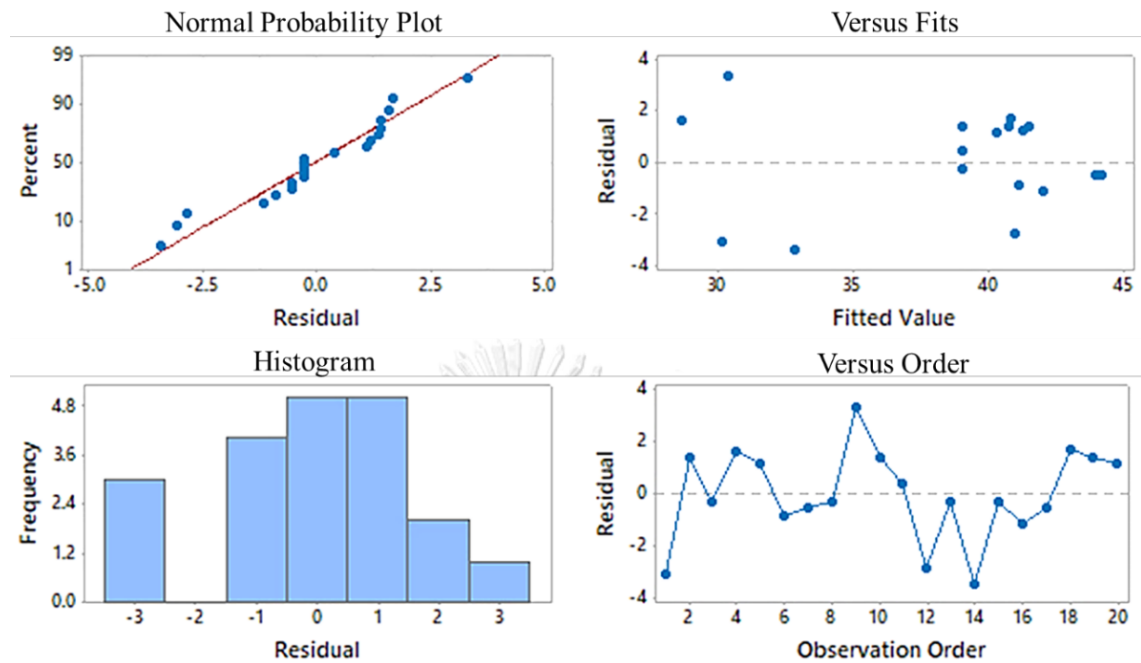
Figure 4.19 Residual plot of model adequacy for TPH removal efficiency

Moreover, the main effect parameters were illustrated in the line-level plot in **Figure 4.20**. It was observed that P_s provided a high percentage of TPH removal when it rose from 2 to 4 bars and so on. Based on this line plot, V_m was effective between 400 rpm and 600 rpm, whereas this value showed a slight decrease at a higher speed. It was noted that the period using in this experiment demonstrated better results, starting from 40 to 80 minutes of washing time. However, in order to determine the optimum level as the interaction for the combination process, these three variables were explained, as given in **Figure 4.21**.
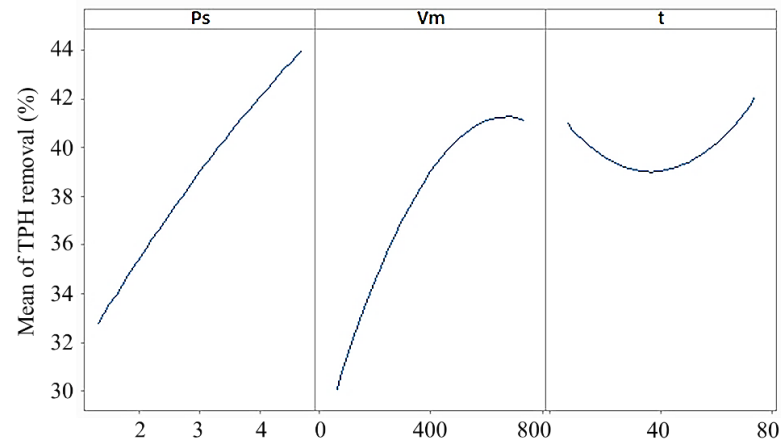
Figure 4.20 Main effects plot of the fitted mean value of TPH removal

Likewise, the contour plot was confirmed that the low rotational speed would not provide a better result if it was used with the lower saturated pressure; however, the increased pressure until 4 bars or higher had a positive effect on TPH removal when the rotational speed regulated to the higher values, such as from 400 to 600 rpm. Furthermore, once the saturated pressure started interacting with washing time, it was shown that at any time between 20, 40, to 60 minutes could give a better percentage of TPH elimination if the P_s were used from 3 to 4 bars. Similarly, the rotational speed V_m was comparable to P_s if they were analyzed with the time t. when the rotational speed used was higher, especially from 400 to 600 rpm, the time t could operate between 20, 40, to 60 min or more than that to obtain higher TPH removal %.
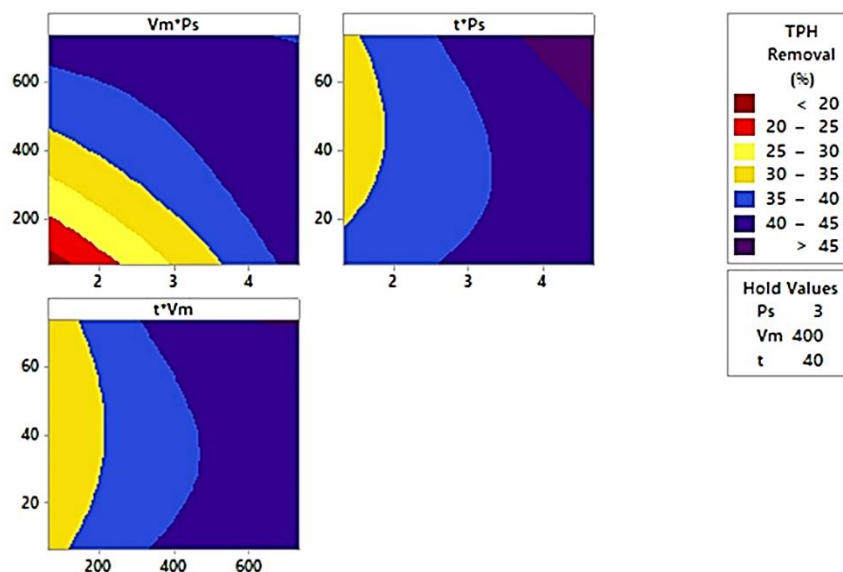
Figure 4.21 Contour plots of two factors interaction for factor optimization

4.5.3 Statistical Analysis

Moreover, from the experimental results, the optimum level could analyze via ANOVA and the second-order polynomial equation (E.q. 2.12, Chapter 2), which could derive into the TPH removal equation as a function of rotational speed (V_m), saturated pressure (P_s), and washing time (t), as given in **Equation 4.3**. According to ANOVA results obtained from RSM design, it was found that F-test was roughly 87% of the confidential level, and the p-value was 0.13, which designated the significance of parameters using in the experiment. The F-test and P-value were determined in **Table 4.11** and showed themselves about their significance. P_s and V_m got the number of F-test of 26.05 and 25.33 with the P-value of 0.000 and 0.001, which were smaller than P = 0.05, respectively. These numbers represented the important number that needed in the experiment. However, from the table, t was not significant since its F-test equal to 0.24, and P-value was 0.634, which was higher than P = 0.05.

From **Equation 4.1**, the predicted response (TPH removal efficiency) was plotted to compared to the actual response to evaluate the precision and the competency of the model. As a result, it was shown that the correlation $R^2 = 0.8691$ indicated a satisfied result of the model fit to the experimental data, as displayed in **Figure 4.22**.

$$\%TPH\ removal = 10.6 + 7.93\ P_s + 0.0711 V_m - 0.309t - 0.219\ P_s^2 - 0.000030\ V_m^2 + 0.00217\ t^2 - 0.01179\ P_s V_m + 0.0355\ P_s t + 0.000112\ V_m t \quad (Eq\ 4.1)$$

Table 4.10 Actual experimental results vs. prediction results in stirring with DAF

Run No.	P_s (bar)	V_m (rpm)	t (min)	%TPH removal Experiments	Prediction
1	2	200	20	33.73	30.44
2	4	200	20	41.45	40.38
3	2	600	20	42.17	40.75
4	4	600	20	42.43	41.25
5	2	200	60	30.35	28.76
6	4	200	60	42.89	41.54
7	2	600	60	42.56	40.86

Run No.	P_s (bar)	V_m (rpm)	t (min)	%TPH removal	
				Experiments	Prediction
8	4	600	60	43.68	44.20
9	1.32	400	40	29.43	32.88
10	4.68	400	40	43.46	44.03
11	3	63.64	40	27.09	30.23
12	3	736.36	40	40.29	41.13
13	3	400	6.36	38.13	41.00
14	3	400	73.64	40.90	42.07
15	3	400	40	40.46	39.08
16	3	400	40	39.45	39.08
17	3	400	40	38.77	39.08
18	3	400	40	38.77	39.08
19	3	400	40	38.77	39.08
20	3	400	40	38.77	39.08
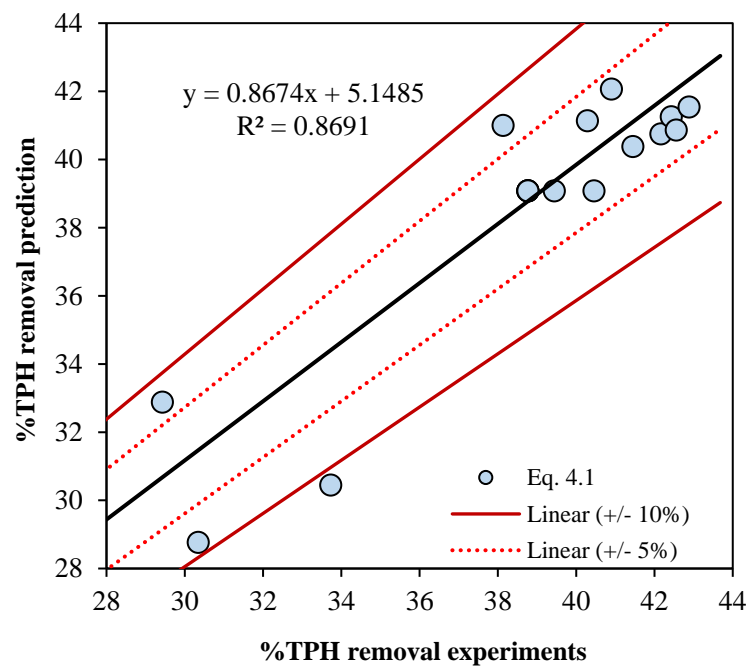
Figure 4.22 Experimental results vs. Predicted results of TPH removal efficiency

Table 4.11 Analysis of variance (ANOVA) for factor optimization

Analysis of Variance						
Source	**DF**	**Adj SS**	**Adj MS**	**F-value**	**P-value**	
Model	9	382.413	42.49	7.38	0.002	
Linear	3	297.092	99.031	17.21	0	
P_s	1	149.928	149.928	26.05	0.000	Significant
V_m	1	145.78	145.78	25.33	0.001	Significant
t	1	1.385	1.385	0.24	0.634	Not significant
Square	3	35.17	11.723	2.04	0.173	
Ps^2	1	0.694	0.694	0.12	0.736	
Vm^2	1	20.511	20.511	3.56	0.088	
t^2	1	10.828	10.828	1.88	0.2	
2-ways interaction	3	50.151	16.717	2.9	0.088	
$Ps*V_m$	1	44.515	44.515	7.74	0.019	
$Ps*t$	1	4.022	4.022	0.7	0.423	
V_m*t	1	1.614	1.614	0.28	0.608	
Error	10	57.549	5.755			
Lack-of-Fit	5	55.166	11.033	23.16	0.002	
Pure Error	5	2.382	0.476			
Total	19	439.961				
Model Summary						
	S	**R-sq**	**R-sq (adj)**	**R-sq (pred)**		
	2.398	86.92%	75.15%	3.71%		

4.5.4 Optimum Conditions

According to the above results, the optimum conditions of stirring combined with the DAF process were found that when saturated pressure **(P_s) was operated at 4 bars**, the rational speed **(V_m) was 400 rpm**, and the washing time **(t) was 70 minutes** so that the maximum TPH removal capacity would achieve around **50%**.

From the actual experiment, this maximum condition was tested by giving a similar prediction. From P_s equal to 4 bars, V_m same to 400 rpm, and t equal to 70 minutes, the efficiency was achieved **47.02%**.

4.6 Study the Effect of a/G Over the Combination Processes

4.6.1 The Effect of a/G Over DAF to the "Stirring-DAF"

In this section, a/G values in the DAF system were analyzed and drawn the comparison to the combination process of "Stirring-DAF" for both tap and salty water. The values of "Stirring-DAF" here were obtained from the optimum conditions that were found from the DOE, which were P_s = 4 bars, V_m = 400 rpm, and t = 70 min. Then, these conditions were experimented, followed by P_s equal to 3 bars, 2.5 bars, and 2 bars in both tap and saline water in order to investigate the removal efficiency of TPH compared to a/G ratio.

As stated in **Figure 4.23**, it was noted that the treatment efficiencies of DAF and "Stirring-DAF" with both tap and saline water grew linearly along with a/G value. It was observed that the differences in removal efficiency from DAF to "Stirring-DAF" were investigated at the same a/G values. However, since "stirring-DAF" was the combination process between tiny bubbles and stirring, the velocity gradient (G) of these two processes were sum up together, which cause the a/G of this combined process was lower than DAF, yet it proved to obtain higher proficiency in TPH removal in both tap and salty water. It was confirmed that not only microbubbles that produced in the DAF unit had an effect on TPH removal, but also the effect of mixing condition that came from the rotational speeds caused the DC suspended and provided the chance for bubbles attachment.
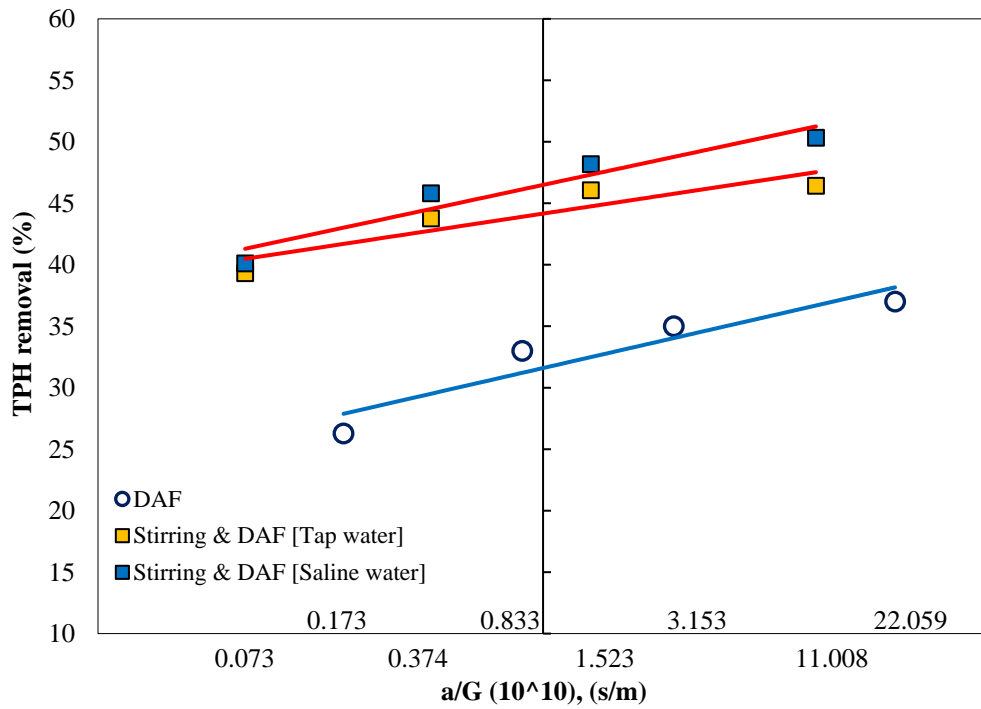
Figure 4.23 The a/G values of DAF compared to "Stirring-DAF" on TPH removal efficiency
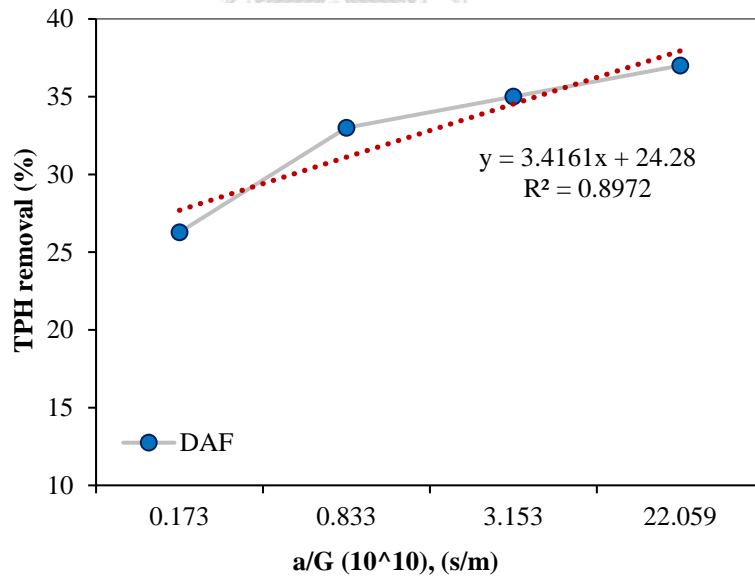
Figure 4.24 Effect of a/G values of DAF on TPH removal efficiency and trendline prediction
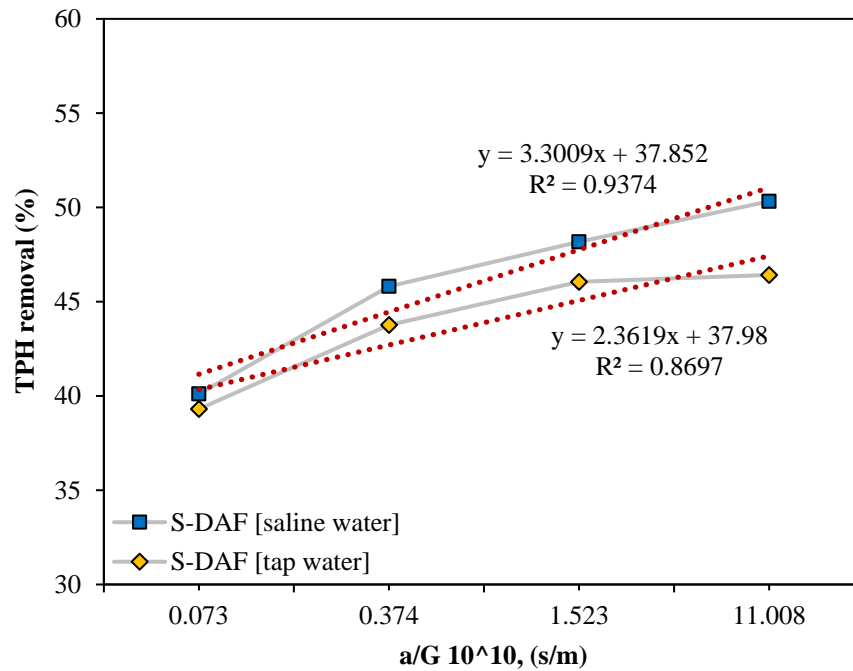
Figure 4.25 Effect of a/G values of "Stirring-DAF" on TPH removal efficiency and trendline prediction

Table 4.12 The values of a/G of stirring-DAF on TPH removal

Ps (bar)	a [DAF] 10^{10} (m^{-1})	G [DAF] (s^{-1})	G (Stirring) 400 rpm	a/G [DAF] 10^{10} (s/m)	a/G [S-DAF] 10^{10} (s/m)
2	19.65	113		0.173	0.073
2.5	105.68	127	156	0.833	0.374
3	459.64	146		3.153	1.523
4	3,427.93	155		22.059	11.008

Table 4.13 The constants that obtained from the linear equations for the DAF and stirring-DAF

Systems	Slope (A)	Intercept (B)	R-square
DAF	3.416	24.280	0.897
Stirring-DAF [Tap water]	2.362	37.980	0.870
Stirring-DAF [Saline water]	3.301	37.852	0.937

According to **Table 4.13**, the values of slope (A), the intercept (B), and the R-square, which was acquired from the linear equations, were presented. From the graph, we could observe and analyze:

➤ It was found that the slope (A) of Stirring-DAF that used salty water was slightly bigger than that used with tap water. It signified that in the same system, the removal efficacy would improve due to the effects of NaCl solutions. Moreover, it could be included that the elevated influence of Stirring-DAF even using tap and saline water was remarkable growth rather than using the DAF alone.

➤ The treatment efficiencies obtained from the DAF, Stirring-DAF with both tap and saline water increased linearly along with a/G values. Likewise, the a/G values of Stirring-DAF were observed to be a bit lower than the DAF system due to the combination of the velocity gradient between stirring and DAF. However, if we investigated at the same values of a/G, the variations of TPH removal from the combination process showed a greater removal percentage compared to the DAF system (**Figure 4.23**). This case confirmed that not only the interaction of the tiny bubbles to the oil droplets inside the tank but also the mixing conditions of stirring was also contributed to the removal performance.

➤ Moreover, the value of slope (A) obtained from the DAF unit tended to be steeper within the a/G ratio, yet it represented a lower percentage of TPH removal efficiency than the combination of Stirring-DAF at the same a/G value (**Figure 4.24**). For this reason, it could be concluded that the mixing condition and the effect of the interfacial area of tiny bubbles in the DAF system alone showed a small effect in TPH removal compared to Stirring-DAF.

➤ In Stirring-DAF by saline water, the value of slope (A) was also sharper than tap water (A = 3.3) (**Figure 4.25**). It was observed that saline water had an effect within the system and was expected to obtain higher TPH removal efficiency when the a/G ratio increased.

➤ In addition, the value of the intercept (B) also indicated TPH removal efficiency obtained from the physical processes. In case DAF or Stirring-DAF were not applied into the system (there were not a and G that were applied into the system), it could represent that there was only DC that was soaked into tap water. So, TPH could also be removed from DC approximately **24%** to **38%,** respectively, according to the studied duration (**Table 4.13**).

➤ Similarly, in case the washing media was changed into another type such as saline water, the percentage of TPH seemed to remain constant and could also be

naturally removed from DC approximately **38%** at the studied duration if stirring and tiny bubbles were not applied into the system.

Therefore, regarding the importance of the above discussion, the trendline prediction between the treatment proficiency and the a/G values in DAF, Stirring-DAF [tap water], and Stirring-DAF [saline water] was employed in order to estimate the further treatment percentages for the combination between 2 main physical processes such as Mbs application and stirring processes.

4.6.2 The Effect of a/G Over DAF to the "Stirring-IAF"

The graph from **Figure 4.26** focused on the study of a/G ratio in the combination of the "Stirring-IAF" process. As seen in the diagram, the a/G of IAF surged linearly within the R^2 of 0.996. These results showed the increase of TPH reduction based on the increase of airflow rate in IAF alone. However, the IAF represented the least percentage of TPH removal compared to the "Stirring-IAF." It was reasonable to explain that the linear increase of a/G value in both IAF and "Stirring-IAF" processes represented the growth of TPH removal from DC. From the results, the largest airflow rate in IAF showed a percentage of approximately 30% and surged to around 35% by combining with the stirring process. It could be concluded that the mixing conditions in both stirring and bubbles application in IAF reveal the small effect in TPH removal from DC.

Therefore, even though the a/G values in "Stirring-IAF" could exhibit the a/G the higher TPH reduction than a single process (IAF), it was still noticed to be lower compared to "Stirring-DAF."
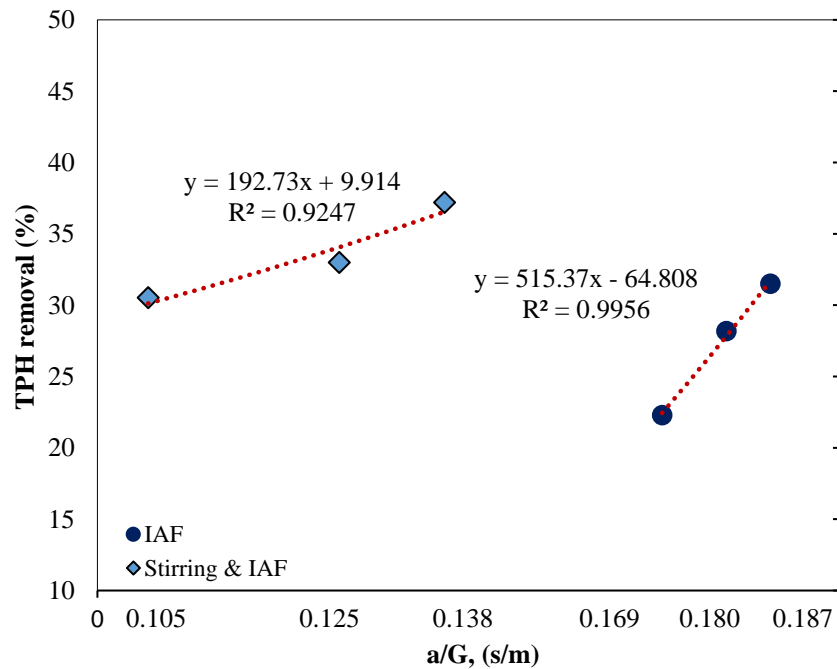
Figure 4.26 Effect of a/G values of DAF comparing to IAF, "Stirring-IAF" and "Stirring-DAF" on TPH removal efficiency

Table 4.14 The values of a/G of "Stirring-IAF" on TPH removal

Q_g (lpm)	a (m^{-1})	G [IAF] (s^{-1})	G (Stirring, 400 rpm)	a/G [IAF] (s/m)	a/G [S-IAF] (s/m)
1	42.96	254		0.169	0.105
2	64.5	359	156	0.18	0.125
3	82.31	440		0.187	0.138

4.7 Study Factor Optimization of the Mechanical Stirring Combined with IAF and DAF Using DOE

From the previous section, three parameters were studied, including P_s (DAF), V_m (Stirring), and time (t). As expected, they provided satisfying results within the optimum conditions obtained from DOE. In this part, four parameters were continuously investigated through DOE in order to find out whether they could give a better percentage of TPH removal or not. These four parameters were Q_g (IAF), P_s (DAF), V_m (stirring), and washing time (t). They were detailed as followed:

4.7.1 The Studied Parameters Using in Experiments

Every parameter was listed and set for their studied levels as designed by central composite deign-response surface methodology (CCD-RSM) and depicted in **Table 4.15**.

Table 4.15 Variables and factor levels using to design in CCD-RSD

No.	Parameters	Unit	Level		
			-1	**0**	**1**
1	Air Flowrate (Q_g)	LPM	1	2	3
2	Saturated Pressure (P_s)	bar	2	3	4
3	Mixing Speed (V_m)	rpm	200	400	600
4	Washing time (t)	min	20	40	60

Based on the CCD-RSM method, the experimental conditions were generated as a single replication and showed the codes of design for 31 experiments, as listed in **Table 4.16**. TPH removal efficiency was the response variable. The airflow rate (Q_g), saturated pressure (P_s), rotational speed (V_m), and washing time (t), were the parameters using in stirring combined with IAF and DAF processes. The results were analyzed by statistical analysis (ANOVA) that was explained based on the F-test with P-value to verify the intimate level of factors optimization. F-test quals to 95% with P-value equals to 0.05 were notified as to the significant conditions for this study. Similarly, every result was checked by the main effect plots of each parameter, and the interaction plots of two parameters, which were displayed as line-level plot and contour plots, correspondingly.

Table 4.16 Experimental results for factors optimization

Run No.	Q_g (lpm)	P_s (Bar)	V_m (rpm)	t (min)	TPH Removal (%)
1	1	2	200	20	21.75
2	3	2	200	20	33.19
3	1	4	200	20	32.38
4	3	4	200	20	34.64
5	1	2	600	20	40.55
6	3	2	600	20	42.01
7	1	4	600	20	40.05
8	3	4	600	20	41.55

Run No.	Q_g (lpm)	P_s (Bar)	V_m (rpm)	t (min)	TPH Removal (%)
9	1	2	200	60	21.09
10	3	2	200	60	33.76
11	1	4	200	60	31.56
12	3	4	200	60	36.13
13	1	2	600	60	51.48
14	3	2	600	60	55.54
15	1	4	600	60	45.51
16	3	4	600	60	54.38
17	0	3	400	40	36.07
18	4	3	400	40	36.03
19	2	1	400	40	38.95
20	2	5	400	40	36.94
21	2	3	000	40	37.68
22	2	3	800	40	51.83
23	2	3	400	00	0.000
24	2	3	400	80	39.98
25	2	3	400	40	47.41
26	2	3	400	40	46.61
27	2	3	400	40	47.01
28	2	3	400	40	46.85
29	2	3	400	40	46.85
30	2	3	400	40	46.85
31	2	3	400	40	46.85

4.7.2 Main Effect Plot of Line Level and Interaction Parameters

1). The Fitted Mean Value of TPH Removal

In accordance with the line plot, it was exhibited the main effect of every parameter, such as Q_g, P_s, V_m, and t, as represented in **Figure 4.27.** It was informed that airflow rate (Q_g) was efficient when it was operated between 2 and 3 l/min; however, it would slightly drop if the operation were higher than 3 l/min. In the meantime, P_s was applicable if it was set up in between 3 and 4 bars. These outcomes were also got confirmed with the number of bubbles produced inside the pressure vessel tank. Moreover, V_m showed a remarkable increase from the lowest to the highest value, which represented more rotational speed provided better TPH removal efficiency. Although it was a remarkable rising of V_m, washing time t was also showed its

effectiveness in the system. The time t started rising when it was operated from 30 minutes to 40 minutes and 60 minutes; however, that value would drop if the system increased higher than that. It meant that in between the time of 30 min to 60 min were the better condition in the washing process, yet it still almost remained the same, even the time t had been increased.
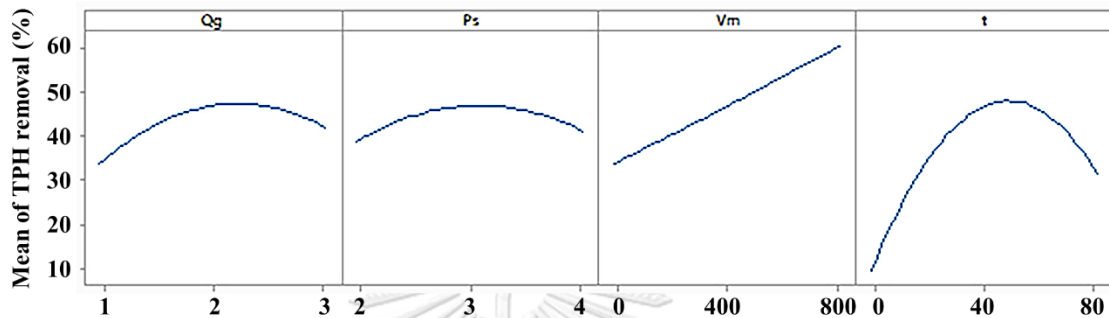
Figure 4.27 Main effects plot of the fitted mean value of TPH removal of "Stirring - IAF-DAF."

2). Contour Plot Value of TPH Removal

Regarding **Figure 4.28**, the four parameters, including P_s, Q_g, V_m, and t were showing about their relationship on TPH removal in order to define the maximum conditions.

For the interaction of P_s*Q_g, it was seen that using 2 to 5 bars of saturated pressure with 2 to 4 l/min of airflow rate would give the maximum proportion of TPH removal approximately 40 to 50%. In case V_m interacted with airflow rate Q_g, it revealed that V_m had a positive effect with Q_g on TPH eradication. For example, from any value between 1, 2, 3, 4 l/min of Q_g and so on could remove TPH from DC around 50 to 60%, while it was operated with V_m from 600 to 800 rpm.

For the interaction of $t*Q_g$, TPH removal seems to have less effect when these two parameters operated together. The operated airflow rate from 1 to 4 l/min would give the result only around 40 to 50% at the time of 30 minutes to 60 minutes. Similarly, in $t*P_s$ interaction, P_s was comparable to Q_g if it interacted with t. P_s that used between 1.5 to 4.5 bars offered the least results, around 40 to 50%, when t started rising from 40 to 60 minutes.

In V_m*P_s interaction, V_m showed as another valid variable when it worked with saturated pressure. It was recognized that from any pressure from 1 to 4.5 bars would give a satisfied TPH removal when V_m regulated from 600 to 800 rpm; thus, the removal efficiency would be 50 to 60% and higher. Likewise, in $t*V_m$ interaction, since V_m played a vital role in emanating TPH from DC, it was also effective comparing to washing time t. When V_m set up from around 600 rpm to 800 rpm, 50 to 60% of TPH removal or higher than that would be achieved even the washing time was counted at any value of 20, 40, 60, or 80 min. This term represented that time t was not significantly affected by TPH elimination that showed a similar result at any time using V_m.
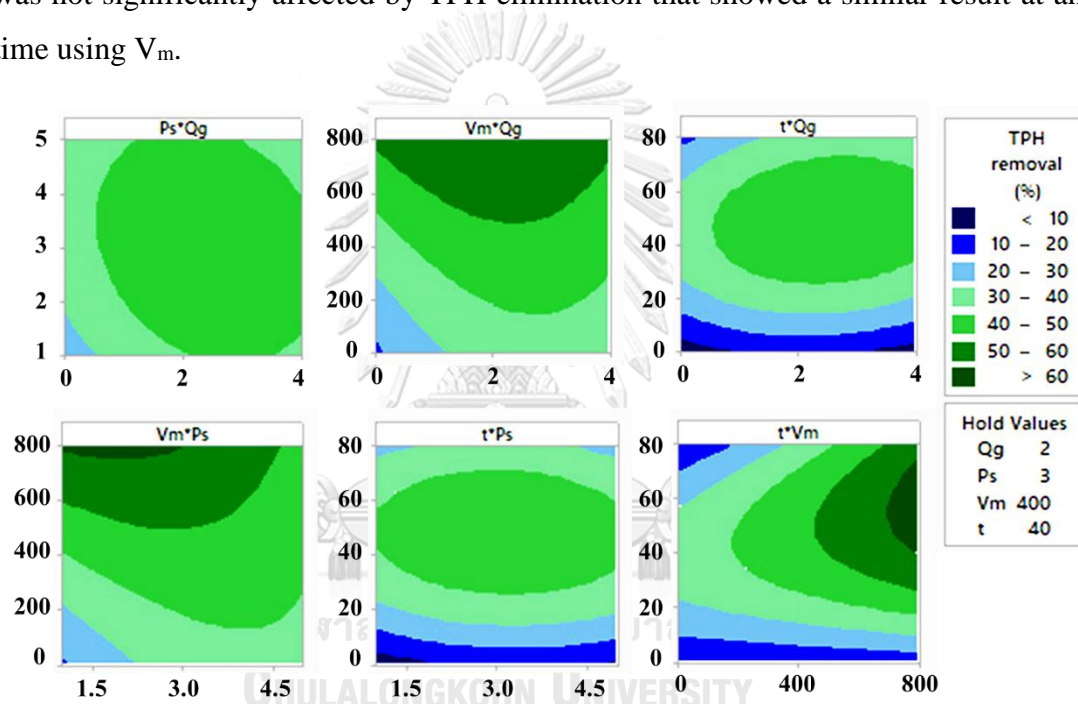
Figure 4.28 Contour plots of four parameters interaction

4.7.3 Statistical Analysis (ANOVA)

Based on ANOVA analysis in **Table 4.17**, it was obviously seen that Q_g got F-value 2.60 with the P-value 0.126 (> P = 0.05), and P_s got F-value 0.19 with P-value 0.665 (> P = 0.05). Therefore, it characterized that Q_g and P_s did not show a significant effect on TPH reduction. However, the mixing speed V_m obtained F-value 28.54 with P-value 0.00 (< P = 0.05), and the treatment time t gained F-value of 18.09 with the P-value of 0.001 (< P = 0.05). Thus, they were notified as a significant effect on TPH reduction from DC (the detailed table was in Appendix 2)

Table 4.17 ANOVA analysis for factor optimization of stirring combined with IAF and DAF

Analysis of Variance						
Source	**DF**	**Adj SS**	**Adj MS**	**F-value**	**P-value**	
Model	14	3117.06	222.65	6.36	0.001	
Linear	4	1730.32	432.58	12.36	0	
Q_g	1	90.97	90.97	2.6	0.126	No significant
P_s	1	6.82	6.82	0.19	0.665	No significant
V_m	1	999.16	999.16	28.54	0.000	Significant
t	1	633.36	633.36	18.09	0.001	Significant
Square	4	1170.43	292.61	8.36	0.001	
Q_g^2	1	124.4	124.4	3.55	0.078	
P_s^2	1	74.31	74.31	2.12	0.164	
V_m^2	1	0.23	0.23	0.01	0.936	
t^2	1	1064.36	1064.36	30.41	0	
2-ways interaction	6	216.31	36.05	1.03	0.442	
Q_g*P_s	1	9.67	9.67	0.28	0.606	
Q_g*V_m	1	14.15	14.15	0.4	0.534	
Q_g*t	1	11.38	11.38	0.33	0.576	
P_s*V_m	1	68.05	68.05	1.94	0.182	
P_s*t	1	1.82	1.82	0.05	0.822	
V_m*t	1	111.24	111.24	3.18	0.094	
Error	16	560.07	35			
Lack-of-Fit	10	559.7	55.97	922.88	0	
Pure Error	6	0.36	0.06			
Total	30	3677.13				

From **Equation 4.2**, the predicted response (TPH removal efficiency) was plotted to compare to the actual response to evaluate the precision and the competency of the model. As a result, the correlation $R^2 = 0.8477$ was indicated in the comparison, as displayed in **Figure 4.29**.

TPH removal (%) = -37.6 + 12.82 Q_g + 16.56 P_s + 0.0444 V_m + 1.180 t - 2.09 Q_g^2 - 1.61 P_s^2 + 0.000002 V_m^2 - 0.01525 t^2 - 0.78 Q_g*P_s - 0.00470 Q_g*V_m + 0.0422 Q_g*t - 0.01031 P_s*V_m - 0.0169 P_s*t + 0.000659 V_m*t   *(Eq 4.2)*

Table 4.18 Actual experimental results vs. prediction in "stirring-IAF-DAF"

Run No.	Q_g (lpm)	P_s (Bar)	V_m (rpm)	t (min)	TPH Removal (%)	
					Experiments	Prediction
1	1	2	200	20	21.75	22.45
2	3	2	200	20	33.19	28.058
3	1	4	200	20	32.38	29.89
4	3	4	200	20	34.64	32.38
5	1	2	600	20	40.55	35.99
6	3	2	600	20	42.01	37.84
7	1	4	600	20	40.05	35.19
8	3	4	600	20	41.55	33.91
9	1	2	200	60	21.09	26.46
10	3	2	200	60	33.76	35.44
11	1	4	200	60	31.56	32.55
12	3	4	200	60	36.13	38.41
13	1	2	600	60	51.48	50.55
14	3	2	600	60	55.54	55.77
15	1	4	600	60	45.51	48.39
16	3	4	600	60	54.38	50.49
17	0	3	400	40	36.07	34.61
18	4	3	400	40	36.03	42.33
19	2	1	400	40	38.95	39.31
20	2	5	400	40	36.94	41.47
21	2	3	000	40	37.68	34.34
22	2	3	800	40	51.83	59.96
23	2	3	400	00	0.000	12.14
24	2	3	400	80	39.98	32.72
25	2	3	400	40	47.41	46.83
26	2	3	400	40	46.61	46.83
27	2	3	400	40	47.01	46.83
28	2	3	400	40	46.85	46.83
29	2	3	400	40	46.85	46.83
30	2	3	400	40	46.85	46.83
31	2	3	400	40	46.85	46.83
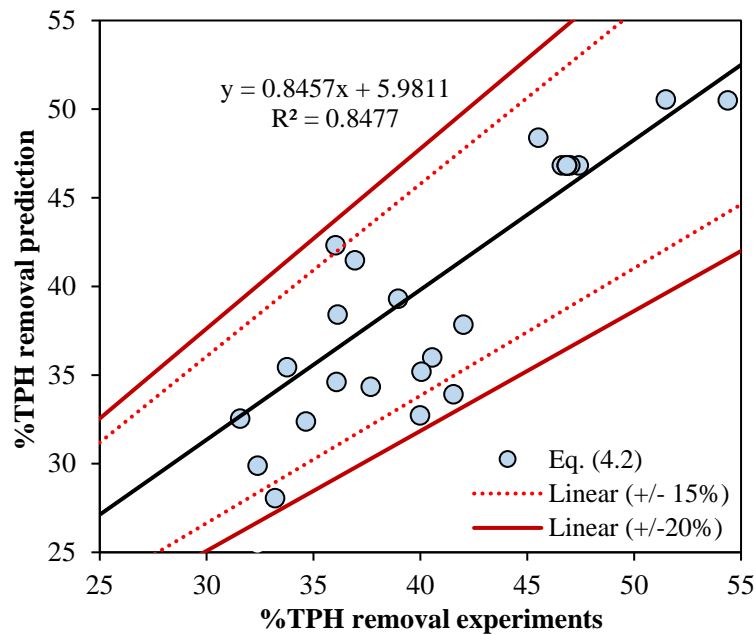
Figure 4.29 Experimental vs. Predicted results of TPH removal efficiency

4.7.4 Optimum Conditions

As a result, the optimum conditions were discovered from the analysis of ANOVA and the interactions between every variable. As mentioned, the level of the airflow rate (Q_g) was defined to be **2 l/min**, saturated pressure **(P_s) was 2 bars**, the rational speed **(V_m) was 800 rpm**, and the washing time **(t) was 60 minutes.** From the study, these optimal terms will provide the maximum TPH removal capacity of approximately **60%**.

In order to confirm the optimal terms for each parameter, the actual experiment was operated. Consequently, the results showed that within Q_g = 2 l/min, P_s = 2 bars, V_m = 800 rpm, and t = 60 min, TPH reduction was defined to be **55%**, which similar to our expectation.

4.8 The Comparison of TPH Removal from Every Process

In this portion, the overall processes used for TPH removal were compared, including the DAF process, the combination of "Stirring-IAF," the combination of "Stirring-DAF," and the three combinations of "Stirring-IAF-DAF," as illustrated in **Figure 4.30**. It was investigated that the DAF system alone seemed to have less influence on

DC remediation than other combined units such as "Stirring-DAF" and "Stirring-IAF-DAF." However, it showed a slight increase in TPH removal if it was compared with "Stirring-IAF." As seen in the graph, DAF was comparable to the combination process of "Stirring-IAF" when it was operated from the time of 40 to 60 minutes.

Furthermore, when the stirring started to combine with the DAF, the removal proficiency was interestingly improved compare to the DAF alone and "stirring with IAF." The result was taking place to rise from the time of 40 min to 60 min with the interesting TPH removal around 40%. Also, when the air flotation included IAF and DAF were mixed together with stirred motor by using different speeds, it also showed the remarkable TPH eradication. About 50% of TPH was removed within the time set from 40 min to 60 min, as displayed in the graph. This percentage was notified to the highest compared to other processes. Yet, it will be discussed more on its operational experiments and installation.

The optimum points that showed in the graph were obtained from the DOE design and estimation. They represented the maximum conditions that could operate and obtain higher results. In the "stirring-DAF" process, the optimum point was about 50%, while the optimum removal from "stirring-IAF-DAF" was approximately 60%.
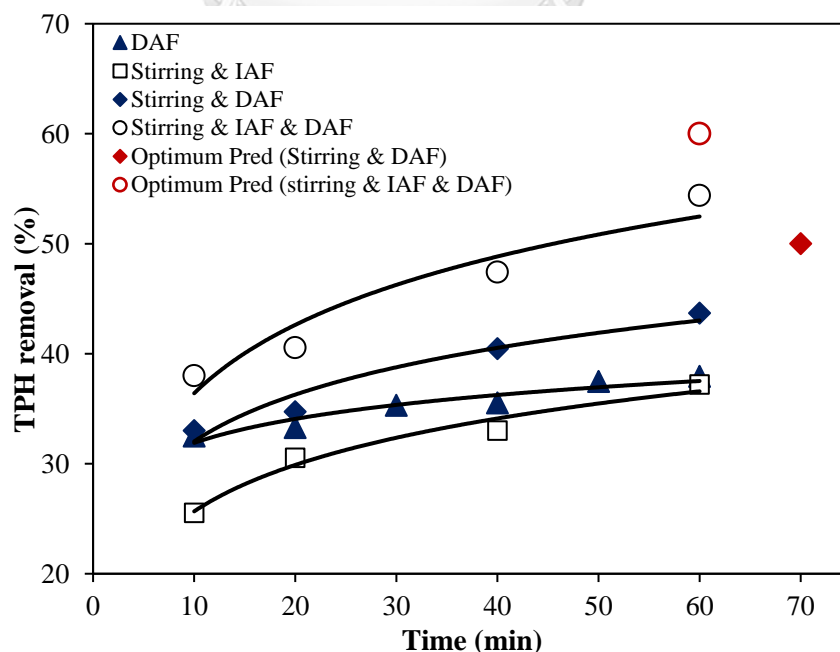
Figure 4.30 The comparison of TPH removal (%) in different processes

4.9 The Effect of NaCl Solutions over DC Washing

Compared to tap water, the saline water (water that mixed with NaCl (30 g/L) to represent as seawater) was markedly shown the positive performance of TPH removal proportion from DC. Therefore, the proportion of saline water was carried out for every process in order to confirm its effectiveness over DC washing compared to tap water.

4.9.1 Effect of Saline Water Over DC Washing from Stirring

In the stirring process, three selected washing conditions, including 600 rpm washed for 20 minutes, 600 rpm washed for 40 minutes, and 600 rpm washed for 60 minutes, were studied by using saline water. Subsequently, it was observed that at the high mixing speed of 600 rpm, TPH was removed from the DC around 25% by Tap water, and it was removed approximately 35% by saline water at the same time of 20 minutes. Moreover, it was a similarity of TPH elimination at the time between 40 min and 60 min. As seen in **Figure 4.31**, TPH was eliminated by almost 30% by tap water and increased to around 40% by just changing to saline water at the time from 40 min to 60 min.
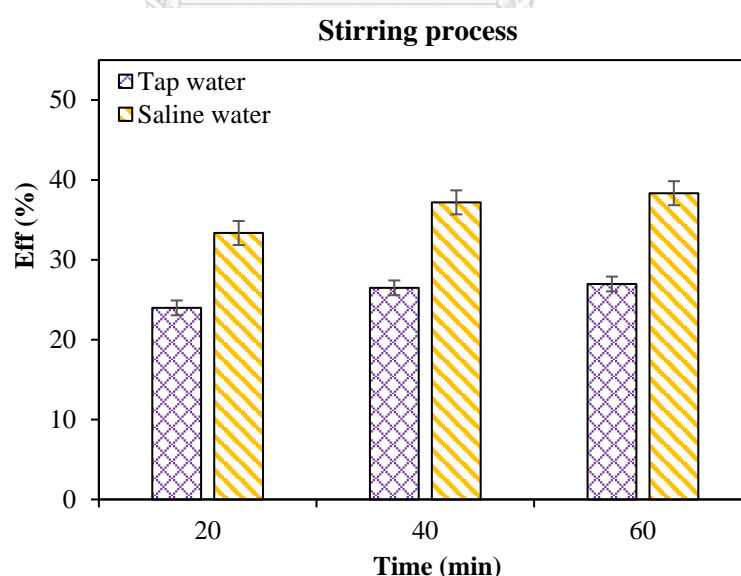
Figure 4.31 Tap water compared to saline water for DC washing in stirring process

4.9.2 Effect of Saline Water over DC Washing from IAF

At the same time, three washing conditions, such as 3 LPM for 20 min, 3 LPM for 40 min, 3 LPM for 60 min, were selected to understand the differences between tap water and saline water in the IAF process. It was stated that at a lower time of 20 min, the efficiency of TPH removal was roughly 25% when DC was washed by tap water, whereas roughly 35% of that was washed by saline water with the same conditions. Likewise, when the time rose to 40 min, the removal capacity increased from around 30% to around 40% that washed by tap and salty water, respectively. Also, at the longest time of 60 min, TPH removal was markedly increased when it was treated by saline water, which was almost 45% compared to roughly 30% treated by tap water.
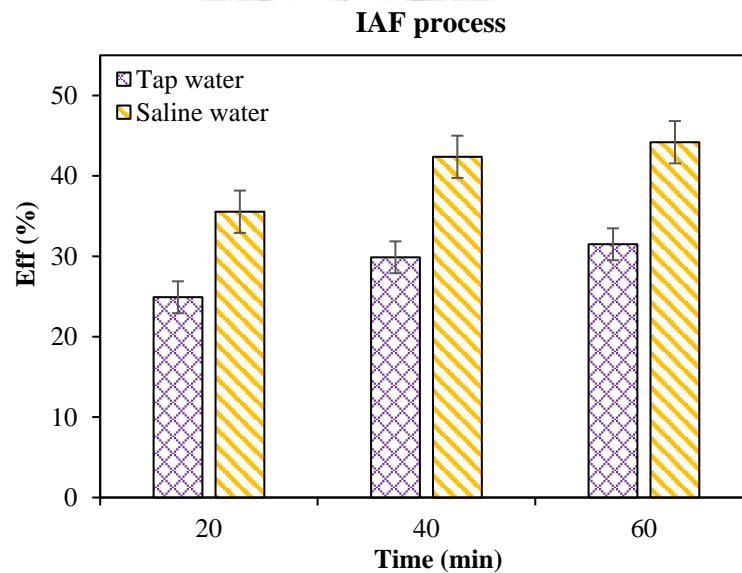
Figure 4.32 Tap water compared to saline water for DC washing in IAF process

4.9.3 Effect of Saline Water over DC Washing from DAF

Along with the DAF process, the was a comparison between using tap water saline water also had been investigated. It was markedly shown in **Figure 4.33** that saline water had a positive effect on TPH removal compared to tap water. It was indicated that from the high saturated pressure of 4 bars and time 20 min, 40 min, and 60 min, the reduction of TPH was remarkably grew from approximately 30% to 40%, 35% to 45%, and from roughly 40% to 50% by tap water and saline water, accordingly.
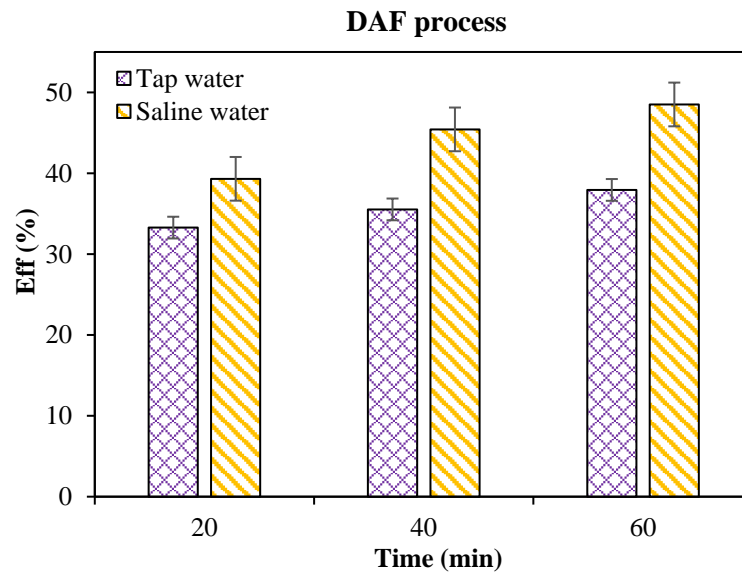
DAF process

Figure 4.33 Tap water compared to saline water for DC washing in the DAF process

4.9.4 Effect of Saline Water over DC Washing from the Stirring Combined with IAF/ DAF

In this section, the investigation was carried out by apply saline water into the three comparable conditions of "Stirring-IAF" and "Stirring-DAF." As mentioned in **Figure 4.34**, it was interesting that the efficiency of TPH eradication was increased by approximately 10% by changing from tap water to saline water for all three experimental conditions.
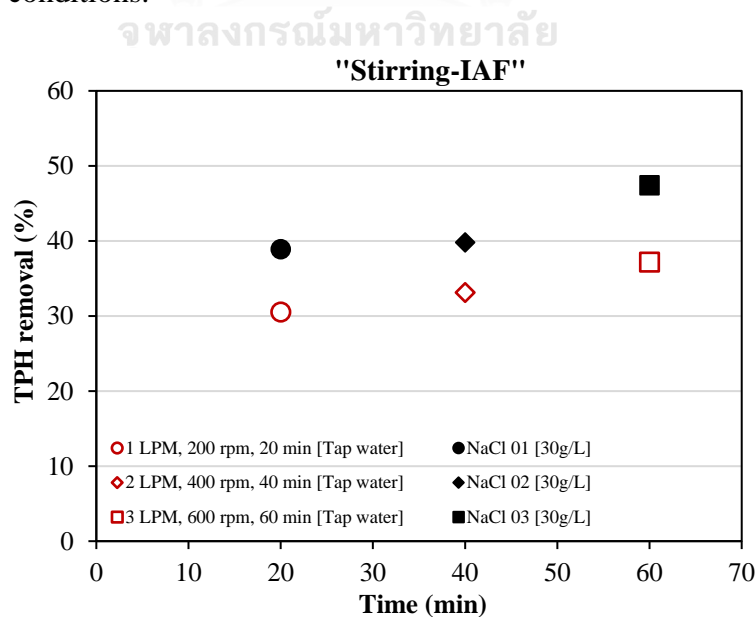
Figure 4.34 The comparison between tap water and saline water from "Stirring-IAF"

In the meantime, in "Stirring-DAF," the effectiveness of adding salty water was not much different from the combination of "Stirring-IAF." The runs with saline water of this combination showed a marginal increase of hydrocarbons removal compared to the experimental running with "Stirring-IAF" with saline water. This reason happened maybe because the NaCl proportion was able to switch over the oil droplets from DC attachment, yet within the Mbs, the physical force that generated by through the bursting of microbubbles became weaker in the presence of sodium chloride (Sun et al., 2019). Thus, the removal of TPH from DC with Mbs was slightly increase compared to other processes.
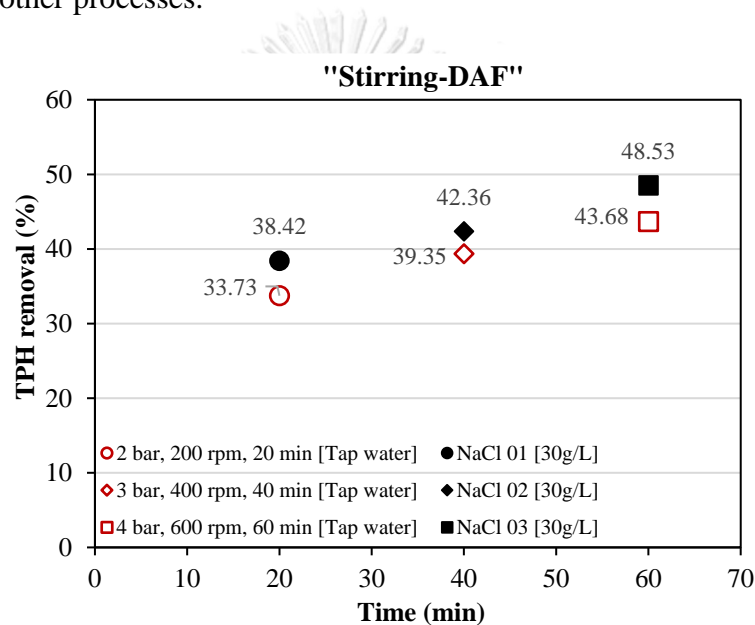
Figure 4.35 The comparison between tap water and saline water from stirring & DAF

4.9.5 Effect of Saline Water over DC Washing from the Optimum Conditions of "Stirring-DAF," and "Stirring-IAF- DAF"

In this part, the investigation was carried out by using the saline water on TPH subtraction from the optimum conditions of "Stirring-DAF" and "Stirring-IAF-DAF." As mentioned from the previous section, the level of the optimum parameter for "S-DAF" was P_s = 4 bars, V_m = 400 rpm, and washing time t = 70 min. Regarding this study, these values were experimentally run and presented the removal capacity of TPH to be almost **50%** by tap water as expected. To compare with this result, the saline water was also applied to this optimum term. It was revealed that the salinity of

water had influenced TPH elimination compared to tap water, which resulted in a higher percentage of about **55%**. In the meantime, the optimum conditions for "Stirring-IAF-DAF" were Q_g = 2 LPM, P_s = 2 bars, V_m = 800 rpm, and washing time t = 60 min. Consequently, these values were experimentally run and offered the removal capacity of TPH to be roughly **55%** by tap water. Similarly, the saline water was applied to this optimum term also in order to observe the effectiveness of water salination on TPH removal. As expected, TPH was reduced by saline water around **60%,** which is higher than tap water approximately 5%, as illustrated in **Figure 4.36**.
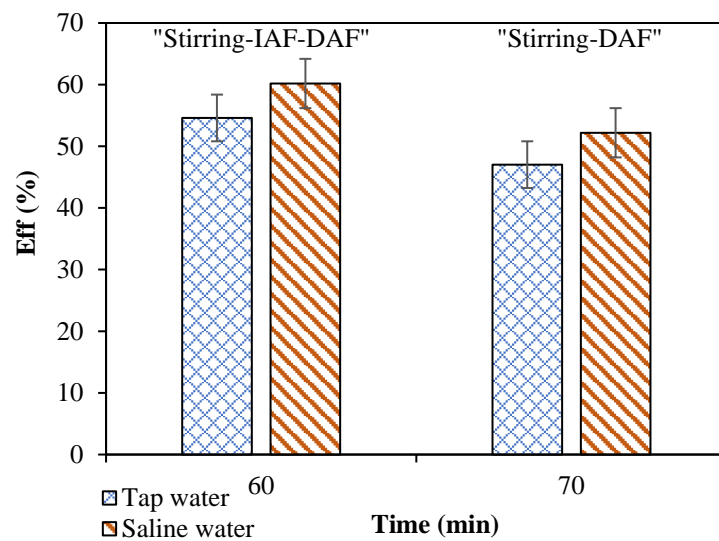
Figure 4.36 Tap water compared to saline water for DC washing from the optimum conditions

According to Wei et al. (2017), the authors reported that cations in salinity could replace the negative charge of oil and clay. It was observed that the electrical double layers (EDL) expanded into surrounding the negative charge of clay mineral when the potential of cations was reduced. Thus, when the thickness of the double layer increases, the salinity created a thicker film, which increased the water wetness and the permeability of oils. Furthermore, while the double layer was more compacted by many ions, the expansion of the double-layer would allow monovalent ions such as sodium (Na^+) to penetrate the layer. So, Na^+ would replace divalent ions, which resulted in growing the electrostatic repulsion between oil droplets and clay particles. Finally, the oil droplets would desorb from clay particles when repulsive forces overcame the attractive forces through cation bridges (**Figure 4.37**).

Through these mechanisms, when the negative charge of DC was immersed in water, an electrical double layer formed surround it. Na^+ in saline water opened the diffuse layer and penetrated the double layer. So, it increased the electrostatic repulsion between soils and oil droplets, which caused the oil droplets attached to air bubbles while the system was operated. In addition, adding salt into the water was known to decrease the chance of bubble coalescence, which cause the average bubble diameter diminished as well. Therefore, the TPH removal from DC would be higher than using freshwater.
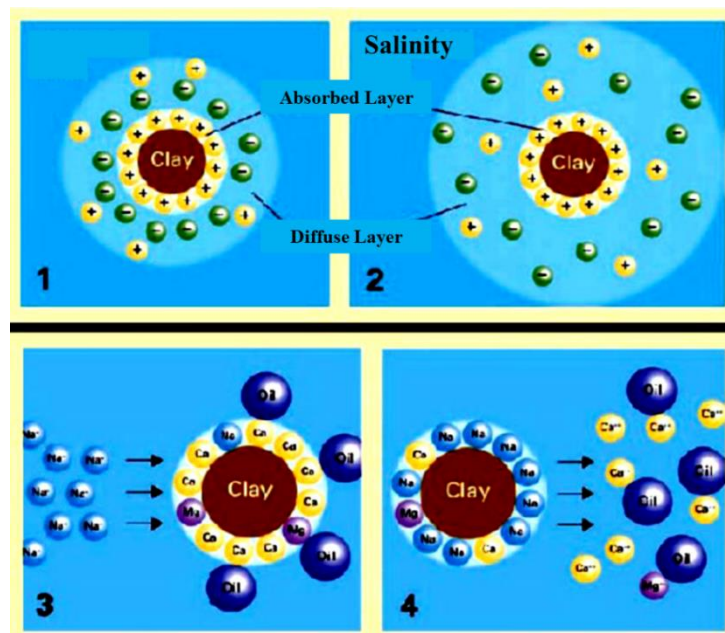
Figure 4.37 The effect of salinity over the electrical double layer

4.10 The Water Effluent from Washing System Evaluation

In this part, the water effluent that came from the optimum condition of "S-DAF" and "Stirring-IAF-DAF" were taken to analyze for two main parameters, including oil and grease (TPH) and total suspended solids (TSS). As reviewed from the previous section, the specifications for an acceptable quality of oil field produced water for reinjection system was followed by TSS $\leq$ 10 mg/L and oil and grease $\leq$ 42 mg/L. Moreover, it is important to prevent the presence of bigger sand and other solids in the reinjection stream to prohibit the plugging and pump damage (Jiménez et al., 2018,

Etchepare et al., 2017). Therefore, the TPH in water effluent and TSS were evaluated in order to compare with these specifications.

4.10.1 Oil in Water Mixture Determination

1). *Calibration Curve*

Ultraviolet-visible spectrophotometry (UV-vis) was used to analyze the samples from washing effluent. The calibration curve was calculated by measuring six points of known concentration of diesel-hexane solutions. The six solutions of diesel oil were 10 mg/L, 30 mg/L, 50 mg/L, 100 mg/L, 150 mg/L, and 200 mg/L, which prepared to do the experiment by measuring its absorbent in the GENESYS^{TM} 10S UV-vis spectrophotometry machine (see **Figure 4.38**). The wavelength used in this work was from 200 to 400 nm and 264 nm for the calibration curve of diesel-hexane mixtures (Agarwal et al., 2016), as displayed in **Figure 4.39**.

Figure 4.38 GENESYS™ 10S UV-Vis spectrophotometer

$$y = 0.0012x + 0.026$$
$$R^2 = 0.9936$$
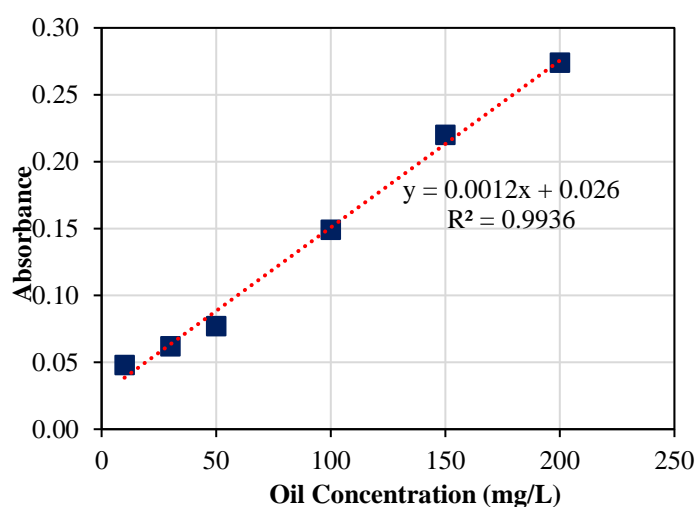
Figure 4.39 Diesel- Hexane calibration curve

From the calibration curve, the oil concentration could be determined by the Eq 4.4:

$$C_{oil} = \frac{Y - 0.026}{0.0012} \ (mg/L) \hspace{3cm} Eq \ 4.3$$

2). The Oil in Water Mixture Measuring

As mentioned by Radzuan et al. (2016), one method that could measure the oil in water was the FastHEX method. 100ml of the sample was collected from the system and was mixed with hexane for 10 ml in the 200 ml beaker. Then, this mixture was gently shaken for 3 minutes in order to permit the layer of hexane and dissolved oil mixing completely. Hexane was used as a blank measurement in the UV-vis machine before measuring the absorbance of the sample. Afterward, each sample was recorded its absorbance and calculated for the oil concentration in the water effluent.

As a result, the water effluent that was coming from both the combination process of "Stirring-IAF-DAF" and "Stirring-DAF" were found to be 62.5 mg/L and 60.83 mg/L of hexane, which represented to be 6.25 mg/L and 6.083 mg/L of water, accordingly. It was observed that these values were much lower than the specifications (< 42mg/L of oil and grease). Therefore, the water effluents from the optimum of every combination process were not the concern for reusing in the reinjection system of oil field industries.

4.10.2 Total Suspended Solid Measurement

The suspended solids of samples were calculated by the evaporation method. Before analysis, the glass fiber filter was dried at 103-105 ℃ for 1hour and keep drying in the desiccator. Then the fiber filter was placed in the filtration assembly and ready for filtration. 20 ml portions of the sample were taken to suck, then dried at 103-105℃ for 1 hr. The mass that remains on the fiber filter represented the suspended solids.

It was found that the process of "Stirring-IAF-DAF" was 865 mg/L, and the process of "Stirring-DAF" was 353 mg/L. These results were much higher than the specifications (> 10 mg/L). Thus, they were not able to use without the removal of these TSS. Further solutions should be considered in order to make these water effluents passed the specs of oil and gas industries before reusing in the reinjection system or disposal.

CHAPTER 5
CONCLUSION AND RECOMMENDATION

5.1 Conclusion

In conclusion, this research aimed to study the effects of modifying the air flotation process, including induced air flotation and dissolved air flotation, to combine with the mechanical stirring process in order to observe their usefulness over TPH removal from drill cuttings. The bubble hydrodynamics of the flotation process was analyzed in terms of interfacial area to velocity gradient (a/G) as the function of TPH removal efficiency. Briefly, this work could be summarized into four main categories, as mentioned below.

5.1.1 The Effects of TPH Removal by The Combination System

Based on the study, every individual process was not provided with satisfying results; therefore, the combination units were selected for detail studying to reveal the effectiveness in TPH removal proficiency. As suggested, "Stirring-DAF" and "Stirring-IAF-DAF" were remarkedly investigated. DOE that utilized the method of central composite design response surface methodology was applied to these two combined processes in order to find out the optimum conditions in operational experiments that could provide the most TPH reduction from DC. As a result, the operational conditions for "Stirring-DAF" was found to be 4 bars of saturated pressure, 400 rpm of rotational speed, which spent the operated time around 70 min. So, the removal capacity would achieve approximately 50%. Moreover, the operational conditions for "Stirring-IAF-DAF" were also determined. It was found that using the saturated pressure from pressure vessel of only 2 bars, airflow rate of 2 l/min, and rotational speed of stirred more for 800 rpm would provide the higher removal efficiency around 60% for an hour of treatment time.

5.1.2 Study the Effects a/G Ratio Over the TPH Remediation

The ratio of the interfacial area (a) and velocity gradient (G) was proved to be an essential parameter to describe the performance of TPH treatment from DC by flotation processes. In this study, the values of a/G were not only studied in a single

flotation process but also analyzed in the combination unit such as "Stirring-IAF" and "Stirring-DAF" compared to the DAF unit. From the study, the process of "Stirring-DAF" was found to be the better conditions in TPH removal efficiency; therefore, this combination was observed along with a/G values for two washing media: tap and salty water solution.

The relation between the treatment proficiency and the a/G values in DAF, "Stirring-DAF" [tap water], and "Stirring-DAF" [salt water] were studied for the further prediction of treatment proficiency because they were associated with the combination between 2 main physical processes such as tiny bubbles application and stirring processes. The linear equation of the DAF unit was proposed within R^2 = 0.897, slope 3.416, and the intercept 24.28, while the "Stirring-DAF" was proposed within R^2 = 0.870, slope 2.362, and the intercept 37.98 by tap water. Moreover, the combination of "Stirring-DAF" that was washed by saline water was investigated with better conditions, which showed by correlation equation that has R^2 = 0.937, slope 3.301, and the intercept 37.852.

5.1.3 Study the Effects of Saline Water over DC Washing

Consequently, it could be drawn to the conclusion that the experiments conducted with saline water showed a better percentage of TPH reduction compared to tap water correspondingly.

- ❖ In every process, such as stirring, IAF, and DAF, "Stirring-IAF," "stirring-DAF," were confirmed the TPH decrease by using the saline water as the washing reagents. It was proven that the salty water would encourage TPH removal from approximately 5% to10% rather than conducting with tap water.

- ❖ For this reason, it could understand that probably the characteristics of salt changed the attachment between oil droplets and DC, which could remove after using the turbulence conditions of stirring and IAF processes (Radzuan et al., 2016). In the same way, in DAF, the bubbles would have more chance to attach with oil droplets when they detached from DC by having the attendance of salty water.

❖ Moreover, it was seen that at the combination process of "stirring-DAF," the runs with saline water show a minimal surge of hydrocarbons removal around 5% compared to the experimental running with tap water. This reason happened maybe because the NaCl was able to change the oil droplets from DC attachment; so far, within the Mbs, the physical force generated through the bursting of microbubbles became weaker when the sodium chloride solution was introduced. Thus, the removal of TPH from DC with Mbs was slightly increase compared to other processes.

5.1.4 Water Effluents Evaluation

The managing of produced water for oil and gas industries was essential in both offshore and onshore since it was largely produced and consumed for the injected system of the drilling operation. However, in order to reuse produced water for reinjection system or discharging, several factors insides produced water were considered to meet the limitation or discharge legislation. In this work, the washed water that remained after washing conditions were also analyzed and checked for its appropriation of reusing and discharge. Hence, in terms of oil and grease (O&G) in this water was obtained about 6.25 mg/L and 6.083 mg/L for the optimum conditions of "Stirring-IAF-DAF" and "Stirring-DAF," respectively, which were acceptable for oil field PW quality in reinjection system. In addition, the TSS of this water was found to be 865 mg/L and 353 mg/L of the effluents from "Stirring-IAF-DAF" and "Stirring-DAF," accordingly, which were higher than the limitation of PW quality for both reinjection and discharging. Therefore, this water has to be further considered to reduce TSS until it meets the specifications.
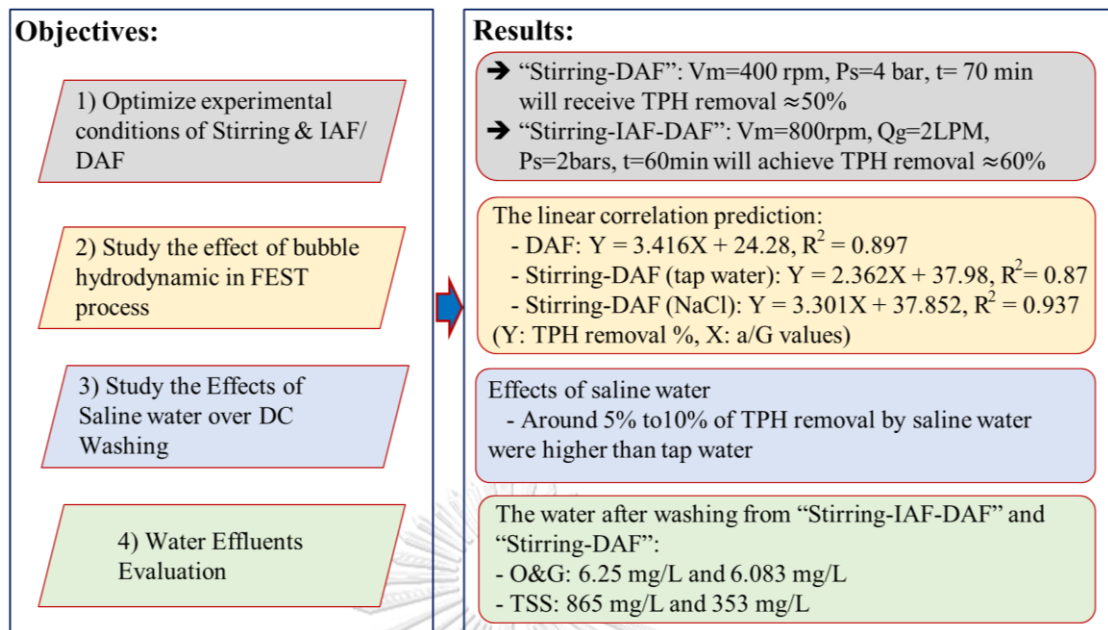
Figure 5.1 The summary of results

5.2 Recommendation

As expected, the combination system between stirring and air flotation was recognized as the novel operational approach that can enhance TPH elimination from DC with a remarkable percentage. Additionally, it was believed that this study was beneficial for further research in order to achieve maximum removal based on environmental regulations. Yet, there were some recommendations and suggestions for further research over TPH removal from drill cuttings, as listed below.

➢ It is essential to continue studying more detail on DC washing since the percentage in this work does not reach the limitation of TPH removal (~99%).

➢ The TPH measurement should be changed to a different method that could save much time and be more accurate.

➢ Additional experiments should be conducted to validate the better output, especially in DOE application in order to obtain precise results.

➢ The next study can consider the enlarged scale of the study for the combination process for the DC washing, especially stirring combined with DAF because it is not so complicated in operational installation and provides a satisfying output.

➢ Water effluents should be further treated for other factors such as TSS; for instance, the water effluent could be treated by the coagulation process in order to meet the regulation before discharging or reusing.

➢ From the study, the two combination processes "Stirring-DAF" is recommended than the three combination processes "Stirring-IAF-DAF." The reasons are that the total removal efficacy is not much different, which shows around a 10% increase from the two to three combination units. Moreover, as suggested, the two combination units, "Stirring-DAF," is more accessible in terms of experimental conditions and cost operations.

➢ For the three combination processes, "Stirring-IAF-DAF," they would need more detailed study since they are such a complicated in the operational experiment and challenging to describe in terms of a/G.

➢ It is beneficial for the next step study of removal TPH from DC by reducing the use of green surfactant (for example, Ethyl Lactate, which is known as the effective media for TPH removal and environmentally friendly, but it is an expensive media) since the combination physical process enhances the removal proficiency approximately 50%. Thus, it would save much money when the combined physical processes are applied before employing green surfactants (**Figure 5.2**).
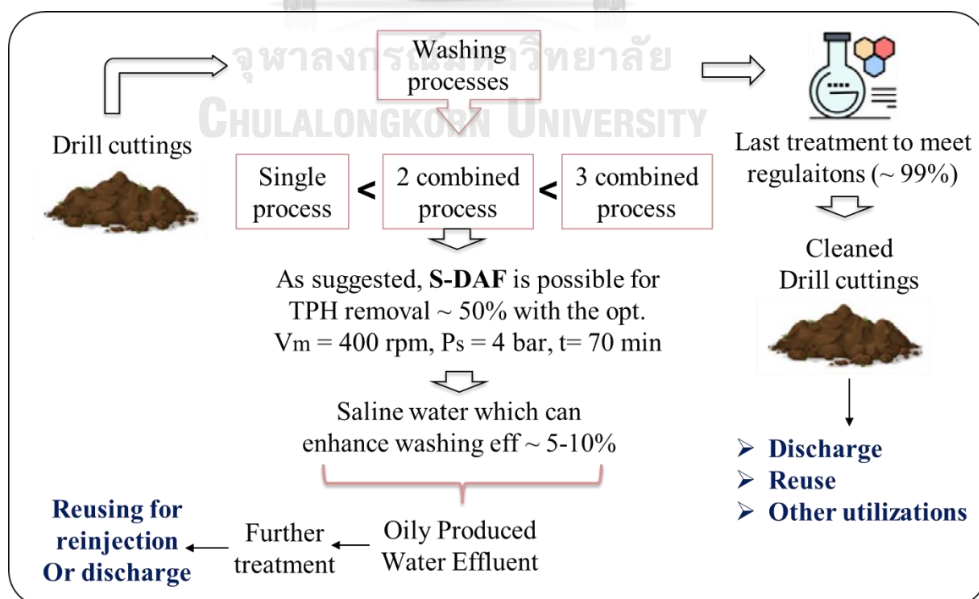

Figure 5.2 Overall diagram for DC management

REFERENCES

Aagaard-Sørensen, S., Junttila, J., & Dijkstra, N. J. M. p. b. (2018). Identifying past petroleum exploration related drill cutting releases and influences on the marine environment and benthic foraminiferal communities, Goliat Field, SW Barents Sea, Norway. *129*(2), 592-608.

Agarwal, A., & Liu, Y. J. M. P. B. (2015). Remediation technologies for oil-contaminated sediments. *101*(2), 483-490.

Agarwal, A., Zhou, Y., Liu, Y. J. E. S., & Research, P. (2016). Remediation of oil-contaminated sand with self-collapsing air microbubbles. *23*(23), 23876-23883.

Ahmad, A., Sumathi, S., & Hameed, B. J. C. E. J. (2006). Coagulation of residue oil and suspended solid in palm oil mill effluent by chitosan, alum and PAC. *118*(1-2), 99-105.

Ahmadkalaei, S. P. J., Gan, S., Ng, H. K., Talib, S. A. J. E. S., & Research, P. (2016). Investigation of ethyl lactate as a green solvent for desorption of total petroleum hydrocarbons (TPH) from contaminated soil. *23*(21), 22008-22018.

Ayranci, I., Kresta, S. M., Derksen, J. J. J. C. E., & Technology. (2013). Experiments and simulations on bidisperse solids suspension in a mixing tank. *36*(11), 1957-1967.

Bakke, T., Klungsøyr, J., & Sanni, S. J. M. e. r. (2013). Environmental impacts of produced water and drilling waste discharges from the Norwegian offshore petroleum industry. *92*, 154-169.

Ball, A. S., Stewart, R. J., Schliephake, K. J. W. M., & Research. (2012). A review of the current options for the treatment and safe disposal of drill cuttings. *30*(5), 457-473.

Bashat, H. J. E. A., SENV. (2002). Managing waste in exploration and production activities of the petroleum industry. *1*, 1-37.

Bensadok, K., Belkacem, M., & Nezzal, G. J. D. (2007). Treatment of cutting oil/water emulsion by coupling coagulation and dissolved air flotation. *206*(1-3), 440-448.

Breuer, E., Stevenson, A., Howe, J., Carroll, J., & Shimmield, G. J. M. P. B. (2004). Drill cutting accumulations in the Northern and Central North Sea: a review of environmental interactions and chemical fate. *48*(1-2), 12-25.

Broni-Bediako, E., Amorin, R. J. R. J. o. A. S., Engineering, & Technology. (2010). Effects of drilling fluid exposure to oil and gas workers presented with major areas of exposure and exposure indicators. *2*(8), 710-719.

Bui, H. (2017). VOxFlotation: Future Solution for Water Treatment.

Chawaloesphonsiya, N. (2014). *Separation of oily emulsion by flotation and coalescer processes for wastewater treatment.* Chulalongkorn University,

Chawaloesphonsiya, N., Wongwailikhit, K., Bun, S., & Painmanakul, P. J. E. J. (2019). Stabilized Oily-Emulsion Separation Using Modified Induced Air Flotation (MIAF): Factor Analysis and Mathematical Modeling. *23*(5), 29-42.

Crittenden, J. C., Trussell, R. R., Hand, D. W., Howe, K. J., & Tchobanoglous, G. (2012). *MWH's water treatment: principles and design*: John Wiley & Sons.

Daud, Z., Awang, H., Nasir, N., Ridzuan, M. B., Ahmad, Z. J. P.-S., & Sciences, B. (2015). Suspended solid, color, COD and oil and grease removal from biodiesel wastewater by coagulation and flocculation processes. *195*, 2407-2411.

de Almeida, P. C., Araújo, O. d. Q. F., & de Medeiros, J. L. J. J. o. C. P. (2017). Managing offshore drill cuttings waste for improved sustainability. *165*, 143-156.

Etchepare, R., Oliveira, H., Azevedo, A., Rubio, J. J. S., & Technology, P. (2017). Separation of emulsified crude oil in saline water by dissolved air flotation with micro and nanobubbles. *186*, 326-332.

Fakhru'l-Razi, A., Pendashteh, A., Abdullah, L. C., Biak, D. R. A., Madaeni, S. S., & Abidin, Z. Z. J. J. o. h. m. (2009). Review of technologies for oil and gas produced water treatment. *170*(2-3), 530-551.

Guerra, K., Dahm, K., & Dundorf, S. (2011). *Oil and gas produced water management and beneficial use in the Western United States*: US Department of the Interior, Bureau of Reclamation.

Hendricks, D. (2006). *Water treatment unit processes: physical and chemical*: CRC press.

Hoseini, S. M., Salarirad, M. M., Alavi Moghaddam, M. R. J. D., & Treatment, W. (2015). TPH removal from oily wastewater by combined coagulation pretreatment and mechanically induced air flotation. *53*(2), 300-308.

Igunnu, E. T., & Chen, G. Z. J. I. J. o. L.-C. T. (2012). Produced water treatment technologies. *9*(3), 157-177.

IOGP. (2016). *Environmental Fates and Effects of Ocean Discharge of Drill Cuttings and Associated Drilling Fluids From Offshore Oil and Gas Developments. Report 543, .* Retrieved from

Irfan, M., Butt, T., Imtiaz, N., Abbas, N., Khan, R. A., & Shafique, A. J. A. j. o. c. (2017). The removal of COD, TSS and colour of black liquor by coagulation–flocculation process at optimized pH, settling and dosing rate. *10*, S2307-S2318.

Ite, A. E., Ibok, U. J., Ite, M. U., & Petters, S. W. J. A. J. o. E. P. (2013). Petroleum exploration and production: Past and present environmental issues in the Nigeria's Niger Delta. *1*(4), 78-90.

Júnior, I. P., Martins, A. L., Ataíde, C. H., & Duarte, C. R. J. J. o. e. m. (2017). Microwave drying remediation of petroleum-contaminated drill cuttings. *196*, 659-665.

Kim, T.-i., Kim, Y.-h., & Han, M. J. M. p. b. (2012). Development of novel oil washing process using bubble potential energy. *64*(11), 2325-2332.

Kubo, Y. s., Kido, Y., Fuwa, Y., Hoshino, H. J. J. R. o. R., & Development. (2016). Experiments on method for washing drill cuttings: evaluation of soaking, stirring, and milling effects. *22*, 39-48.

Kuppusamy, S., Thavamani, P., Venkateswarlu, K., Lee, Y. B., Naidu, R., & Megharaj, M. J. C. (2017). Remediation approaches for polycyclic aromatic hydrocarbons (PAHs) contaminated soils: Technological constraints, emerging trends and future directions. *168*, 944-968.

Lai, C.-C., Huang, Y.-C., Wei, Y.-H., & Chang, J.-S. J. J. o. H. M. (2009). Biosurfactant-enhanced removal of total petroleum hydrocarbons from contaminated soil. *167*(1-3), 609-614.

Lersjintanakarn, S. (2008). *Treatment of lubricant oily emulsion wastewater by combining flotation and coagulation process.* Chulalongkorn University,

Liu, H., Wang, Z., Wang, J., & He, X. J. E. (2016). Improvement of emission characteristics and thermal efficiency in diesel engines by fueling gasoline/diesel/PODEn blends. *97*, 105-112.

Machado, M. B., Nunhez, J. R., Nobes, D., & Kresta, S. M. J. A. j. (2012). Impeller characterization and selection: Balancing efficient hydrodynamics with process mixing requirements. *58*(8), 2573-2588.

Meyssami, B., & Kasaeian, A. J. B. t. (2005). Use of coagulants in treatment of olive oil wastewater model solutions by induced air flotation. *96*(3), 303-307.

Neff, J. M. J. I. E. A., & Management. (2008). Estimation of bioavailability of metals from drilling mud barite. *4*(2), 184-193.

Onwukwe, S., Nwakaudu, M. J. I. J. o. E. S., & Development. (2012). Drilling wastes generation and management approach. *3*(3), 252.

Osuji, L. C., & Nwoye, I. J. A. J. o. A. R. (2007). An appraisal of the impact of petroleum hydrocarbons on soil fertility: the Owaza experience. *2*(7), 318-324.

Painmanakul, P., Sastaravet, P., Lersjintanakarn, S., Khaodhiar, S. J. C. E. R., & Design. (2010). Effect of bubble hydrodynamic and chemical dosage on treatment of oily wastewater by induced air flotation (IAF) process. *88*(5-6), 693-702.

Poyai, T. (2018). *Development of a treatment process for petroleum drill cuttings via soil washing technique.* Chulalongkorn University,

Radzuan, M. A., Belope, M. A.-B., Thorpe, R. J. C. E. R., & Design. (2016). Removal of fine oil droplets from oil-in-water mixtures by dissolved air flotation. *115*, 19-33.

Reynolds, T. D., & Richards, P. A. (1996). Unit Operation and Processes in Environmental Engineering.

Rubio, J., Souza, M., & Smith, R. J. M. e. (2002). Overview of flotation as a wastewater treatment technique. *15*(3), 139-155.

Saththasivam, J., Loganathan, K., & Sarp, S. J. C. (2016). An overview of oil–water separation using gas flotation systems. *144*, 671-680.

Stuckman, M. Y., Lopano, C. L., Berry, S. M., Hakala, J. A. J. J. o. N. G. S., & Engineering. (2019). Geochemical solid characterization of drill cuttings, core and drilling mud from Marcellus Shale Energy development. *68*, 102922.

Sun, H., Liu, H., Wang, S., & Liu, Y. J. J. o. h. m. (2019). Remediation of oil spill-contaminated sands by chemical-free microbubbles generated in tap and saline water. *366*, 124-129.

Takahashi, M. J. T. J. o. P. C. B. (2005). ζ potential of microbubbles in aqueous solutions: electrical properties of the gas− water interface. *109*(46), 21858-21864.

Tom D. Reynolds, P. A. R. (1996). *Unit operations and processed in environmental engineering*.

Torres, L., Climent, M., Saquelares, J., Bandala, E., Urquiza, G., Iturbe, R. J. I. J. o. E. S., & Technology. (2007). Characterization and treatability of a contaminated soil from an oil exploration zone. *4*(3), 311-322.

Urum, K., Pekdemir, T., Ross, D., & Grigson, S. J. C. (2005). Crude oil contaminated soil washing in air sparging assisted stirred tank reactor using biosurfactants. *60*(3), 334-343.

Urum, K., & Pekdemir, T. J. C. (2004). Evaluation of biosurfactants for crude oil contaminated soil washing. *57*(9), 1139-1150.

Veil, J. A. (2011). Produced water management options and technologies. In *Produced Water* (pp. 537-571): Springer.

Von Lau, E., Gan, S., Ng, H. K., & Poh, P. E. J. E. p. (2014). Extraction agents for the removal of polycyclic aromatic hydrocarbons (PAHs) from soil in soil washing technologies. *184*, 640-649.

Wang, L. K., Shammas, N. K., Selke, W. A., & Aulenbach, D. B. (2010). *Flotation technology*: Springer.

Wei, B., Lu, L., Li, Q., Li, H., Ning, X. J. E., & Fuels. (2017). Mechanistic study of oil/brine/solid interfacial behaviors during low-salinity waterflooding using visual and quantitative methods. *31*(6), 6615-6624.

Wongwailikhit, K., Warunyuwong, P., Chawaloesphonsiya, N., Dietrich, N., Hébrard, G., Painmanakul, P. J. C. E., & Technology. (2018). Gas Sparger orifice sizes and solid particle characteristics in a bubble column–relative effect on hydrodynamics and mass transfer. *41*(3), 461-468.

Xionghu, Z., Fengchun, W. J. D. F., & Fluid, C. (2004). Research development of waste drilling fluids disposal. *21*(2), 43-48.

Yan, P., Lu, M., Guan, Y., Zhang, W., & Zhang, Z. J. B. t. (2011). Remediation of oil-based drill cuttings through a biosurfactant-based washing followed by a biodegradation treatment. *102*(22), 10252-10259.

Yap, C. L., Gan, S., & Ng, H. K. J. J. o. E. S. (2012). Evaluation of solubility of polycyclic aromatic hydrocarbons in ethyl lactate/water versus ethanol/water mixtures for contaminated soil remediation applications. *24*(6), 1064-1075.

Yu, L., Han, M., & He, F. J. A. j. o. c. (2017). A review of treating oily wastewater. *10*, S1913-S1922.

Zhang, L., Somasundaran, P., Ososkov, V., Chou, C. J. C., Physicochemical, S. A., & Aspects, E. (2001). Flotation of hydrophobic contaminants from soil. *177*(2-3), 235-246.

Zheng, J., Chen, B., Thanyamanta, W., Hawboldt, K., Zhang, B., & Liu, B. J. M. p. b. (2016). Offshore produced water management: A review of current practice and challenges in harsh/Arctic environments. *104*(1-2), 7-19.

จุฬาลงกรณ์มหาวิทยาลัย

CHULALONGKORN UNIVERSITY
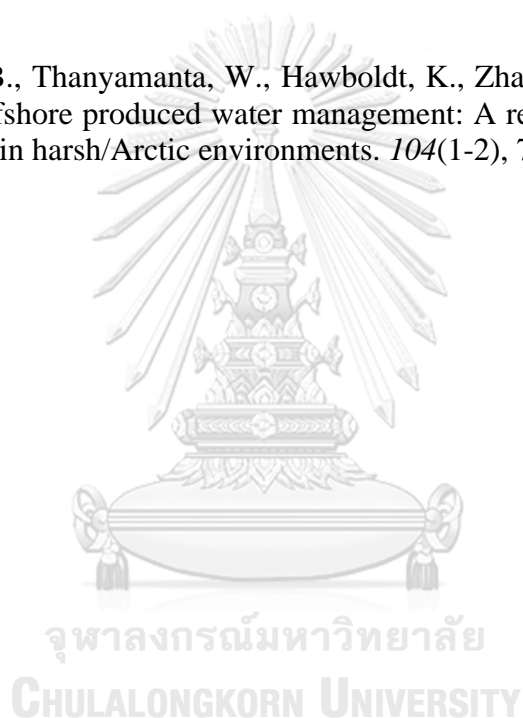
APPENDICES

Appendix 1

Table 1.1. Analysis of variance (ANOVA) for factor optimization of "S-DAF" (1)

Analysis of Variance					
Source	**DF**	**Adj SS**	**Adj MS**	**F-value**	**P-value**
Model	9	382.413	42.49	7.38	0.002
Linear	3	297.092	99.031	17.21	0.000
Ps	1	149.928	149.928	26.05	0.000
Vm	1	145.78	145.78	25.33	0.001
t	1	1.385	1.385	0.24	0.634
Square	3	35.17	11.723	2.04	0.173
Ps^2	1	0.694	0.694	0.12	0.736
Vm^2	1	20.511	20.511	3.56	0.088
t^2	1	10.828	10.828	1.88	0.200
2-ways interaction	3	50.151	16.717	2.9	0.088
Ps*Vm	1	44.515	44.515	7.74	0.019
Ps*t	1	4.022	4.022	0.7	0.423
Vm*t	1	1.614	1.614	0.28	0.608
Error	10	57.549	5.755		
Lack-of-Fit	5	55.166	11.033	23.16	0.002
Pure Error	5	2.382	0.476		
Total	19	439.961			

Model Summary					
	S	**R-sq**	**R-sq (adj)**	**R-sq (pred)**	
	2.398	86.92%	75.15%	3.71%	

Table 1.2. *Analysis of variance (ANOVA) for factor optimization of "S- DAF" (2)*

Term	Effect	Coef	SECoef	T-value	P-value
Coded Coefficients					
Constant		39.05	0.978	39.91	0.000
Ps	6.627	3.313	0.649	5.100	0.000
Vm	6.534	3.267	0.649	5.030	0.001
t	0.637	0.318	0.649	0.490	0.634
Ps^2	-0.439	-0.219	0.632	-0.350	0.736
Vm^2	-2.386	-1.193	0.632	-1.890	0.088
t^2	1.734	0.867	0.632	1.370	0.200
Ps*Vm	-4.718	-2.359	0.848	-2.780	0.019
Ps*t	1.418	0.709	0.848	0.840	0.423
Vm*t	0.898	0.449	0.848	0.530	0.608

จุฬาลงกรณ์มหาวิทยาลัย

CHULALONGKORN UNIVERSITY

Appendix 2

Table 2.1. *Analysis of variance of stirring combined with IAF and DAF (1)*

Source	DF	Adj SS	Adj MS	F-value	P-value	
Analysis of Variance						
Model	14	3117.06	222.65	6.36	0.001	
Linear	4	1730.32	432.58	12.36	0.000	
Q_g	1	90.97	90.97	2.60	0.126	No significant
P_s	1	6.82	6.82	0.19	0.665	No significant
V_m	1	999.16	999.16	28.54	0.000	Significant
t	1	633.36	633.36	18.09	0.001	Significant
Square	4	1170.43	292.61	8.36	0.001	
Q_g^2	1	124.40	124.40	3.55	0.078	
P_s^2	1	74.31	74.31	2.12	0.164	
V_m^2	1	0.23	0.23	0.01	0.936	
t^2	1	1064.36	1064.36	30.41	0.000	
2-ways interaction	6	216.31	36.05	1.03	0.442	
Q_g*P_s	1	9.67	9.67	0.28	0.606	
Q_g*V_m	1	14.15	14.15	0.40	0.534	
Q_g*t	1	11.38	11.38	0.33	0.576	
P_s*V_m	1	68.05	68.05	1.94	0.182	
P_s*t	1	1.82	1.82	0.05	0.822	
V_m*t	1	111.24	111.24	3.18	0.094	
Error	16	560.07	35.00			
Lack-of-Fit	10	559.70	55.97	922.88	0.000	
Pure Error	6	0.36	0.06			
Total	30	3677.13				
Model Summary						

S	R-sq	R-sq (adj)	R-sq (pred)
5.91643	84.77%	71.44%	12.31%

Table 2. *Analysis of variance of stirring combined with IAF and DAF (2)*

Term	Effect	Coef	SE Coef	T-value	P-value
Coded Coefficients					
Constant		46.92	2.240	20.98	0.000
Q_g	3.890	1.950	1.210	1.610	0.126
P_s	1.070	0.530	1.210	0.440	0.665
V_m	12.90	6.450	1.210	5.340	0.000
t	10.27	5.140	1.210	4.250	0.001
Q_g^2	- 4.170	- 2.090	1.110	- 1.890	0.078
Ps^2	- 3.220	- 1.610	1.110	-1.460	0.164
Vm^2	0.180	0.090	1.110	0.080	0.936
t^2	-12.20	- 6.100	1.110	- 5.510	0.000
Q_g*P_s	- 1.550	- 0.780	1.480	- 0.530	0.606
Q_g*V_m	- 1.880	- 0.940	1.480	- 0.640	0.534
Q_g*t	1.690	0.840	1.480	0.570	0.576
P_s*V_m	- 4.120	- 2.060	1.480	- 1.390	0.182
P_s*t	- 0.670	- 0.340	1.480	-0.230	0.822
V_m*t	5.270	2.640	1.480	1.780	0.094

VITA

NAME	Marina Phea
DATE OF BIRTH	06 July 1993
PLACE OF BIRTH	Prek Koy Commune, Kong Meas District, Kampong Cham Province, Cambodia
INSTITUTIONS ATTENDED	Bachelor's Degree of Water Resources and Rural Infrastructure Engineering, Institute of Technology of Cambodia Mater's Degree in Environmental Engineering, Chulalongkorn University, Thailand
HOME ADDRESS	Krangyov Commune, Saang District, Kandal Province, Cambodia
PUBLICATION	Joining the SUT International Virtual Conference (IVCST) on science and technology on 28th August 2020. Joining The 9th International Conference on Environmental Engineering, Science, and Management of Environmental Engineering Association of Thailand (EEAT).
AWARD RECEIVED	Received the scholarship from ASEAN and Non-ASEAN country of Chulalongkorn University, Thailand for Master's Degree in Environmental Engineering, Department of Environment, Faculty of Engineering, Chulalongkorn University, Thailand.

จุฬาลงกรณ์มหาวิทยาลัย
CHULALONGKORN UNIVERSITY